FLUORESCENCE AS A DIAGNOSTIC OF NUTRIENT STRESS

BY
JEAN-PAUL PARKHILL

Submitted in partial fulfillment of the requirements for the degree of Doctor of Philosophy

DALHOUSIE UNIVERSITY
Halifax, Nova Scotia
April 2003

DALHOUSIE UNIVERSITY

FACULTY OF GRADUATE STUDIES

The undersigned hereby certify that they have read and recommend to the Faculty of Graduate Studies for acceptance a thesis entitled "Fluorescence as a diagnostic of nutrient stress" by Jean-Paul Parkhill in partial fulfillment for the degree of Doctor of Philosophy.

Dated: March 31, 2003

External Examiner:

Research Supervisor:

Examining Committee:

Departmental Representative:

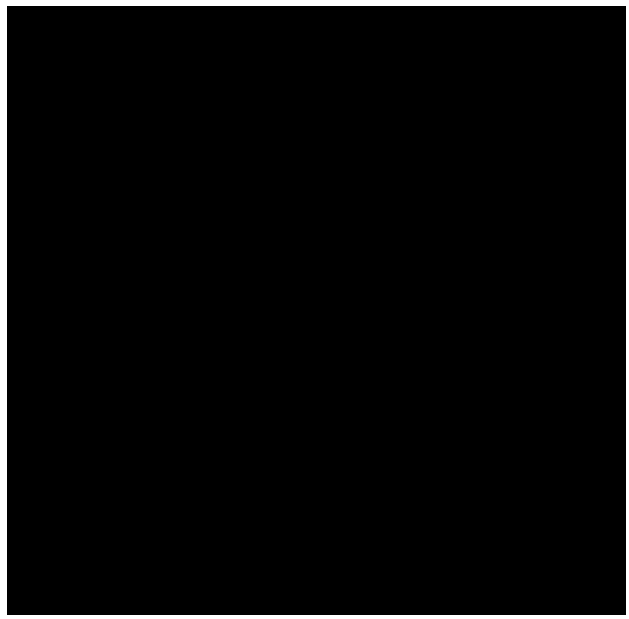

Copyright Agreement Form
Dalhousie University

Date: April 7th, 2003

Author: Jean-Paul Parkhill

Title: Fluorescence as a diagnostic of nutrient stress

Department: Oceanography Department, Dalhousie University

Degree: Ph.D.
Convocation: May
Year: 2003

Permission is herewith granted to Dalhousie University to circulate and to have copied for non-commercial purposes, at its discretion, the above title upon the request of individuals or institutions.

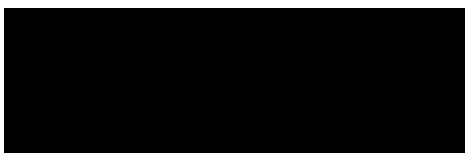

Signature of Author

The author attests that permission has been obtained for the use of any copyrighted material appearing in the thesis (other than the brief excerpts requiring only proper acknowledgement in scholarly writing), and that all such use is clearly acknowledged.

Table of Contents

List of Figures

Figure 2.5 Nutrient starvation for cultures previously acclimated to nitrate-limited growth. F_v/F_m as a function of the duration of nutrient stress defined as the time after the flow of nutrients is stopped (Time = 0) for four different pre-conditioned nutrient-limited relative growth rates at two different growth irradiances: (A) 350 μmol m^{-2} s^{-1} (μ_{max} = 1.50 d^{-1}) and (B) 55 μmol m^{-2} s^{-1} (μ_{max} = 0.71 d^{-1}). Error bars show SD of triplicate cultures. (C) Fv/Fm, determined from PAM fluorometry, as a function of nutrient-dependent relative growth rate for perturbed continuous cultures, 4 days after the flow of nutrients was stopped for three different irradiances (n = 55 μmol m^{-2} s^{-1}, 5 = 350 μmol m^{-2} s^{-1}, □ = 150 μmol m^{-2} s^{-1}). The points for μ/μ_{max} = 1.0 represent nutrient replete semi-continuous cultures for which replacement of medium was stopped at time zero (t_o). Means ± SE for three replicate cultures. **42**

Figure 2.6 (A) F_v/F_m determined from active fluorometry (PAM) under balanced growth conditions for a range of nutrient-dependent growth rates and growth irradiance (● = 55 μmol m^{-2} s^{-1}, ▲ = 350 μmol m^{-2} s^{-1}, □ = 150 μmol m^{-2} s^{-1}). Estimates of F_v/F_m from the findings of Kolber et al. (1988), who reported F_v/F_o measured with a Pump and Probe fluorometer on Thalassiosira pseudonana (3H), are shown for comparison (symbol = O). (B) F_v/F_m determined by conventional fluorometry (DCMU methodology, no neutral density screen) for continuous cultures grown at different irradiances and N-limited growth rates. Data from previous experiments (Cullen et al. 1992 and Zhu et al. 1992). Mean ± SE for three replicates. **44**

Figure 2.7 Physiological parameters of Thalassiosira pseudonana as a function of time for determining balanced growth conditions. Representative cultures grown under low nutrient-limited growth rates (●) and high nutrient-limited growth rates (O) for different irradiance levels: 55 μmol m^{-2} s^{-1}, with growth rates of 0.43 and 0.21 d^{-1} (A-C), 150 μmol m^{-2} s^{-1}, with growth rates of 1.0 and 0.17 d^{-1} (D-F), 350 μmol m^{-2} s^{-1}, with growth rates

ensures that the fiber-optic cable to the photomultiplier tube (PMT) and saturating flash lamp are at right angles. The metal guard has a guide with stoppers which allow for accurate and rapid changes from one sample to the next. A secondary cooling unit using a fan system provides further heat dissipation. A light shield (not shown) blocks out all ambient irradiance, which allows measurement of individual samples under dark-adapted conditions prior to exposure to their respective incubation irradiances. Once these initial readings are taken the light shield is removed. The signal from each sub-sample is propagated down a fibre-optic light guide and amplified by the PMT; it is then recorded for further data analysis. Sampling time for an individual sub-sample is 10 seconds. A run of 12 cuvettes requires 2 minutes and a sample is observed over a 20 minute period. The PAM system is run using a program generated from a Labview 4.0 software package. **71**

Figure 3.3 Daily routine measurements of replete cultures grown under three different irradiance levels (150 (●), 350 (g) and 1000 μmol m^{-2} s^{-1} (O)) provides evidence of steady-state exponential growth and irradiance limitation of growth. (A) Growth rate was determined by daily dilutions and provides evidence that cultures grown under higher irradiance levels had higher growth rates. (B) Measurements of a fluorescence parameter normalized to chlorophyll provides evidence of little physiological change over time. (C) F_v/F_m, an indicator of nutrient starvation, was high and constant for all light levels investigated, indicating nutrient replete growth conditions. Means ± SE for three replicate cultures. **80**

Figure 3.4 Fluorescence signal measured by PAMoTron. (A) Fluorescence signal of F_o and F_m for 12 blank subsamples of 0.22 μm filtered artificial media under ambient light conditions with the delivery of a 600 ms saturation pulse (>5000 μmol m^{-2} s^{-1}) at the end of the monitoring interval for each respective cuvette. F_m is not different from F_o. The monitoring interval of an individual sample is 10 s. Following completion of the saturation pulse, measurement moves to the next sample. No changes in the fluorescence signal are

List of Tables

THESIS ABSTRACT

Fluorescence measurements have been used for decades for determination of algal biomass and assessment of physiological status both in the laboratory and the field. They can provide rapid non-invasive indicators of algal physiological stress. Fluorescence-based studies of nutrient stress in phytoplankton have been predominately limited to the measurement of maximum quantum yield for photosystem II (F_v/F_m). Reported results for cultures grown under acclimated N-limited growth conditions showed a decrease in F_v/F_m as a function of N-limited growth rate. My research reports contradictory results using two independent measurement systems showing consistently high F_v/F_m (~ 0.65) independent of irradiance and N-limited growth rate. Experiments on nutrient-replete and N-starved cultures contribute to the growing body of evidence for using F_v/F_m as a proxy for N-stress, and show that a decrease in F_v/F_m under N-starved conditions is also a function of pre-conditioned N-limited growth rate. The two independent measurement systems, Turner Designs and Pulse Amplitude Modulation (PAM) Fluorometer, showed strong correlation, although reduction of the actinic measuring beam in the Turner Designs system was required for cultures grown under low-light. Since the basic relationship between N-stress and F_v/F_m breaks down under acclimated balanced N-limited growth, a complementary or more sensitive diagnostic is required.

Active fluorometers (i.e. PAM) have the capability to resolve fluorescence measurements under actinic light providing an opportunity to investigate other fluorescence metrics as a function of irradiance to provide proxies for quantifying physiological stress. I interfaced a light incubation chamber and a PAM fluorometer to allow parallel measurements of fluorescence parameters such as calculated electron transport rates and maximum non-photochemical quenching (NPQ_{max}) over time as a function of irradiance. This new measurement system eliminates the confounding effects of varying irradiance during measurement that influence results of the established rapid-light-curve method. The new measurement system allows for determination of the parameter of light saturation (E_{KF}) in F vs. E curves, as well as NPQ_{max}. Both parameters were a function of growth irradiance. Further investigation of these parameters under N-stress (limitation and starvation) show that E_{KF} and NPQ_{max} are sensitive to N-stress, although the relationship was less apparent in N-limited cultures, and the growth irradiance played a more dominant role. The relationship of increased NPQ_{max} and reduced E_{KF} under increased N-stress is also supported by the accessory photo-protective pigment data and comparison to radio-labeled carbon uptake experiments. Because effects of growth irradiance and N-nutrition on NPQ_{max} and E_{KF} are not easily separated, the method has limited utility for assessing N-stress in the field. Although the instrument has some limitations including poor sensitivity and the need for controlled laboratory settings, it is an important step in identifying viable fluorescence metrics that can replace insensitive or labor-intensive techniques currently used. Also, the strong correlation between E_{KF} and the saturation parameter for photosynthesis suggests that the fluorescence parameter E_{KF} can be used as a tool for understanding and predicting variability in primary production in the oceans, while NPQ_{max} provides insight into the effect of N-stress on the photo-protective strategies of an algal population.

List of Symbols and Abbreviations

Symbols and units, from a compilation of fluorescence research (Kooten and Snel 1990; Falkowski and Kolber 1993; Geider et al. 1993a; Kolber and Falkowski 1993; Schreiber et al. 1995; Rohácek and Barták 1999).

Symbols	Definitions	Units
chl	Chlorophyll *a* concentration	$\mu g\ L^{-1}$
DD	Diadinoxanthin concentration	$\mu g\ L^{-1}$
DT	Diatoxanthin concentration	$\mu g\ L^{-1}$
E	Irradiance	$\mu mol\ photons\ m^{-2}\ s^{-1}$
E_K	Parameter of light saturation determined from ^{14}C incubation experiments	$\mu mol\ photons\ m^{-2}\ s^{-1}$
E_{KF}	Parameter of light saturation determined from fluorescence measurements	$\mu mol\ photons\ m^{-2}\ s^{-1}$
ETR*	Relative electron transport rate ($\Delta F/F_m'$) * E	$\mu mol\ photons\ m^{-2}\ s^{-1}$
ETR^*_{max}	Maximum relative electron transport rate	$\mu mol\ photons\ m^{-2}\ s^{-1}$
F_o	Minimum fluorescence measured on dark adapted sample with open PSII RCs (qP = 1) and all NPQ in the thylakoid membrane minimized (qN = 0)	mV (Relative)

F_o'	Minimum fluorescence measured on light adapted sample	mV (Relative)
F_m	Maximum fluorescence measured on dark adapted sample with closed PSII RCs (qP = 0) and all NPQ in the thylakoid membrane minimized (qN = 0)	mV (Relative)
F_m'	Maximal fluorescence measured on ambient light sample with closed PSII RCs (qP = 0) in the presence of NPQ (qN > 0)	mV (Relative)
F_s	Steady-state fluorescence measured on ambient light sample (qP > 0, qN > 0)	mV (Relative)
F_v	Maximum variable fluorescence on dark adapted sample $F_v = F_m - F_o$	mV (Relative)
F_v'	Variable fluorescence on ambient light sample $F_v' = F_m' - F_o'$	mV (Relative)
F_v/F_m	Fluorescence-based maximum quantum yield for PSII	Dimensionless
$\Delta F/F_m'$	Photochemical quenching determined from fluorescence $((F_m' - F_s)/ F_m')$	Dimensionless
GY	Genty yield = $\Delta F/F_m'$	Dimensionless
NPQ	Non-photochemical quenching of fluorescence $((F_m - F_m')/ F_m)$	Dimensionless
NPQ_{max}	Maximum non-photochemical quenching of fluorescence $((F_m - F_m')/ F_m)$ determined from 20 minute incubated cultures	Dimensionless

P^B_{max}	Maximal rate of photosynthesis normalized to chlorophyll	gC $gchl^{-1}$ h^{-1}
qN	Non-photochemical quenching of variable fluorescence $((F_v-F_v')/F_v)$	Dimensionless
qE	Component of non-photochemical quenching assigned to high energy state transitions	Dimensionless
qI	Component of non-photochemical quenching assigned to photoinhibition processes	Dimensionless
qT	Component of non-photochemical quenching assigned to state transitions	Dimensionless
qP	Photochemical quenching of variable fluorescence $((F_m'-F_s)/ F_v')$	Dimensionless
ψ_f	Probability of fluorescence	Dimensionless
ψ_d	Probability of heat dissipation	Dimensionless
ψ_p	Probability of photochemistry	Dimensionless
ϕ_C	Quantum yield of carbon fixation	mol C fixed (mol photons absorbed)$^{-1}$
$(\phi_C)_m$	Maximum quantum yield of carbon fixation	mol C fixed (mol photons absorbed)$^{-1}$
ϕ_{PSII}	Quantum yield of PSII	mol electron (mol photons absorbed)$^{-1}$
$(\phi_{PSII})_m$	Maximum quantum yield of PSII	mol electron (mol photons absorbed)$^{-1}$
μ	Specific growth rate	d^{-1}

μ_{max}	Maximum growth rate at a growth E and Temp.	d^{-1}
μ/μ_{max}	Relative growth rate	Dimensionless

Abbreviations

D1	Reaction center protein
DCMU	3'-(3,4-dichlorophenyl)-1',1'dimethyl urea
LHC	Light Harvesting Complex
PAM	Pulse Amplitude Modulation
PSI	Photosystem I
PSII	Photosystem II
Q_A	Primary electron acceptor after PSII
Q_B	Secondary electron acceptor after PSII
RC	Reaction Center
SD	Standard deviation
SE	Standard error

Acknowledgements

I would like to thank John Cullen for providing me with his continuous support and guidance. You are an excellent scientist and supervisor; your high standards have made me a better investigator. With your wisdom, encouragement and patience you have made this thesis possible.

Technical support from Gary Maillet needs to be acknowledged. Your countless hours and meticulous nature in the lab made this large multi-measurement experimental design possible. You are a good friend and this thesis represents your work as much as it does mine. Yannick Huot, for his advice, statistical knowledge and never-ending proofreading, I know I am going to say one day, that I knew this world class scientist and I used to crush him on the badminton court. I would like to thank the rest of the CEOTR group, especially Richard Davis, for being there with helpful ideas, criticisms, technical support and friendship. Also, Erica Head and the group from Bedford Institute of Oceanography who allowed me countless hours on the HPLC for little more than a bottle of Chardonnay.

I thank my thesis committee who has vetted me on every aspect of the research. Each member provided insightful comments, discussions and revisions.

A heartfelt thanks goes to my family. Especially my parents, whom this endeavor has aged considerably, who have been there emotionally and financially at every turn. Also, my wife, Sarah whose support, quiet persistence and example of what a dedicated scientist should be, has guilted me to completion.

This research, invaluable training and education were made possible from financial support from Dalhousie University Scholarship and grants from NSERC, NSERC Research Partnerships, and ONR.

Chapter 1

General introduction

1.1 Introduction

This chapter introduces the reader to photosynthetic reactions, the measurement and interpretation of fluorescence, and general terminology. In addition, an overview of how different fluorescence metrics may be used as measures of physiological stress is presented. This section serves only as a brief review of basic principles necessary to understand fluorescence as a diagnostic of physiological stress and to provide the structure for the thesis. More detailed descriptions of the specific topics are found in the background sections of each chapter; readers wishing more information on photosynthesis, fluorescence and nutrient stress are referred to more extensive reviews (Prézelin 1981; Krause and Weis 1991; Govindjee 1995; Falkowski and Raven 1997; Maxwell and Johnson 2000; Beardall et al. 2001).

1.1.1 Photosynthesis and absorbed light

The general principles of photosynthesis are described in introductory biology texts and books on aquatic photosynthesis (Barber 1992; Lalli and Parsons 1993; Kirk

1994; Falkowski and Raven 1997; Lawlor 2001). The following summary is compiled from these sources.

Photosynthesis is a metabolic process that occurs in cells of green plants, certain protists, algae, and bacteria. During the process, energy from the sun is trapped and used to convert the inorganic raw materials carbon dioxide (CO_2) and water (H_2O) to carbohydrates and oxygen (O_2). Overall, photosynthesis is a conversion of light energy to chemical energy stored in the form of molecular bonds.

The photons that drive this biologically mediated reaction are absorbed by cellular compounds called photosynthetic pigments. The principal pigment active in photosynthesis is chlorophyll *a*. When a photon of light energy is absorbed, it changes the electron configuration of the absorbing molecule. A molecule with all its electrons in their most stable low energy orbitals is said to be in its ground state. A photon of the appropriate wavelength striking a pigment molecule in its ground state can transfer its energy and excite the electron into a higher energy orbital (Figure 1.1). This happens only if the energy of the photon is equal to the difference in energy between the two electronic states of the molecule and all accompanying vibrational or rotational states (Clayton 1980). This excitation is an all-or-nothing process, whereby if the excitation energy is not in the correct energy range the electrons will not achieve a higher orbital state (Figure 1.1).

Once energy is absorbed, photosynthesis can occur. Photosynthesis involves two different sets of partial reactions. In the first, water is oxidized; in the second, carbon dioxide is reduced. When water is oxidized, O_2 is released to the environment. Through a

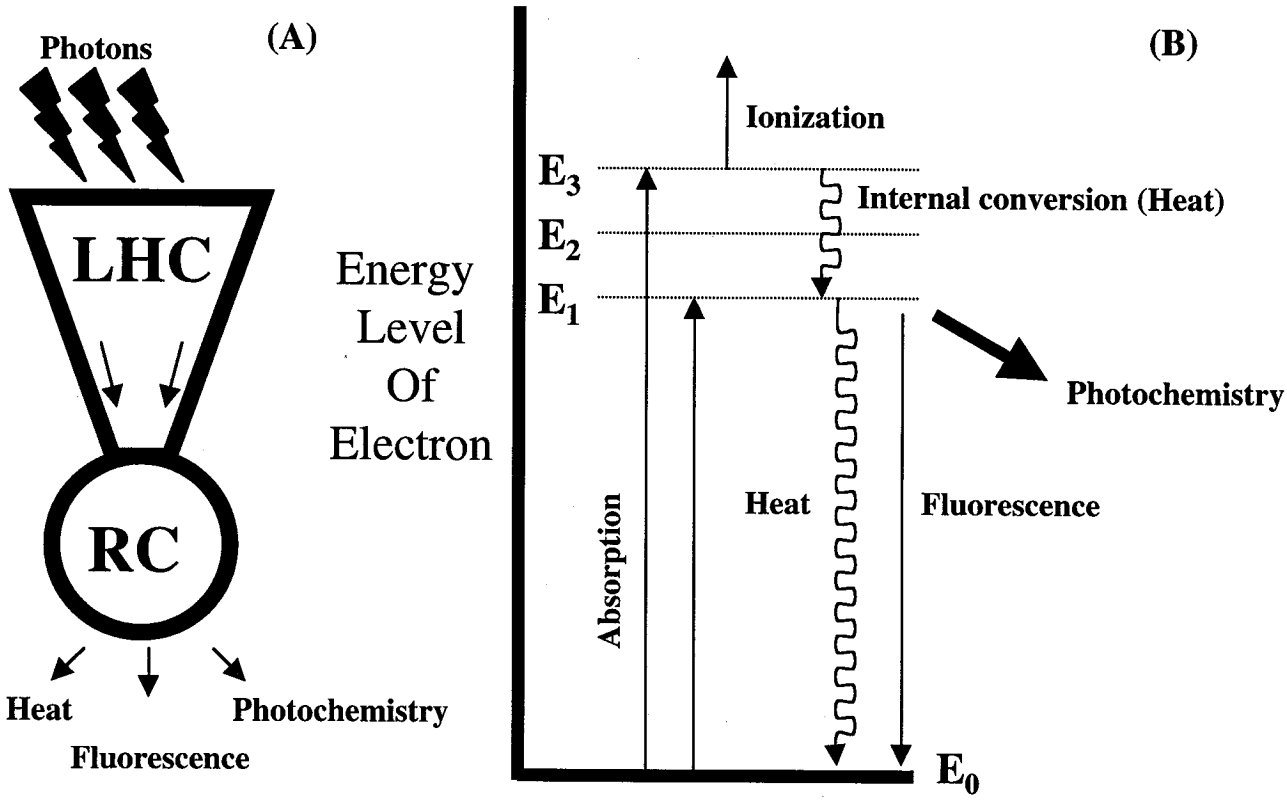

Figure 1.1 (A) Photons are absorbed by the light harvesting complex (LHC) which consists of antennae pigments (chlorophylls, carotenoids, and phycobilins). A portion of this energy is transferred as an exciton to the reaction center (RC) where it can be dissipated in one of three possible pathways (heat, photochemistry, or fluorescence). (B) The energy level diagram shows excited states of electrons from absorbed light energy in the chlorophyll molecules of the reaction center. An absorbed photon excites an electron from its ground state (E_0) and if the energy absorbed is too much it will exceed the nuclear attraction and cause the loss of the electron from the molecule, a process called ionization. When the absorbed energy corresponds to an excited state (E_3-E_1) the electron will return to the lowest excited state (E_1) through an internal conversion leading to non-radiative dissipation (heat). Once the lowest excited state is achieved, the excited state has three possible pathways - emission as fluorescence, photochemistry, or loss as heat.

series of steps, the liberated electrons then reduce CO_2 to carbohydrate, which is used in the synthesis of cellular constituents (Prézelin 1981).

The first phase of photosynthesis, directly dependent on light absorption, involves a series of protein complexes, electron carriers, and lipids. Photosynthetic electron transport consists of a series of electron transfers from one electron carrier to another. The first step in the conversion of a photon to an excited electronic state occurs in the antennae system. The antennae system, referred to as the light harvesting complex (LHC), consists of hundreds of pigment molecules, mainly chlorophylls (chl) and carotenoids, that are anchored to proteins within the photosynthetic membrane (thylakoid membrane) and funnel the energy to a specialized protein complex known as the reaction center (Figure 1.1) (Govindjee 1995). The photosynthetic pigments serve a light harvesting function for the reaction center (RC), and expand the spectral range of light energy that can be absorbed in the chloroplast and transferred to RC to drive the photochemical reactions of photosynthesis. The electronic excited state is transferred over the antennae molecules. These mobile concentrations of energy consisting of excited electrons are called excitons. Some excitons are converted back into photons and emitted as fluorescence, some are converted into heat and some are trapped by a reaction center protein and used for photochemistry (Krause and Weis 1991). These are the only three possible fates for absorbed photons (excitons) (Figure 1.1).

Excitons trapped by a reaction center provide energy for photochemistry through reactions of donor and acceptor molecules called the electron transport chain. The electron transport chain can be discussed in three sections: the donor side of photosystem II

(PSII), the acceptor side of PSII, and the acceptor side of photosystem I (PSI) (Figure 1.2). On the donor side of PSII the water molecule is oxidized; oxygen is evolved and protons are released from the water molecule. A water-splitting enzyme very efficiently donates electrons to PSII, a chl *a* dimer driving photosynthesis after transfer of excitation energy from the light harvesting complex. Oxygen ions from water combine to form O_2. By assessing the amount of oxygen evolution that occurs over a given time period and by measuring absorbed light, a measurement of photosynthetic quantum efficiency (ϕ_{O2}) can be determined (Falkowski and Raven 1997; Flameling and Kromkamp 1998).

On the acceptor side of PSII, absorbed photons excite PSII and an electron donated by water is transferred from the chlorophyll complex to pheophytin, then to Q_A, and Q_B, and onto the plastoquinone pool through these chemical electron carriers. Once primary charge separation occurs, at the pheophytin level, the subsequent electron transfer reactions are energetically downhill (Figure 1.2). During charge separation, the absorbed energy not used for photosynthesis is dissipated as heat and fluorescence. Assuming a constant ratio between heat and fluorescence, a measurable relationship between chlorophyll fluorescence and the efficiency of photosynthetic energy conversion (ϕ_{PSII}) can be obtained.

On the acceptor side of PSI, the final stage of conversion of radiant energy into chemical bond energy begins when another photon excites the protein complex, PSI, providing energy to reduce a higher energy acceptor, ferredoxin. Then subsequent electron transfers culminate in the reduction of NADP, and along with ATP generated from proton (H^+) gradients, converts inorganic carbon into a reduced chemical form (Figure 1.2). The

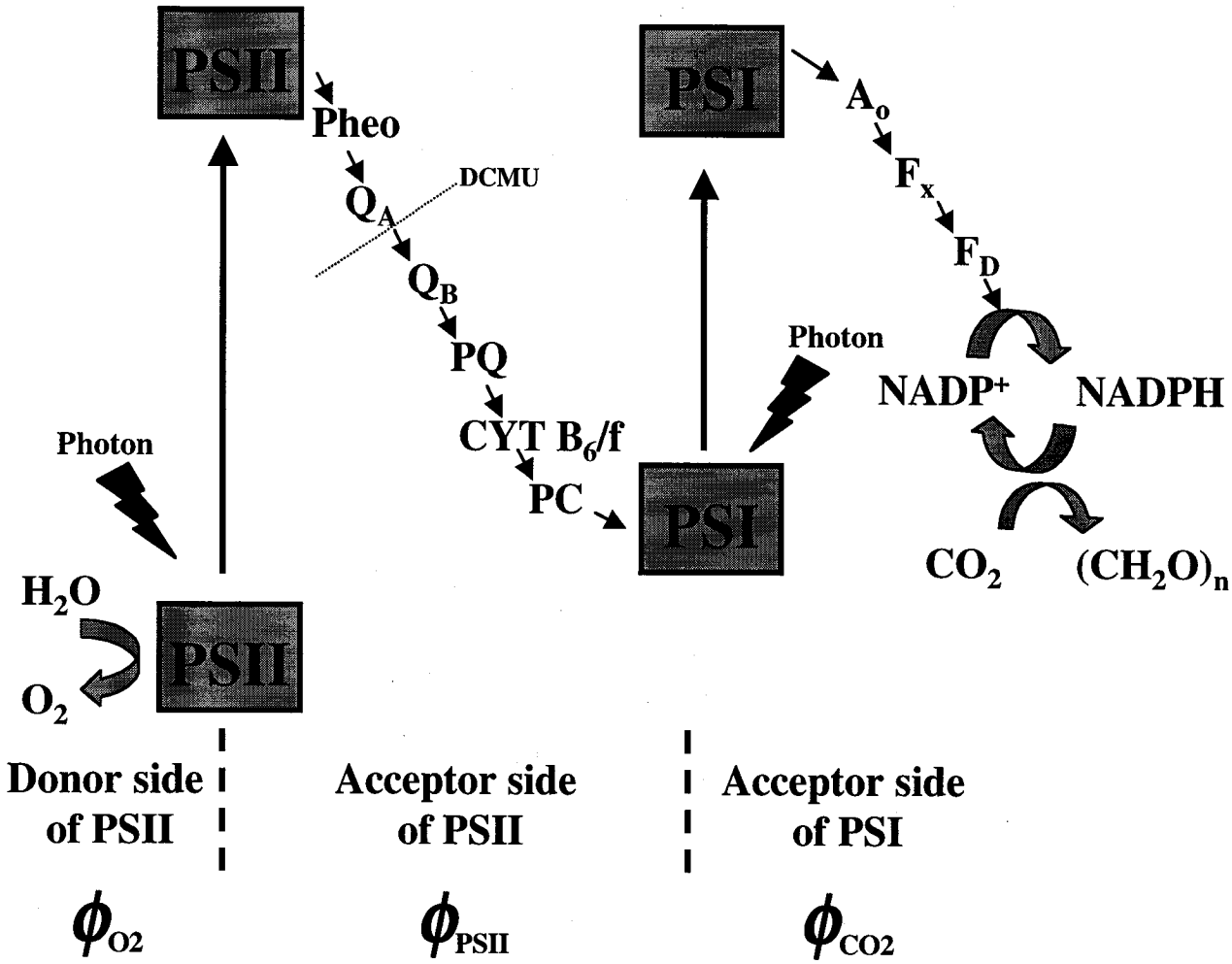

Figure 1.2 Electron transport chain. Electrons extracted from water in PSII are sequentially transferred to an excited state of PSII and transported to pheophytin (Pheo) which subsequently reduces the primary acceptor Q_A. Two electrons are then transferred from Q_A to the secondary acceptor Q_B which dissociates from the PSII protein complex and diffuses into the plastoquinone pool (PQ) until it reaches the cytochrome B_6/f complex. The complex delivers the electrons to the plastocyanin (PC) which ferries the electron to PSI. With another absorbed photon at PSI, an electron moves though a series of electron carriers and iron sulfur clusters (A_o, F_x) and then to a molecule of ferredoxin (F_D) and through the enzyme ferredoxin-$NADP^+$ reductase allows for the production of reductant NADPH to facilitate the incorporation of carbon. The reduction of CO_2 by $NADPH_2$ (catalysed by carboxylase enzymes) requires the chemical energy of ATP and these processes are called the "dark reactions". The efficiency of incorporation of inorganic carbon can be determined (ϕ_{CO2}) at this point. The efficiency of the donor side of PSII can be determined from the amount of oxygen evolution (ϕ_{O2}), while the efficiency of electron transfer on the acceptor side of PSII (ϕ_{PSII}) can be determined through fluorescence parameters.

quantum efficiency of this conversion can be determined by ^{14}C incubation experiments (ϕ_{CO2}).

1.1.2 Photosynthesis and fluorescence

The fundamental relationship between fluorescence and photosynthetic energy conversion is that fluorescence originates from the same excited states, created by light absorption, which alternatively can be photochemically converted or dissipated as heat. Hence the relationship between the fraction of absorbed energy going to fluorescence, photosynthesis, and heat is constrained by the conservation of energy in the first law of thermodynamics, that is, the probabilities of all fates of absorbed light energy must equal the total amount of absorbed light energy (Equation 1.1, where Ψ_p, Ψ_d and Ψ_f are the probabilities for photosynthesis, dissipation as heat, and fluorescence, respectively).

$$\psi_p + \psi_d + \psi_f = 1 \qquad 1.1$$

Since, under some conditions, the probabilities of heat and fluorescence remain in relatively constant proportions, one can determine relative electron transport through fluorescence measurements (see section 2.3.1 for more detail). This is a simplified view of relationships based on energy conversion theory and biophysical models (Butler 1978; Weis and Berry 1987; Genty et al. 1989; Owens 1991; Kolber and Falkowski 1993; Kroon et al. 1993; Lavergne and Trissl 1995). The key point is that changes in the

probability of fluorescence will correspond inversely to changes in the probability of photosynthesis. At room temperature, fluorescence originates primarily from photosystem II (PSII) because energy transfer within photosystem I (PSI) is very efficient (Govindjee 1995). Since PSII is responsible for over 90% of the fluorescence in eukaryotic algae, then changes in fluorescence can be a direct indicator of the status of PSII (Butler 1978; Kiefer and Reynolds 1992; Schreiber and Bilger 1993). Further review and theory of the calculation of fluorescence parameters is shown in the background section of Chapter 2.

1.1.3 Measurement of fluorescence

In this research, two different measurement systems, a conventional and an active fluorometer, were used to measure fluorescence parameters for determination of the physiological status of an algal species. A conventional fluorometer uses the same light for fluorescence excitation and for driving photosynthesis; fluorescence is detected at 90° in the presence of excitation/actinic light by the use of appropriate combinations of optical filters (e.g. a blue filter for excitation and a long-pass emission filter that transmits red fluorescence to the photodetector). Such conventional fluorometers are of limited use for photosynthesis research, as they are not designed to measure fluorescence in ambient light.

In active fluorometers, in particular the Pulse Amplitude Modulation (PAM) fluorometer, excitation light can be "modulated" to distinguish between fluorescence and

other sources of light at the same wavelengths. When a special "measuring light" is switched on/off, the fluorescence signal follows the on/off pattern and the modulated signal can be selectively amplified. This signal is then recorded in a data acquisition program and analyzed to provide important fluorescence metrics both in the dark and under ambient light levels.

As discussed, chlorophyll fluorescence competes with photochemical energy conversion and dissipation as heat in the de-excitation of the singlet excited states in PSII (Figure 1.1). A common measurement from conventional and active fluorometers has been the maximal quantum yield of photosystem II (PSII) (Geider et al. 1993a). This measurement is a proxy for the maximum efficiency of electron transfer to photochemistry from the light harvesting complex and the reaction center of PS II. This measurement uses the minimal (F_o) and maximal (F_m) fluorescence for a dark-adapted sample (Figure 1.3; Chapter 2). With both the conventional and active fluorometer, F_o is measured using a weak measuring light. For the PAM fluorometer F_m is achieved by a saturating pulse of bright light, while in the conventional case, 3'-(3,4-dichlorophenyl-1',1'-dimethyl urea (DCMU) is used to block electron transfer (Figure 1.2) allowing for measurement of F_m, thereby ensuring that photosynthesis is minimal and fluorescence is maximal. From these measurements, variable fluorescence, F_v (= F_m - F_o) is determined. A reliable proxy of maximal quantum yield of PSII is determined from F_v/F_m. Inhibition of PSII reaction centers (i.e. nutrient, light, and/or temperature stress) causes an increase in heat dissipation and a lower quantum yield of PSII (Cullen et al. 1992b; Falkowski and Kolber 1993). Both an increase in F_o or a decrease in F_m may

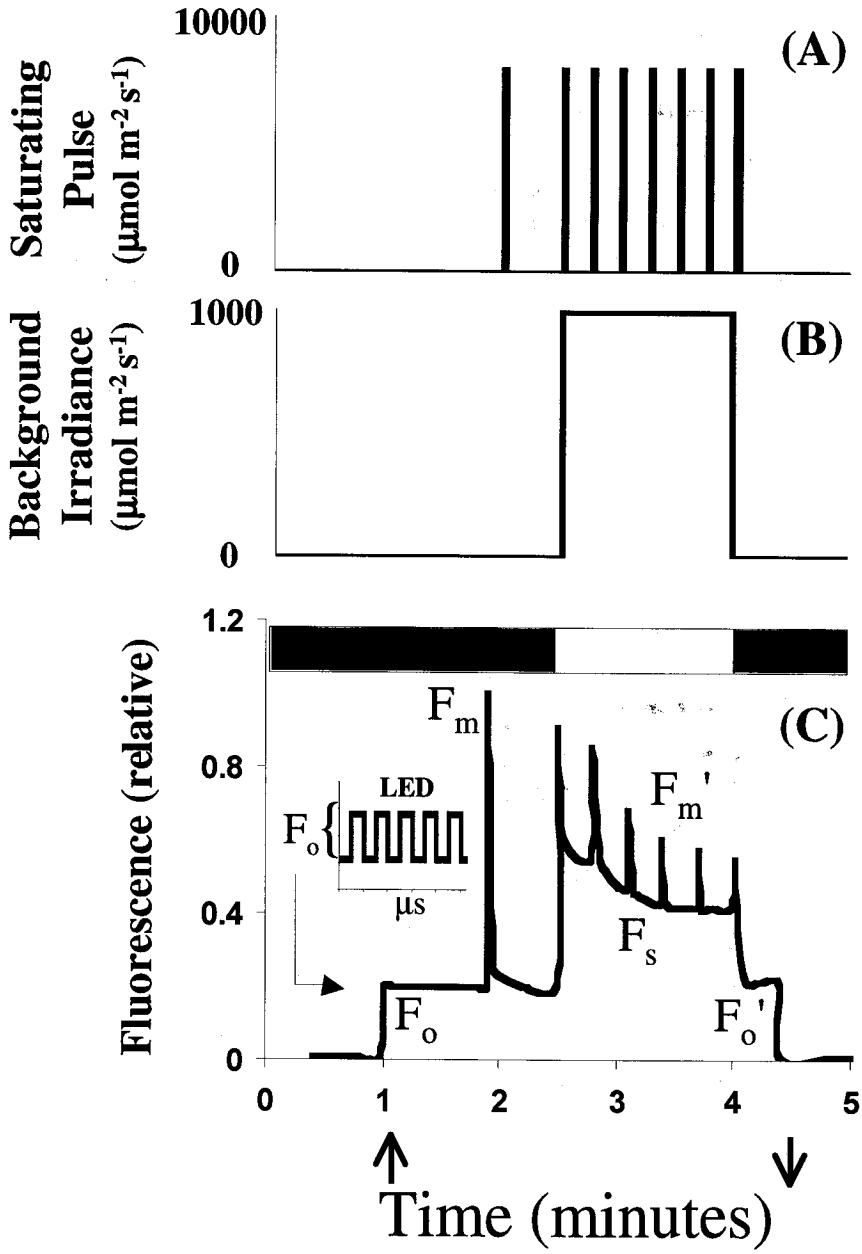

Figure 1.3 The PAM measurement system uses (A) saturating pulses, (B) background irradiance and a (C- inset) µs-modulated Light Emitting Diode (LED) to determine relative fluorescence parameters measured under dark (■) and ambient light (□) conditions. (C) The LED light is turned on (↑) and determination of minimal fluorescence (F_o) for a dark-adapted sample can be done. Subsequently, a saturation pulse, which closes all the reaction centers, allows determination of maximal fluorescence (F_m) under dark adaptation. Under ambient light, steady state fluorescence (F_s) and maximal fluorescence (F_m') can be determined. After the sampling period is complete the ambient light can be turned off (↓) and determination of minimal fluorescence after ambient light exposure can be determined (F_o'). For further explanation see text.

contribute to a decrease in F_v/F_m. While an increase of F_o points to photodamage, a decrease in F_m reflects enhanced non-radiative energy loss (heat dissipation), which can be viewed as an expression of photoprotection (Demmig-Adams and Adams III 1992; Anderson et al. 1997; Niyogi 1999; Laisk and Oja 2000). When a photosynthetically active sample is exposed to ambient irradiance, its fluorescence yield can vary between two extreme values, F_o and F_m.

The PAM allows measurement of fluorescence yields under ambient light, F_s. If a saturation pulse is then administered and closes the remaining reaction centers the measurement is termed maximal fluorescence under ambient light conditions, F_m' (Kooten and Snel 1990). These fluorescence parameters are the basis for the fluorescence metrics investigated in this research (List of Symbols and Abbreviations-xviii, Figure 1.3).

1.1.4 Fluorescence and non-photochemical quenching

Any reduction of fluorescence with respect to F_m may be caused either by enhanced photochemical energy conversion or by increased dissipation of absorbed photon energy as heat. Increased heat dissipation is commonly referred to as non-photochemical quenching. The saturation pulse method from a PAM fluorometer can distinguish between these two fundamentally different types of fluorescence quenching. Determination of quenching coefficients such as photochemical quenching (qP), and non-photochemical quenching (qN and NPQ), requires measurement of fluorescence metrics under ambient light conditions (List of Symbols and Abbreviations on p. xviii and

equations within). The definitions of qP and qN (explained in Chapter 3) imply that fluorescence quenching affects only variable fluorescence and not F_o. In reality, at higher levels of qN, there can also be significant quenching of F_o, resulting in the lower yield F_o'. This can be estimated upon light off, when the acceptor side of PSII is quickly re-oxidized (1-2s), whereas significant relaxation of non-photochemical quenching requires a longer time period (Rohácek and Barták 1999). Far-red light which excites mainly PSI can enhance Q_A-reoxidation and facilitate assessment of F_o'. The assessment of F_o' was not performed in this research, so accurate determination of qN could not be done; instead the proxy NPQ was investigated, which does not require the measurement of F_o', but provides similar information.

Non-photochemical quenching of fluorescence simply implies that de-excitation pathways other than photochemistry increase to quench fluorescence. This down-regulation is usually achieved by increased heat dissipation in the light harvesting antennae complexes (Demmig-Adams and Adams III 1992). Non-photochemical quenching can be divided into different processes related to their mechanisms. The three main categories include high energy state quenching (qE), state transitions (qT), and photoinhibition (qI). High energy state quenching refers to the rapid photoprotective mechanisms of the light-harvesting complex when a change in pH occurs causing a gradient over the thylakoid membrane. This activates conformational changes in some of the accessory pigments to dissipate a larger portion of the absorbed light as heat. For example, in diatom species under high-light conditions, the xanthophyll cycle is observed (i.e. de-epoxidation of diadinoxanthin to diatoxanthin) causing an increase in non-

photochemical quenching by diatoxanthin (Bilger and Björkman 1990; Long et al. 1994; Casper-Lindley and Björkman 1998; Schofield et al. 1998). These reactions are rapid and can be observed on the time scales of minutes. In state transitions, the light-harvesting complex can be moved from PSII to facilitate PSI absorption of light causing a reduced fluorescence quantum yield. This mechanism can be observed on time scales of 10-20 minutes, though it may not be important in the ocean (Falkowski and Raven 1997). Photoinhibitory damage to the reaction centers of PSII occurs when the capacity of these photoprotective mechanisms is exhausted. Classically, photoinhibition results from the degradation of the PSII reaction center protein (Neale 1987), D1, which is normally repaired in a few hours (Kyle et al. 1984; Prasil et al. 1992). The damaged reaction centers continue to trap excitation energy but dissipate it as heat (Krause and Weis 1988). The extended exposure of the photosynthetic apparatus to excessive light can lead to even more severe degradation of PSII where a slow recovery of days or longer can be observed (Krause and Weis 1988; Osmond 1994). NPQ should be a function of the ability for an algal cell to cope with excess energy, which should also be a function of the nutritional status of the algal cell.

1.1.5 Fluorescence and physiological stress

Since the three pathways (fluorescence, heat and photochemistry) compete for absorbed light energy, the proportion of energy used for photochemistry should be inversely related to the amount of fluorescence emitted. Photochemical systems require

nutrients for their maintenance, therefore fluorescence metrics should reflect changes due to N-stress. Nutrient stress has many effects on the photosynthetic apparatus of phytoplankton (Graziano et al. 1996) including a decrease in nitrogen rich pigments (i.e. chlorophyll) per cell causing a subsequent decrease in fluorescence per cell. Conversely, under N-stress, a decrease in protein may be observed, or changes in configuration of the photosynthetic apparatus due to protein loss, which would lead to an increase in fluorescence yield (Geider et al. 1993b; Olaizola et al. 1996; Falkowski and Raven 1997).

Fluorescence metrics have shown promise as a diagnostic of N-stress (Genty et al. 1989; Geider et al. 1993a; Babin et al. 1996a), although no clear consensus has been reached. With the advent of active fluorometers, investigation into other potential fluorescence metrics under an ambient light field is now possible, allowing investigation into fluorescence parameters as indicators of N-stress. By measuring fluorescence parameters during controlled physiological shifts related to N-stress, relationships between fluorescence and N-stress can be developed.

1.2 Structure of thesis research

This thesis is structured as three independent reports (Chapters 2, 3, and 4) with a general introduction (Chapter 1) and general conclusion (Chapter 5). This has resulted in some degree of reiteration in the background sections of Chapters 2, 3, and 4.

In Chapter 2, I examine an existing paradigm that F_v/F_m is an indicator of N-stress under all growth conditions. The investigation was performed using two independent measurement systems, an active fluorometer and a conventional fluorometer, which showed strong correlation although a correctable artifact may occur with a conventional fluorometer used for measurements on cultures acclimated to low irradiance. My results show that F_v/F_m remains high and independent of growth irradiance for nutrient-replete cultures which is consistent with the literature. Under batch-growth conditions, F_v/F_m decreases as a function of time without nutrients, and after full acclimation to N-limited conditions, the decrease in F_v/F_m during subsequent starvation is a function of pre-conditioned N-limited growth rate. Under N-limited growth conditions after acclimation of cultures, the relationship between F_v/F_m and N-stress breaks down, and therefore F_v/F_m is not robust for all nutrient growth conditions. The results question the generality of F_v/F_m as a diagnostic and highlight the importance of searching for complementary or new diagnostics of nutrition under all types of N-stress.

In Chapter3, I introduce the use of a new measurement system, PAMoTron, which interfaces a light incubation chamber and a PAM fluorometer. PAMoTron provides fluorescence vs. irradiance curves for a suite of 12 irradiances as a function of time. The two minute intervals between fluorescence measurements of different subsamples allows parallel investigation of the samples, obviating the problems with pre-conditioning and potential erroneous determination of electron transport rates that are associated with the sequential changes of light used in rapid light curves (White and Critchley 1999). The measurement system shows the rapid kinetics of NPQ under high

irradiance and shows that high energy state quenching is the dominant quenching process. The advantages and limitations of the new system are explored and investigation under different growth irradiances for nutrient-replete cultures shows that the parameter of light saturation determined from fluorescence (E_{KF}) is a function of light history and shows a strong correlation to the parameter of light saturation determined from ^{14}C incubation experiments (E_K). Also, non-photochemical quenching (NPQ) maxima are a function of incubation irradiance and the pre-conditioned growth rates for nutrient-replete cultures. The PAMoTron shows promise as a tool for detecting physiological stress.

In Chapter 4, the new measurement system is used to investigate N-limited and N-starved cultures at two different irradiance levels (350 and 1000 μmol m^{-2} s^{-1}). E_{KF} and NPQ_{max} were indicators of both N-limitation and N-starvation although the compound effect of light history and nutrient pre-conditioning makes resolution of a definitive fluorescence diagnostic of N-stress difficult. Regardless, when the light history is known, both parameters are functions of N-stress and can be used as a potential diagnostic. A decrease in the E_K and E_{KF} and an increase in NPQ_{max} were observed under increased N-stress. Both E_{KF} and NPQ_{max} increased as a function of growth irradiance. These findings are supported by photoprotective pigment analysis and the strong correlation observed between E_{KF} determined from the new measurement system and E_K determined from conventional ^{14}C incubation experiments.

Finally, the most relevant findings are highlighted in Chapter 5. I discuss the measurement of maximal quantum yield of photosystem II, F_v/F_m, under different growth conditions evaluate the new measurement system, suggesting improvements to the current

system and directions for future research. Finally, I summarize the evidence for using different fluorescence metrics as diagnostics of N-stress.

Chapter 2

Fluorescence-based maximal quantum yield for photosystem II as a diagnostic of nutrient stress

2.1 Chapter overview

In biological oceanography, it has been widely accepted that the maximum quantum yield of photosynthesis is influenced by nutrient-stress. A closely related parameter, the maximum quantum yield for stable charge separation of photosystem II, $(\phi_{PSII})_m$, can be estimated by measuring the increase in fluorescence yield from dark-adapted minimal fluorescence (F_o) to maximal fluorescence (F_m) associated with the closing of photosynthetic reaction centers with saturating light or with a photosynthetic inhibitor such as DCMU (3'-(3,4-dichlorophenyl)-1',1'-dimethyl urea). The ratio F_v/F_m $(= (F_m-F_o)/F_m)$ is thus used as a diagnostic of N-stress. Published results indicated that F_v/F_m is depressed for N-stressed phytoplankton, both during N-starvation (unbalanced growth) and acclimated N-limitation (steady-state or balanced growth). In contrast to published results, fluorescence measurements from my laboratory indicate that F_v/F_m is high and insensitive to N-limitation for cultures in steady-state under a wide range of relative growth rates and irradiance levels. This discrepancy between results could be

attributed to differences in measurement systems or to differences in growth conditions. To resolve the uncertainty about F_v/F_m as a diagnostic of N-stress, I grew the neritic diatom *Thalassiosira pseudonana* (Hustedt) Hasle and Heimdal under nutrient-replete and N-stressed conditions, using replicate semi-continuous, batch, and continuous cultures. F_v/F_m was determined using a conventional fluorometer and DCMU, and with a Pulse-Amplitude-Modulated (PAM) fluorometer. Reduction of excitation irradiance in the conventional fluorometer eliminated overestimation of F_o in the DCMU methodology for cultures grown at lower light levels, and for a large range of growth conditions there was a strong correlation between the measurements of F_v/F_m with DCMU and PAM ($R^2 = 0.77$, $n = 460$). Consistent with the literature, nutrient-replete cultures showed consistently high F_v/F_m (~ 0.65), independent of growth irradiance. Under N-starved (batch culture and perturbed steady-state) conditions, F_v/F_m was significantly correlated to time without the limiting nutrient and to N-limited growth rate prior to starvation. In contrast to published results, my continuous culture experiments showed that F_v/F_m was not a good measure of N-limitation under balanced growth conditions, and remained constant (~ 0.65) and independent of nitrogen-limited growth rate under different irradiance levels. Since variable fluorescence can only be used as a diagnostic for N-starved, unbalanced growth conditions, a robust measure of nutritional status in N-depleted oceanic waters is still required.

2.2 Introduction

The determination of phytoplankton biomass, photosynthetic capacity and photosynthetic efficiency is essential for understanding variability of primary production in the oceans. Photosynthesis is dependent on light, temperature, and nutrients (Eppley 1972; Cullen et al. 1992a; Falkowski and Kolber 1993; Kirk 1994). The relationship between photosynthesis and irradiance (Jassby and Platt 1976) and the influence of light on growth rates (Eppley 1980; Langdon 1988), and photosynthetic efficiency (Dubinsky 1992) have been well documented and quantified, as well as other light-dependent physiological effects such as acclimation (Ibelings et al. 1994; Geider et al. 1996), and inhibition of photosynthesis (Marra 1978; Neale 1987). The effects of temperature on algal physiology and growth have also been reviewed extensively (Eppley 1972; Davison 1991). However, disparate results persist for the role of nutrients in the growth and physiology of phytoplankton (Cullen et al. 1992b). Dugdale (1967), Eppley (1981), and Levasseur et al. (1993) have suggested that nitrogen limits growth rates of microalgae in regions of the ocean, although Goldman (1980) suggested that phytoplankton in the field were growing at or near their maximum relative growth rate. Although N-stress is known to cause changes in cellular physiology of microalgae, a review by Cullen et al. (1992b) suggested that photosynthetic parameters could not be used as robust indicators of nitrogen stress for both unbalanced (N-starved) and acclimated, N-limited growth because published studies produced fundamentally different results for relationships between photosynthetic capacity and N-limited growth rates. This study called into question the

use of measures of photosynthetic performance as diagnostics of nutritional status, particularly N-limitation. A robust diagnostic of N-stress is required to resolve uncertainties about the relationships between photosynthesis, nutrition and growth rates.

Diagnostic tools such as fluorescence metrics have shown promise for determination of photosynthetic efficiency (Schreiber et al. 1986; Falkowski 1992), and, in turn, for describing the effects of nutrition on photosynthetic performance of phytoplankton (Genty et al. 1989; Geider et al. 1993a; Kolber and Falkowski 1993; Babin et al. 1996a). Fluorescence measurements have the advantage of being rapid, sensitive, and minimally invasive. A particularly useful measure is the fluorescence-based maximum quantum yield of charge separation for PSII (F_v/F_m; List of Symbols and Abbreviations-xviii summarizes significant symbols). This measure is calculated from the ratio of maximal fluorescence (photosynthetic pathways saturated by light or blocked with an inhibitor) minus minimal fluorescence (determined using a non-actinic light source) over the maximal fluorescence, determined from a dark-adapted sample. However, the relationships between fluorescence patterns and N-limitation may not be as straightforward as some studies suggest. For example, Kolber et al. (1988) investigated five species of marine unicellular algae, representing three phylogenetic classes, and found that a fluorescence-based measure of photosynthetic quantum yield of PSII was high and constant for nutrient-replete cultures, regardless of irradiance, and was depressed for nitrogen-limited cultures grown in chemostats. Batch cultures starved of nitrogen similarly showed depression of fluorescence-based quantum yield (Cleveland and Perry 1987). If sensitivity of fluorescence-based quantum yield for PSII to N-stress holds for all growth

conditions and light levels, fluorescence can be used as a diagnostic for N-stressed growth of phytoplankton. However, Cullen et al. (1992b) showed that F_v/F_m, based on fluorescence with or without the addition of the photosynthetic inhibitor DCMU, was insensitive to N-limitation of growth rate for cultures of a neritic diatom in balanced growth. Subsequently, MacIntyre et al. (1997) demonstrated that F_V/F_m of the toxic dinoflagellate *Alexandrium tamarense* was not reduced when cultures were fully acclimated to N-limited growth. In this study, I examined the role of N-stress on phytoplankton physiology and its effect on F_v/F_m of unialgal cultures in controlled laboratory experiments. Two methods for measuring F_v/F_m were compared in order to test the generalization that maximum quantum yield of PSII is reduced under N-stress in steady-state (i.e. fully acclimated) cultures (Kolber et al. 1988). Starvation experiments with batch cultures were used to demonstrate the difference between N-limited and N-starved conditions and the effect of N-status on photosynthetic physiology.

2.3 Background

2.3.1 F_v/F_m as a proxy for maximum quantum yield of PS II

The relationship between fluorescence and photosynthesis (Figure 2.1 and assumptions below) is based on energy conversion theory and biophysical models (Butler 1978; Weis and Berry 1987; Genty et al. 1989; Owens 1991; Kolber and Falkowski 1993; Kroon et al. 1993; Lavergne and Trissl 1995). To use fluorescence parameters as a proxy for maximal quantum yield for PSII (F_v/F_m), three assumptions and several simplifications

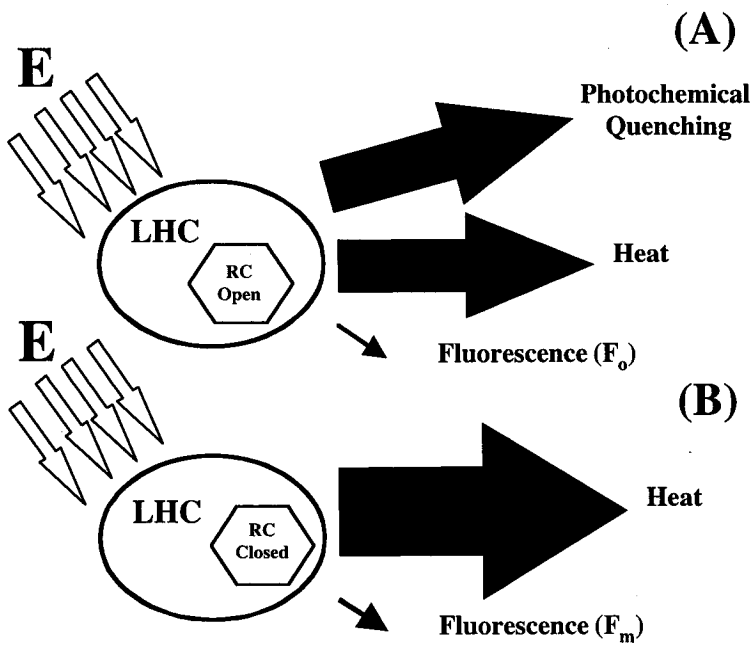

Figure 2.1 A schematic showing the interaction between fluorescence, heat, and photochemical quenching. (A) If the reaction centers (RC) are open, the incident irradiance (E) is absorbed by the light harvesting complex (LHC) where it is dissipated by fluorescence, heat and photochemical reactions. (B) If the reaction centers are closed, photochemical reactions cannot occur and the dissipation of the energy absorbed by the LHC is directed to heat and fluorescence exclusively. Area of the arrows represent the probability of energy transfer by the respective pathways for energy absorbed by the photosynthetic unit through to charge stabilization in PSII.

must be made (Schreiber et al. 1995). First, the sum of the three probabilities of photochemistry (Ψ_p), heat dissipation (Ψ_d) and fluorescence (Ψ_f) represents all possible energy fates:

$$\psi_p + \psi_d + \psi_f = 1 \qquad 2.1$$

Second, just after a saturating light pulse or treatment with an electron transport inhibitor (i.e. DCMU), when all the reaction centers are closed (subscript $_m$), the probability of photochemistry becomes zero:

$$(\psi_d)_m + (\psi_f)_m = 1 \qquad 2.2$$

Finally, the ratio between the quantum yield of fluorescence and the quantum yield for dissipation is constant (Schreiber et al. 1995), regardless of the physiological status of the cell:

$$\frac{\psi_d}{\psi_f} = \frac{(\psi_d)_m}{(\psi_f)_m} \qquad 2.3$$

Through algebraic manipulation of equation 2.2 and 2.3, $(\psi_d)_m$ can be replaced by 1 - $(\psi_f)_m$, and ψ_d can be expressed as $\frac{\psi_f}{(\psi_f)_m} - \psi_f$, so the probability of photochemistry can be expressed solely in terms of probability of fluorescence.

$$\psi_p = 1 - \psi_f - \left[\frac{\psi_f}{(\psi_f)_m} - \psi_f\right] = 1 - \frac{\psi_f}{(\psi_f)_m} = \frac{(\psi_f)_m - \psi_f}{(\psi_f)_m} \qquad 2.4$$

Knowing the relative increase in fluorescence allows quantification of an algal cell's ability to undergo photosynthetic processes, and changes in fluorescence yield can be attributed to the probability of photochemical energy conversion (Falkowski et al. 1986; Schreiber et al. 1986; Kiefer and Reynolds 1992; Schreiber et al. 1995). Fluorescence-based

measures of maximum quantum yield reflect the probability that PSII reaction centers will use the available excitation energy. Therefore, the quantum yield of fluorescence and the quantum yield of PSII (ϕ_{PSII}) should be inversely related (Butler and Kitajima 1975).

A problem with using fluorescence-based maximum quantum yield as an indicator of N-stress is the assumption that a constant relationship exists between ψ_d and ψ_f (Equation 2.3), the ratio between heat dissipation and fluorescence, regardless of conditions. Olaizola and Yamamoto (1994) showed changes in these ratios under light-saturated conditions and concluded a breakdown of the fundamental assumptions relating ψ_d, ψ_f and ψ_p (Equations 2.3 and 2.4). They attributed the departure from the linear relationship to non-photochemical quenching (NPQ). Dark acclimation of samples (> 30 minutes) minimizes the effects of NPQ, but the assumption of a constant ratio between dissipation as heat and fluorescence (Equation 2.3) may be an oversimplification of a complex relationship.

2.3.2 Nutrition and growth

Precise definitions help to focus discussions of the nutrition and growth of phytoplankton. When growth and photosynthesis of phytoplankton are not restricted by the supply of nutrients, growth conditions are considered nutrient-replete and growth rate is limited by irradiance and temperature (μ_{max}). Nutrient-replete conditions can be achieved using semi-continuous cultures, involving periodic addition of nutrients and

removal of algae at a rate consistent with the incorporation into biomass, thereby maintaining a relatively low biomass and high nutrient concentration.

Nutrient stress refers to both N-limitation and N-starvation. Nutrient limitation refers to balanced growth, where growth rate is determined by the rate of nutrient supply and the cells are fully acclimated to this restriction (Bannister and Laws 1980; Cullen et al. 1992b). During acclimated growth on light:dark cycles, growth is balanced over a photoperiod (Shuter 1979). Nutrient starvation refers to unbalanced growth during which the availability of a limiting nutrient decreases relative to the cellular demand so that the rates of photosynthesis and growth decline (Shuter 1979; Eppley 1981; Cullen et al. 1992b). The terms steady-state and acclimated growth are appropriate for conditions of N-limitation, while unbalanced and unacclimated growth refer to N-starvation. Although there are fundamental physiological differences between acclimated and unbalanced growth, the distinction between N-limitation and starvation is not always recognized. All conditions except for nutrient-replete growth can be considered nutrient stress.

Under batch-culture experiments, an essential nutrient can be provided in short supply so it is depleted from the medium and becomes limiting, resulting in unbalanced growth, altered physiological status, and eventual cessation of growth. Limiting nutrients, in this case nitrogen, influence the physiological status of the cell, including its photosynthetic efficiency and ability to react to environmental stresses. Falkowski (1992) showed that N-starvation is correlated to the decline of key reaction center proteins, leading to the inactivation of PSII reaction centers and changes in chemical composition.

Balanced growth can be achieved in continuous cultures where cells grow in an invariable environment with respect to nutrients and light. In these conditions, cells exhibit constant cellular compositions because carbon and nutrients are assimilated at identical cell-specific rates (Shuter 1979; Eppley 1981; Cullen et al. 1992b). Cyclostat cultures, allowing for light:dark cycles, will never truly be in steady-state because variations in growth rate and cellular constituents will occur over a photoperiod; but these cultures can be in acclimated growth, balanced over a 24 hour period. Nutrient-limited growth rate is determined by the rate of dilution of the culture with fresh media. Biomass is determined by the concentration of the limiting nutrient in the supply media. Sampling the cultures at the same time each day can minimize confounding signals from diel variations. Continuous culture systems allow for the investigation of nutrient effects on phytoplankton physiology by minimizing the uncertainties of changing growth rates and growth conditions associated with sampling batch cultures. Comparisons between cyclostat, chemostat, and batch culture can reveal different aspects of nutrient stress.

2.3.3 Conventional versus active fluorometry

Conventional fluorometers can be used to estimate F_v/F_m. These measurements can play an important role in probing physiological state, but they have the disadvantage of requiring an electron transport inhibitor (i.e. DCMU) for determination of maximal fluorescence yield, and thereby lose the ability to resolve important physiological parameters in situ under ambient light (Owens 1991). The body of knowledge on

phytoplankton fluorescence using inhibitors (Prézelin et al. 1977; Samuelsson and Öquist 1977; Cullen and Renger 1979; Roy and Legendre 1979; Neale et al. 1989) and the increasing number of experiments in which active fluorescence techniques are used (Falkowski et al. 1986; Schreiber et al. 1986; Genty et al. 1989; Oquist and Chow 1992; Kolber and Falkowski 1993; Babin et al. 1996a; Flameling and Kromkamp 1998) to determine different physiological parameters, depends on the validity of the methods for resolving fluorescence metrics. Disagreement among studies are difficult to resolve. The experiments described here allow a direct intercomparison between conventional and active fluorometers.

2.4 Materials and methods

2.4.1 General culture conditions

Semi-continuous, batch, and chemostat/cyclostat culture experiments were performed to determine the variability of F_v/F_m in cultures of a neritic diatom, *Thalassiosira pseudonana*, Clone 3H, provided by the Provasoli-Guillard National Center for Culture of Marine Phytoplankton (CCMP 1015). Triplicate cultures for each experimental treatment were grown under 40W Vita-lite full-spectrum fluorescent bulbs (Duro-test Canada Inc., Rexdale, Ontario, Canada) under a 12:12 light cycle, except for chemostat cultures and a set of nutrient-replete cultures grown under continuous light. Desired light levels were achieved using neutral density cellulose acetate screening (Lee Filters, Dartmouth, Nova Scotia, Canada) to reduce ambient light conditions.

Photosynthetically available radiation (μmol m^{-2} s^{-1}) was measured with a Biospherical Instruments Inc. (San Diego, CA) QSL-100 4π sensor. The temperature for all cultures was controlled at 20 ± 0.5°C and the chemostat/cyclostat samples were continuously mixed with magnetic stirrers and aerated with sterile air. Batch and nutrient-replete cultures were manually agitated daily. The medium was f/2 (Guillard and Ryther 1962), made from artificial seawater (Keller et al. 1987), modified by omission of all nitrogen sources. Nitrogen was added to the medium aseptically in desired concentrations (Table 2.1). Chemostat and semi-continuous cultures were set up to repeat the experiment of Kolber et al. (1988) using the same clone (3H) and growth conditions.

2.4.2 Growth conditions

Cultures were preconditioned on their respective light regimes for a minimum of two weeks prior to each experiment. Continuous cultures were grown under low nitrogen f/2 medium (50 μmol L^{-1}) prior to the experiments so that the physiological stress on the cultures investigated would be minimized.

Semi-continuous cultures were maintained in f/2 medium through many generations to study acclimated growth, replete in all nutrients. Cultures (2.5 L) were grown in triplicate in 4 L Erlenmeyer flasks for each treatment. They were diluted daily to maintain a constant cell concentration, and after acclimation, a constant maximal specific growth rate (μ_{max}). Chlorophyll concentrations did not exceed 150 mg chl m^{-3}. Data for

other semi-continuous experiments grown at different irradiance levels (Table 2.1) are from previously described experiments (Cullen et al. 1992b; Zhu et al. 1992).

Triplicate N-deficient batch cultures (2.5 L each) were grown in 4 L Erlenmeyer flasks and were maintained until the culture reached late senescence (26 d) to observe changes in physiological and cellular parameters. The cultures had an initial concentration of 150 μmol L^{-1} $NaNO_3$. Nutrient concentrations were monitored to ensure that nitrogen was the limiting resource and to show when nitrate was depleted.

Nitrogen starvation was also imposed by stopping flow of the medium in N-limited continuous cultures acclimated to different growth rates. Therefore, N-starvation experiments were conducted on both nutrient-replete cultures and N-limited acclimated cultures (Table 2.1).

Triplicate chemostat or cyclostat cultures were grown for a minimum of 10 generations allowing cells to acclimate to the N-limited conditions. It is important to stress the importance of pre-conditioning (light levels, nutrient concentration) of the cultures to facilitate physiological acclimation with minimal disruption. Chemostat cultures were grown under continuous light of 150 μmol quanta m^{-2} s^{-1}, while cyclostat cultures were grown at 55 and 350 μmol quanta m^{-2} s^{-1} (PAR) on a 12:12 light cycle (Table 2.1). Cultures (2.1 L) were grown in 2.5 L polycarbonate bottles. The growth rates of the chemostat cultures were predetermined by controlling the dilution rates (inflow/outflow of medium). The nitrogen source for the chemostat cultures was 75 μmol

$NH_4^+ L^{-1}$, while the cyclostat cultures were diluted with fresh medium containing 50 μmol $NO_3^- L^{-1}$. Data from other cyclostat experiments (Table 2.1) are from previously described experiments (Cullen et al. 1992b; Zhu et al. 1992) using essentially the same culturing methods.

2.4.3 Measurements

Routine sampling was conducted 3 h into the light period (10:00h) and included measures of chlorophyll concentration, cell size and cell concentration, nutrient concentration, dilution and overflow volumes and fluorescence as determined by Pulse Amplitude Modulation (PAM Schreiber et al. 1995) and DCMU methodology (Samuelsson and Öquist 1977). Cultures were sampled at the same time (± 30 min) to minimize effects of diel periodicity in algal physiological factors (Prézelin et al. 1977). Chlorophyll *a*, corrected for phaeopigments (Strickland and Parsons 1972), was measured using a Turner Designs (Sunnyvale, CA) fluorometer (10-005 R) calibrated with pure chlorophyll *a* (Sigma Chemical Co., St Louis, MO). Duplicate volumes of 1 mL each were filtered on Whatman GF/F filters (Whatman Inc., Clifton, NJ) and extracted in 10 mL of 90% acetone in the dark at –15°C for at least 24 h. Cell size and concentration were determined on diluted triplicate samples using a Coulter Multisizer II Particle Analyzer (Coulter Electronics of Canada, Ltd., Burlington, Ontario, Canada) calibrated with latex beads. Concentrations of NO_3^- and NH_4^+ were determined from filtered (0.22 μm) samples of culture medium by a Technicon II Autoanalyzer (Technicon Co., Tarrytown, NY)

(Grasshoff et al. 1976). Ammonium concentration was determined for chemostat cultures only. The overflow volumes and dilution rate for chemostat and cyclostat cultures were measured on a daily basis. For semi-continuous cultures, growth rate (μ, d^{-1}) was determined using the exponential growth equation to describe changes in cell concentration (N, cells mL^{-1}), accounting for dilution (D) (volume fresh medium/total volume) over a discrete period of time (ΔT, d):

$$\mu = \frac{1}{\Delta T}\left(\ln \frac{[N_{T+\Delta T}]/(1-D)}{[N_T]}\right) \qquad 2.5$$

For fluorescence measurements, samples from each culture were dark-adapted for 30 minutes. For the DCMU methodology, fluorescence was measured on triplicate 10 mL samples, before and 30 seconds after the addition of 50 µL of 3 mM DCMU in ethanol. To test if the initial light levels within the fluorometer were high enough to close reaction centers, thereby violating the assumption for measurement of F_o, neutral screening (cellulose acetate: 60% transmission) was placed around the cuvettes and fluorescence was measured on a parallel set of sub-samples for comparison. PAM fluorescence measurements employing the PAM101/102/103 system (Walz, Effeltrich, Germany) with a photomultiplier tube (PMT) accessory as well as the emitter-detector-cuvette assembly (ED101) were done on duplicate samples. The digital signal was recorded using Labview 4.0 (National Instruments, Austin, TX). Minimal fluorescence (F_o) was measured using a light emitting diode delivering a modulated measuring light beam (λ = 650nm), too weak to induce reaction center closure. For the measurement of maximal fluorescence (F_m), a

Table 2.1 A summary of all the experiments performed, with the initial nutrient concentrations, light levels, growth rates, maximal growth rates and duration of the individual experiments. Cultures were grown under 12:12 light dark cycles, unless otherwise indicated.

Type of Experiment	Initial N levels (μmol L^{-1})	Irradiance (μmol m^{-2} s^{-1})	μ (d^{-1})	μ_{max}[B] (d^{-1})	Duration (Days)
BALANCED GROWTH					
Batch: N-Starvation	150 (NO_3^-)	350	Variable	1.5	26
N-Starvation of	<0.2 (NO_3^-)	350	Variable (Initial=0.8)	1.5	7
N-limited	<0.2 (NO_3^-)	350	Variable (Initial=0.4)	1.5	7
Continuous Cultures	<0.2 (NH_4^+)[A]	150	Variable (Initial=0.3)	1.78	5
	<0.2 (NO_3^-)	55	Variable (Initial=0.4)	0.7	7
	<0.2 (NO_3^-)	55	Variable (Initial=0.2)	0.7	7
BALANCED GROWTH					
Semi-Continuous	880 (NH_4^+)[A]	150	1.78	1.78	15
(N-replete)	880 (NO_3^-)[C]	9	0.05	0.05	36
	880 (NO_3^-)[C]	25	0.38	0.38	20
	880 (NO_3^-)[C]	50	0.67	0.67	12
	880 (NO_3^-)[C]	75	0.85	0.85	8
	880 (NO_3^-)[C]	100	0.97	0.97	12
	880 (NO_3^-)[C]	200	1.33	1.33	9
	880 (NO_3^-)[C]	410	1.56	1.56	6
	880 (NO_3^-)[C]	912	1.82	1.82	6

Table 2.1 (Continued)

Chemostat	75 (NH_4^+)[A]	150	0.30	1.78	26
(N-limited)					
Cyclostat	50 (NO_3^-)	350	1.20	1.50	34
(N-limited)	50 (NO_3^-)	350	0.80	1.50	35
(PAM and DCMU)	50 (NO_3^-)	350	0.40	1.50	35
	50 (NO_3^-)	350	0.40	1.50	35
	50 (NO_3^-)	55	0.43	0.71	37
	50 (NO_3^-)	55	0.21	0.71	35
Cyclostat[C]	50 (NO_3^-)[A]	75	0.13	0.85	15
(N-limited)	50 (NO_3^-)[C]	75	0.35	0.85	11
(DCMU only)	50 (NO_3^-)[C]	75	0.56	0.85	15
	50 (NO_3^-)[C]	75	0.61	0.85	25
	50 (NO_3^-)[C]	200	0.20	1.33	32
	50 (NO_3^-)[C]	200	0.43	1.33	26
	50 (NO_3^-)[C]	200	0.59	1.33	13
	50 (NO_3^-)[C]	200	0.84	1.33	25
	50 (NO_3^-)[C]	200	1.11	1.33	17

A - 24 hour light cycle

B - Growth rate in nutrient-replete semi-continuous culture at the same irradiance

C - Data from previously described experiments of Zhu et al. (1992) and Cullen et al. (1992)

minimum of 16 saturating pulses (Schott KL1500-E; E > 5000 μmol m^{-2} s^{-1}) each of 600 ms duration were delivered at 30 s intervals. The interval between saturation pulses allows for reoxidation of the reaction centers. Investigation into the duration, intensity and time between saturation pulse was performed to ensure the proper settings on the PAM fluorometer (data not shown).

2.5 Results

2.5.1 Comparison of measurement systems

Two independent fluorescence measurement systems were compared for describing F_v/F_m of cultures under nutrient-replete, N-starved and N-limited growth conditions. Comparison between PAM fluorometry (active) and DCMU methodology (conventional) showed a strong positive linear correlation ($R^2 = 0.63$, $P < 0.001$, $n = 460$), although departure from a one-to-one relationship was apparent (slope = 0.79 ± 0.03 (95% CI)) and deviations for the individual experiments grown under varying light levels was observed (Figure 2.2A). F_v/F_m measured by conventional fluorometry using DCMU was lower than when measured with PAM for cultures grown in low irradiance (< 150 μmol m^{-2} s^{-1}) (Figure 2.2B).

Neutral density screen was used to reduce excitation irradiance from the Turner Designs fluorometer for cultures grown at 55 μmol m^{-2} s^{-1}. This eliminated the artifactually low F_v/F_m, due to actinic (able to induce photochemical reactions and close

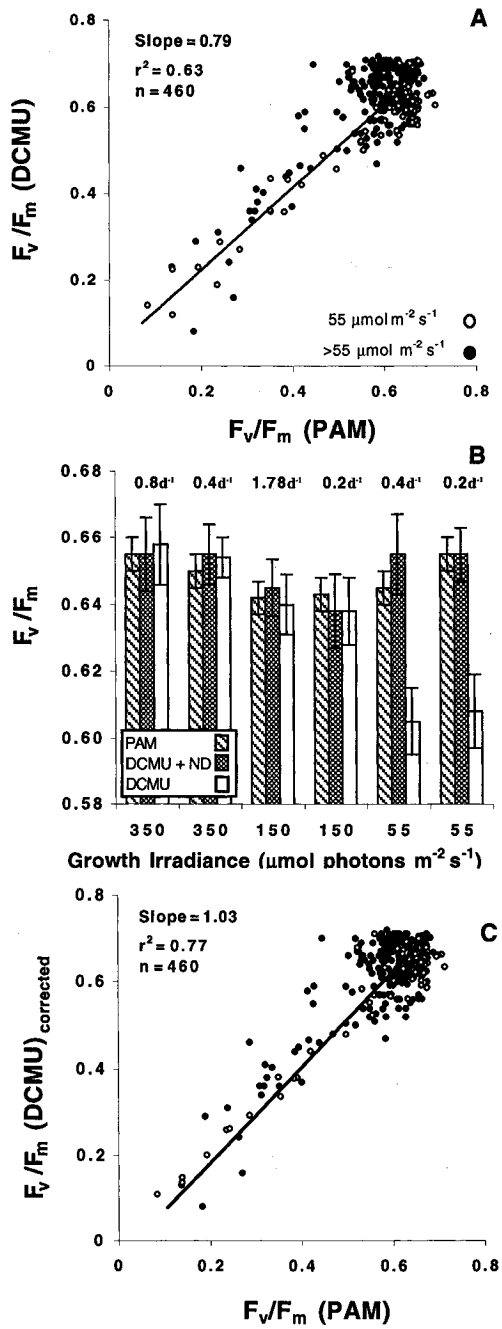

Figure 2.2 Comparison between active fluorometry (PAM) and fluorometry determined by DCMU methodology. (A) F_v/F_m determined with PAM vs. DCMU (no neutral density screen) for different growth conditions and light levels from Table 2.2 (n = 460). Although the relationship shows agreement, clusters are apparent for low light cultures (55 µmol m^{-2} s^{-1} = O). (B) F_v/F_m for acclimated cyclostat cultures of *Thalassiosira pseudonana* at different growth irradiance and different N-limited growth rates for the PAM (▨) and DCMU methodology with 60% neutral density screening (▩) and without 60% neutral density screening (□). Means ± SD for three replicates. Correction of the method through the use of neutral density screening around the cuvettes was necessary for cultures grown under low light to prevent closing of reaction centers and overestimation of F_o. (C) Comparison of the two fluorescence measurement systems when the corrected DCMU methodology is used (see text).

reaction centers) light closing reaction centers, thereby giving elevated values of F_o for low-light cultures. With this modification of the method, a much better agreement between DCMU and PAM methodologies was observed (Figure 2.2C): the regression line from this comparison explains 77% of the variance and shows a strong one:one agreement (slope = 1.03 ± 0.02 (95% CI)). A paired Student t-test identified no significant difference when neutral density screening was used in the measurement of F_v/F_m for acclimated and subsequently starved cultures grown under 150 μmol m^{-2} s^{-1} and 350 μmol m^{-2} s^{-1} ($P >$ 0.10, n = 144, F_v/F_m range = 0.11 - 0.73). Therefore, neutral density screen was used only for cultures grown at the lower irradiance.

2.5.2 F_v/F_m for nutrient-replete cultures

Triplicate semi-continuous cultures, replete in all nutrients and grown under continuous light (150 μmol m^{-2} s^{-1}), showed nearly identical growth rates (average of daily determinations; 1.78 d^{-1} ± 0.04 d^{-1} (± SE, n = 3), Figure 2.3). Measurements of F_v/F_m (PAM) during this time course were relatively high and changed little (0.60 ± 0.02 (± SE, n = 45)) (Figure 2.3A), consistent with previous studies of F_v/F_m in nutrient-replete cultures. Estimates of F_v/F_m with DCMU (0.61 ± 0.03 (± SE, n = 45)) were nearly the same as with PAM, confirming the strong agreement between instruments.

For semi-continuous nutrient-replete cultures, grown on a 12:12 light:dark regime, growth rate (μ_{max}) was a saturation function of irradiance (Figure 2.3B). Using DCMU

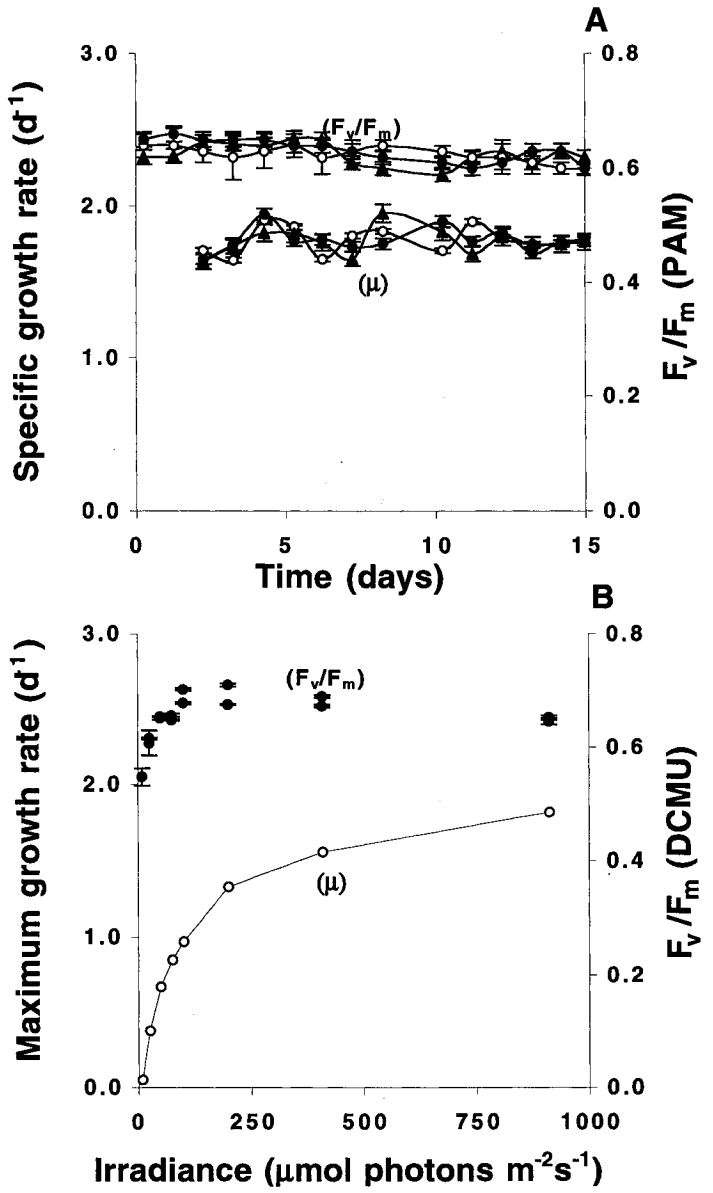

Figure 2.3 (A) Specific growth rate as a function of time (lower points) for NH_4^+ replete cultures of *Thalassiosira pseudonana* grown under 150 μmol $m^{-2}s^{-1}$ continuous light. Growth rate was determined at daily intervals (ΔT = 1d) using equation 2.5. The upper points show F_v/F_m determined from active fluorometry (PAM) over the same time-course. The symbols represent triplicate cultures and error bars represent standard error. (B) μ_{max} and F_v/F_m, determined from a conventional fluorometer (DCMU methodology), as a function of irradiance for nutrient-replete cultures grown under a 12:12 light regime. Actinic light from the fluorometer was not reduced, so the slight decline of F_v/F_m for low-light cultures may be an artifact as described in Figure 2.2. Means ± SE for three replicate cultures.

methodology, F_v/F_m remained consistently high (~ 0.65) for all growth irradiances tested except for decreases in F_v/F_m at low irradiances (< 150 μmol m^{-2} s^{-1}), which can be attributed to underestimation due to the artifact for low-light adaptation that was subsequently identified (Figure 2.2).

2.5.3 F_v/F_m during N-starvation

For N-starved cultures, reduced F_v/F_m and growth rate as determined from cell concentration and fluorescence measurements were apparent after nitrogen was depleted (Figure 2.4). For the N-starved batch experiment, routine measures showed cultures under unbalanced growth conditions and showed a reduced F_v/F_m as a function of N-starvation (Figure 2.4). F_v/F_m determined by DCMU (Figure 2.4C) agreed well with F_v/F_m determined by PAM for batch cultures ($R^2 = 0.91$, $n = 150$).

Starvation was also imposed on the N-limited continuous cultures by stopping the inflow of nutrients into the system. When the cultures were perturbed by turning off the pump, F_v/F_m of the previously acclimated algal cultures declined as a function of both time without nutrient supply and pre-conditioned N-limited growth rate (Figure 2.5). The rate of decrease of F_v/F_m, was determined from linear regression for the final four days of each nitrate-starvation experiment (triplicate cultures at four growth rates). The slopes varied little (mean = -0.09 ± 0.02 d^{-1} (± SE, $n = 12$)), indicating that the decline of F_v/F_m was independent of N-limited growth rate preconditioning and irradiance level.

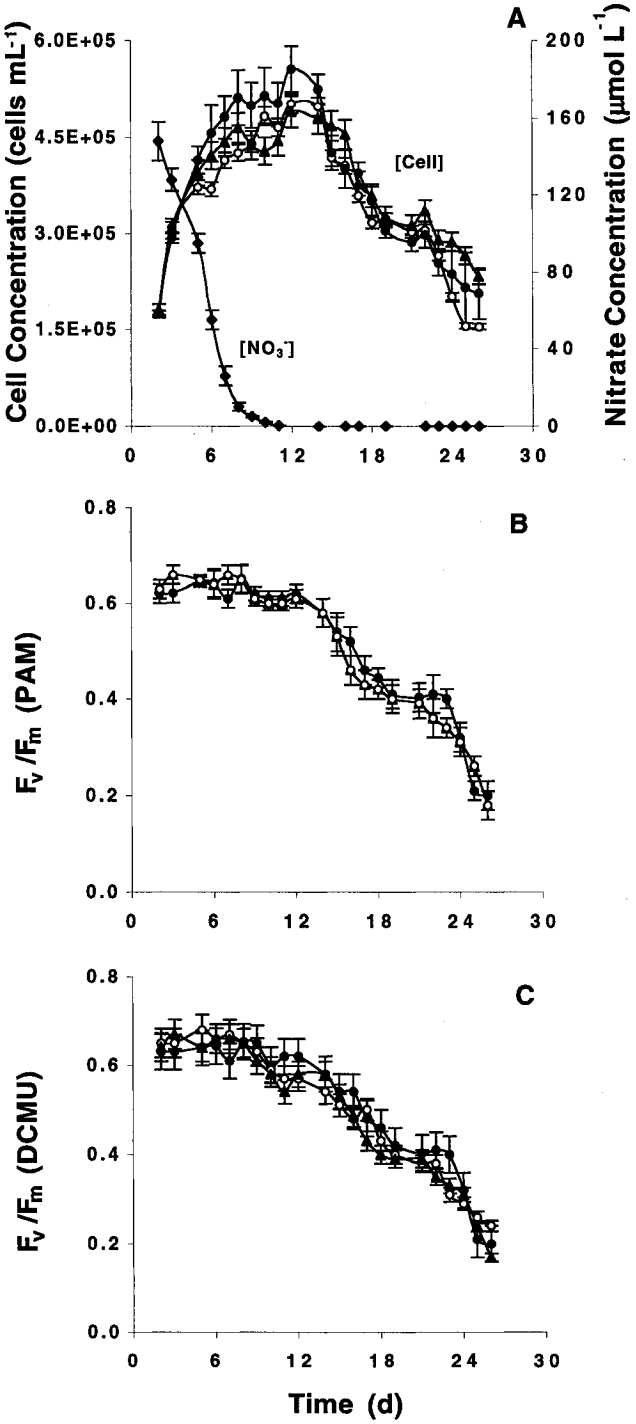

Figure 2.4 (A) Cell concentration and ambient nitrate concentration (symbol = ◆) as a function of time for *Thalassiosira pseudonana* batch cultures (350 µmol m^{-2} s^{-1} PAR), while F_v/F_m for the same triplicate cultures is shown as a function of time as measured with active fluorometry (PAM) (B), and DCMU methodology using a conventional fluorometer (C). Means ± SE for three replicates for all three graphs. Nitrate concentrations with values below detection limit (< 0.1 µM) are represented with a zero value. Nitrate data represent means ± SD of triplicate cultures.

Cultures that were previously acclimated to lower N-limited growth rates had a shorter time interval before the decline of F_v/F_m during N-starvation compared to higher N-limited growth rates (Figure 2.5). For each culture, changes in F_v/F_m for the five days prior to the termination of nutrient flow and three days after were analyzed by repeated measures ANOVA. No significant difference in F_v/F_m through time was observed prior to imposed N-starvation, although significant declines were detected after termination of nutrient supply. The time of onset of the decline in F_v/F_m was determined *post hoc* using a least squares means comparison to find the first sample with significantly lower F_v/F_m. Significant declines in F_v/F_m were evident at 0.5 ± 0.2 d (mean ± SE, $n = 3$) after imposed N-starvation for both the $\mu/\mu_{max} = 0.26$ and $\mu/\mu_{max} = 0.29$ cultures, while cultures previously acclimated to $\mu/\mu_{max} = 0.53$ and 0.60 showed an onset of F_v/F_m decline at 1.0 ± 0.5 and 2.0 ± 0.5 d respectively (Figure 2.5A, B). Cultures grown replete for nutrients ($\mu/\mu_{max} = 1.0$; initial nitrate concentration 880 μmol L^{-1}) showed no decline in F_v/F_m when replenishment of the medium was stopped for 4 days. The NH_4^+-limited 0.17 μ/μ_{max} cultures, grown under continuous light, showed the most rapid onset of the decline of F_v/F_m (0.4 ± 0.2 d, $n = 3$) (Figure 2.5C). In other words, the start of the decline of F_v/F_m was related to the N-limited pre-conditioning, although the rate of decline, once it began, was independent of pre-conditioning. Consequently, F_v/F_m four days after interruption of the nutrient supply is a strong function of N-limited growth rate at the time of the interruption (Figure 2.5C). The assumption of normality underlying ANOVA was tested for in each analysis using a G-test at $\alpha = 0.10$.

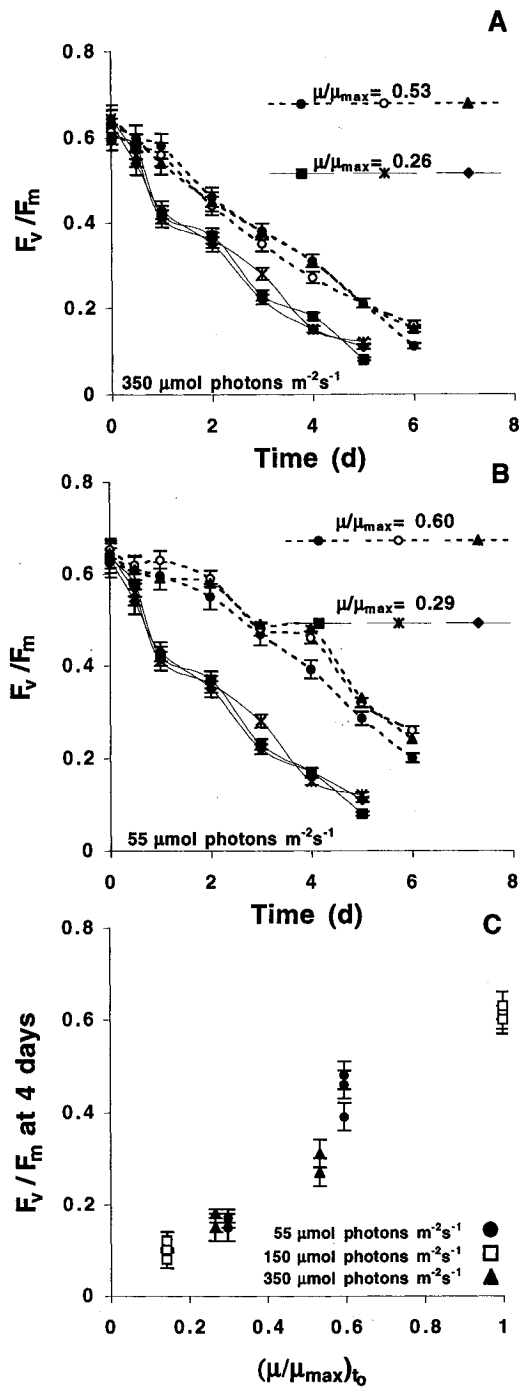

Figure 2.5 Nutrient starvation for cultures previously acclimated to nitrate-limited growth. F_v/F_m as a function of the duration of nutrient stress defined as the time after the flow of nutrients is stopped (Time = 0) for four different pre-conditioned nutrient-limited relative growth rates at two different growth irradiances: (A) 350 μmol m^{-2} s^{-1} (μ_{max} = 1.50 d^{-1}) and (B) 55 μmol m^{-2} s^{-1} (μ_{max} = 0.71 d^{-1}). Error bars show SD of triplicate cultures. (C) F_v/F_m, determined from PAM fluorometry, as a function of nutrient-dependent relative growth rate for perturbed continuous cultures, 4 days after the flow of nutrients was stopped for three different irradiances (● = 55 μmol m^{-2} s^{-1}, ▲ = 350 μmol m^{-2} s^{-1}, □ = 150 μmol m^{-2} s^{-1}). The points for μ/μ_{max} = 1.0 represent nutrient replete semi-continuous cultures for which replacement of medium was stopped at time zero (t_o). Means ± SE for three replicate cultures.

2.5.4 F_v/F_m under acclimated N-limitation

When chemostat and cyclostat cultures were acclimated to N-limitation, F_v/F_m was maximal (~ 0.65) for the range of light intensities investigated (Figure 2.6). Both the fluorescence measurement systems (PAM and DCMU) provided similar evidence for F_v/F_m being independent of both irradiance and acclimated, N-limited growth rate (Figure 2.6) for all balanced growth experiments conducted in the current study and previous experiments (Cullen et al. 1992b; Zhu et al. 1992) (Figure 2.6B). This contradicts the findings of Kolber et al. (1988), who showed that F_v/F_m was dependent on the degree of N-limitation in chemostats (Figure 2.6A).

Acclimation of the cultures was determined by constancy from day-to-day of cell concentration, cell size, chlorophyll, ambient nutrient concentrations, and fluorescence. Steady-state was assumed when several parameters (i.e. chlorophyll, fluorescence, cell and nutrient concentration) remained constant (± 10%) over a three-day period (Figure 2.7). Figure 2.7 shows only the chlorophyll and fluorescence parameters over the duration of three representative experiments at the different growth irradiances, while cell concentration and nutrient concentrations also played a role in determining status of the algal growth conditions being investigated (data not shown). It is clear that physiological changes can proceed for many days (7-14) before acclimation is achieved.

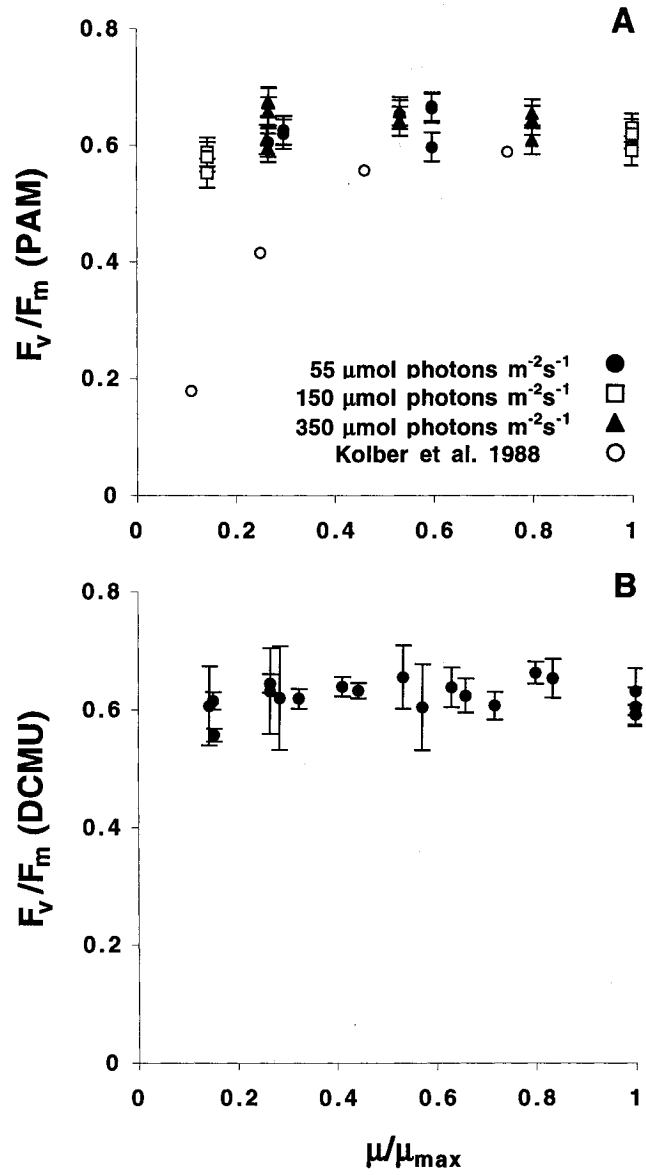

Figure 2.6 (A) F_v/F_m determined from active fluorometry (PAM) under balanced growth conditions for a range of nutrient-dependent growth rates and growth irradiance (● = 55 µmol m^{-2} s^{-1}, □= 150 µmol m^{-2} s^{-1}, ▲ = 350 µmol m^{-2} s^{-1}). Estimates of F_v/F_m from the findings of Kolber et al. (1988), who reported F_v/F_o measured with a Pump and Probe fluorometer on *Thalassiosira pseudonana* (3H), are shown for comparison (symbol = O). (B) F_v/F_m determined by conventional fluorometry (DCMU methodology, no neutral density screen) for continuous cultures grown at different irradiances and N-limited growth rates. Data from previous experiments (Cullen et al. 1992 and Zhu et al. 1992). Mean ± SE for three replicates.

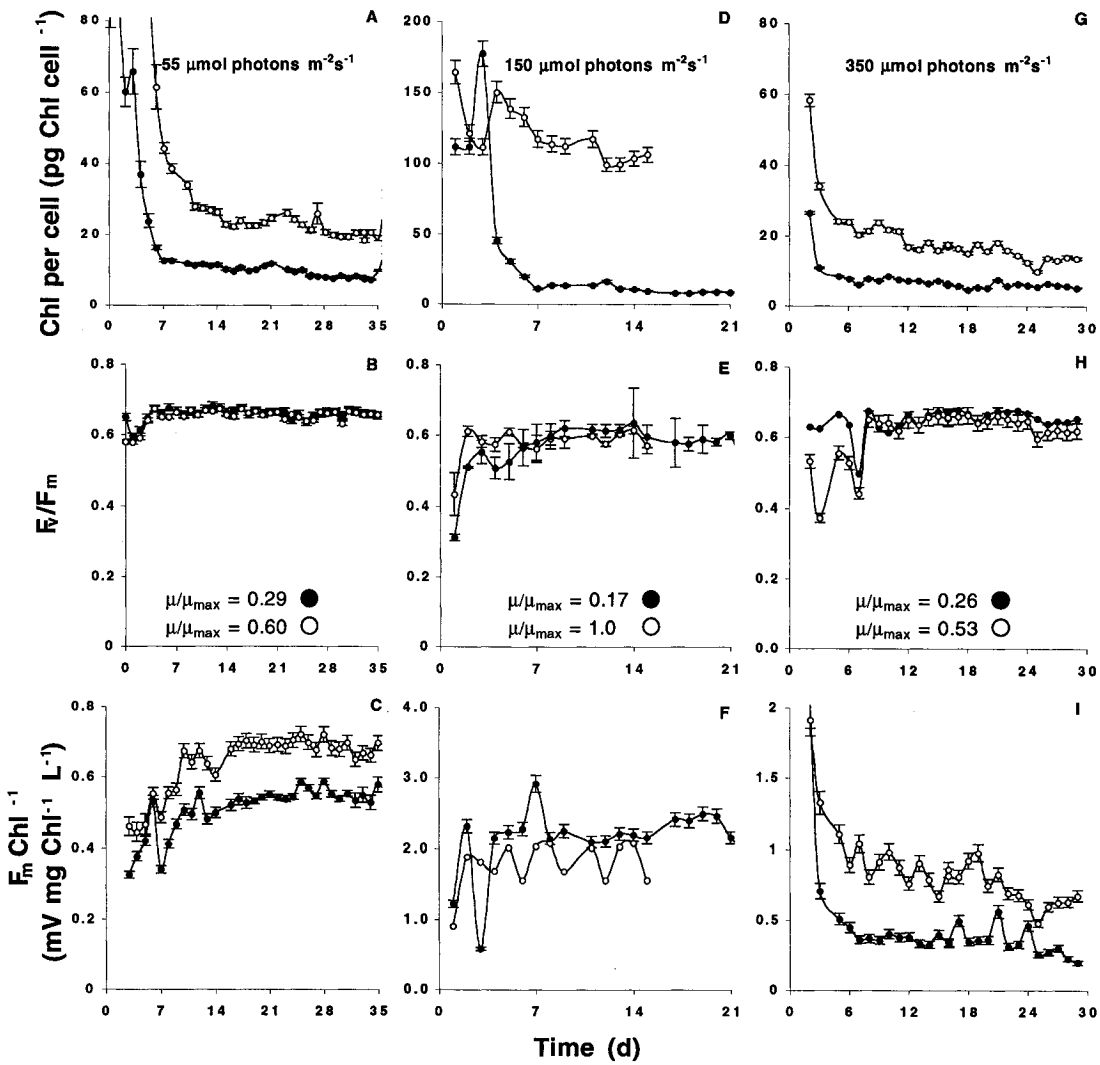

Figure 2.7 Physiological parameters of *Thalassiosira pseudonana* as a function of time for determining balanced growth conditions. Representative cultures grown under low nutrient-limited growth rates (●) and high nutrient-limited growth rates (O) for different irradiance levels: 55 µmol m^{-2} s^{-1}, with growth rates of 0.43 and 0.21 d^{-1} (A-C), 150 µmol m^{-2} s^{-1}, with growth rates of 1.0 and 0.17 d^{-1} (D-F), 350 µmol m^{-2} s^{-1}, with growth rates of 0.80 and 0.40 d^{-1} (G-I)). Parameters shown as a function of time include changes in chl per cell, F_v/F_m and F_m per unit chl. Means ± SE for three replicate cultures.

2.6 Discussion

Results from experiments on N-starved batch and nutrient-replete semi-continuous cultures support the established body of evidence that F_v/F_m can be used as a diagnostic of N-stress. However, this research also shows that this fluorescence metric is insensitive to N-limitation when cultures are fully acclimated to N-stressed conditions. This result conflicts with previously published work on cultures grown in continuous cultures identified as being in steady-state (Kolber et al. 1988). Possible reasons for this discrepancy may be due to instrumentation or growth conditions.

2.6.1 PAM vs. DCMU methodology

The possibility exists that differences in methodology could explain the fundamental contrast between our results using PAM and DCMU, and the results of Kolber et al. (1988) who used a Pump and Probe measurement system (Falkowski et al. 1986). While the results show a strong positive correlation between the PAM and the DCMU methodology, no direct comparison between the PAM fluorometer and the Pump and Probe system was done. Geider et al. (1993a) showed a significant correlation between measurements of F_v/F_m from the Pump and Probe fluorometer and from a Turner Designs fluorometer using DCMU, both in the laboratory ($R^2 = 0.613$, $n = 28$) and during a cross-shelf transect in the Western North Atlantic ($R^2 = 0.637$, $n = 24$). Since this research shows a strong correlation between the Turner Designs fluorometer (DCMU

methodology) and the PAM system, and Geider et al. (1993a) show agreement between the Turner Designs and the Pump and Probe system, I conclude that the fundamental differences in results (Figure 2.6A and 2.8) are not likely due to instrumentation.

I have not conducted a detailed comparison of methods for measuring F_v/F_m and I do not assert that any one method is "best". This study shows that fundamental patterns in F_v/F_m as functions of nutrition can be reproduced by two methods (PAM and DCMU) and that differences between these and other studies is not likely due to differences in methodology.

Measurement of F_v/F_m with a conventional fluorometer and DCMU is convenient, relatively inexpensive and easy, with a wide range of past and future ecophysiological applications (Cullen and Renger 1979; Neale et al. 1989; Krause and Weis 1991; Geider et al. 1993a). I show that the method compares well to the more sophisticated PAM approach when an artifact for cultures grown under low-light is avoided through reduction of excitation irradiance (Figure 2.2). This artifact is created by increased light sensitivity of the algae due to a physiological adaptation of increased chlorophyll concentration per cell, and likely increased chlorophyll per photosystem, for cultures grown under low-light. Harris (1978) states that the low energy source from the Turner Designs fluorescence measurement system would not create the artifact of elevated initial fluorescence, although the studies did not include low-light adapted cultures. Further supporting evidence for an actinic light artifact for conventional fluorometers comes from the semi-continuous experiments, which showed a reduction in F_v/F_m for cultures grown under low-light conditions using the conventional measurement system (Figure 2.3). Once

the artifact is eliminated, the regression line explains 77% of the variance (Figure 2.2). I conclude that conventional and active fluorometry can be used interchangeably to assess fluorescence-based measurements of maximal quantum yield, if excitation energy in the fluorometer is reduced to ensure that reaction centers are not significantly closed by the measurement system.

2.6.2 F_v/F_m for nutrient-replete cultures

My findings on nutrient-replete cultures support the current literature (Kolber et al. 1988; Falkowski and Kolber 1995) that under semi-continuous exponential growth conditions the fluorescence-based measure of maximum quantum yield for PSII (F_v/F_m) remains maximal and constant and is insensitive to irradiance levels (Figure 2.3). This result is not novel and only serves to increase the growing body of evidence that F_v/F_m is not sensitive to growth irradiance for cultures grown under nutrient-replete conditions.

2.6.3 F_v/F_m during N-starvation

The batch culture experiment showed that under N-starved conditions, F_v/F_m declined, reflecting the degree of N-stress (Figure 2.4). After the cell has utilized its stores and is in a state of N-starvation, the culture will show adverse physiological effects (Cleveland and Perry 1987; Falkowski and Raven 1997; Berman-Frank and Dubinsky 1999). Once essential cellular components can not be synthesized and balanced growth

conditions have been perturbed for days, fluorescence-based maximal quantum yield for PSII is significantly reduced. The results from the batch culture experiments contribute to the established body of evidence that maximal quantum yield is a good indicator of N-starvation (Cleveland and Perry 1987; Geider et al. 1993a; Falkowski and Raven 1997).

This research also reports that the reduction in fluorescence-based maximal quantum yield as a consequence of starvation is also a function of the pre-conditioned N-dependent growth rates (Figure 2.5). The onset of the decrease in F_v/F_m occurred more rapidly in the cultures previously acclimated to lower N-limited growth rates. These findings show that phytoplankton experiencing lower N-limited growth rates would be more susceptible to interruptions in nutrient supply in the laboratory or the field, consistent with the decline of F_v/F_m being related to depletion of cellular stores.

2.6.4 F_v/F_m under acclimated N-limitation

Results for chemostat and cyclostat cultures at multiple light intensities and growth rates show that under fully acclimated growth a constant fluorescence-based maximum quantum yield for PSII is obtained (Figure 2.6). This is contradictory to the study of Kolber et al. (1988), which showed reduced fluorescence-based maximal quantum yield as a function of N-limited relative growth rate (Figure 2.8). I tried to replicate the experiments of Kolber et al. (1988), but I did not have the same measurement system. Nevertheless, I minimized this discrepancy by utilizing two independent measurement systems and giving strict adherence to steady-state criteria. I hypothesize

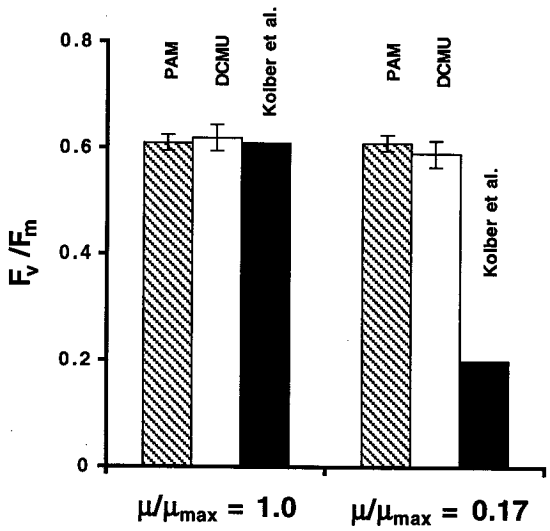

Figure 2.8 Comparison of F_v/F_m determined during this study and in the study of Kolber et al. (1988) for both nutrient-replete (μ/μ_{max} = 1.0) and ammonium-limited (μ/μ_{max} = 0.17) steady-state cultures. Two independent measurement systems, PAM and DCMU methodology using a conventional fluorometer (means ± SE for three replicates), were compared to F_v/F_m determined using a Pump and Probe fluorometer by Kolber et al. (1988). Those values are obtained from graphical representation and may not be exact.

that disparate results may be attributed to the attention given to ensure that balanced growth conditions for all N-limited growth rates were achieved (Figure 2.7). Kolber et al. (1988) sampled cultures 7 days into the chemostat experiment, which may not provide sufficient time for the cultures to acclimate to their N-dependent growth rate. Pre-conditioning the algal cultures to their growth irradiance and nutrient concentrations, and waiting a minimum of 10 generations for the cultures to acclimate was done in these experiments. Nutrient-interruption experiments and daily monitoring showed that slower growing N-stressed cultures are more susceptible to perturbations and slower to reach and maintain acclimated growth. Therefore, scrutiny of different physiological indicators of acclimated balanced growth, especially at low growth rates, is important in studies of cultures in steady-state growth.

Zhu et al. (1992) reported a constant fluorescence ratio for most N-limited relative growth rates, which supports my findings. The ratio broke down in their batch cultures similar to my experiments, which is shown in their paper as a relative growth rate of zero. Zhu et al. (1992) show a decreased ratio of enhanced fluorescence to initial fluorescence (F_m/F_o) for the lowest relative growth rate (~ 0.15) in the continuous culture for the low-light cultures (75 μmol m^{-2} s^{-1}). This result might be due to the overestimate of initial fluorescence by the Turner Designs measurement system in low-light adapted cultures. Further evidence of a high and constant F_v/F_m under N-limitation was reported by MacIntyre et al. (1997) for a dinoflagellate, *Alexandrium tamarense* grown in semi-continuous culture. This support for my findings also emphasizes a limitation of my

study. The results are limited to one coastal species, and the investigation of F_v/F_m as a function of N-stress for other species, including oceanic isolates, is still required.

2.6.5 F_v/F_m as a diagnostic of N-stress

Cleveland and Perry (1987) and Kolber et al. (1988) provided evidence that F_v/F_m can be used as an indicator of N-stress, showing reductions under nitrogen starvation and limitation respectively. Graziano et al. (1996) and Geider et al. (1993a) support this hypothesis of reduced F_v/F_m being an indicator of N-stress in the field. However, the conclusions of Graziano et al. (1996) may relate primarily to growth conditions of a eutrophic environment at the final sampling station (station 8), since no other oligotrophic stations sampled (stations 1-7) showed significant correlation between nutrients, determined by nutrient addition experiments, and the fluorescence-based measure of maximum quantum yield (F_v/F_m). Babin et al. (1996a) provided further support for the role of nitrogen stress in reducing maximum quantum yield of carbon fixation $(\phi_C)_m$, but also identified co-varying factors such as the contribution of non-photosynthetic pigments to reduce maximum quantum yield. Kolber et al. (1990) and Babin et al. (1996a) have shown patterns of fluorescence suggestive of N-stress in nature. However, my results suggest that, using F_v/F_m as a diagnostic, it is difficult to assess whether some natural populations are in acclimated N-limitation. The literature supports a dynamic environment hypothesis in which true balanced growth is never really achieved (Richerson et al. 1970; Harris 1978; Harris 1980; Falkowski and Raven 1997), although a

biological system will tend towards a steady-state condition and may be expected in some conditions to be nearly balanced (Shuter 1979; Eppley 1981). Thus if N-limitation persists in nature, a degree of balanced growth is probable, causing uncertainty in F_v/F_m as an indicator of the degree of N-stress.

2.7 Summary and conclusions

In summary, two independent fluorescence measurement systems, PAM fluorometry (active) and DCMU methodology (conventional), showed a strong 1:1 correlation when the DCMU method was corrected for over-excitation of minimal fluorescence for cultures grown under low light. These independent systems provide evidence that under nutrient-replete growth conditions, F_v/F_m for the neritic diatom *Thalassiosira pseudonana* (3H) is high and independent of growth irradiance, while during N-starvation F_v/F_m declines and is correlated to time spent without nutrients. These findings are consistent with the current literature. When N-starvation was imposed on acclimated N-limited cultures, the onset of the decline of F_v/F_m was a function of preconditioned N-limited growth rate, although the subsequent rate of decline of F_v/F_m was independent of preconditioned N-limited growth rates. This suggests that F_v/F_m is more susceptible to perturbations in nutrient supply for phytoplankton with lower N-limited growth rates. In contrast to published results, F_v/F_m remained high and constant (~ 0.65) for my acclimated steady-state cultures at different nitrogen-limited growth rates,

independent of growth irradiance. This result should be verified for a range of species isolated from different environments.

I conclude that fluorescence-based maximal quantum yield for photosystem II is not a robust diagnostic for all N-stressed conditions. It is a sensitive indicator of N-stress during unbalanced growth, but when phytoplankton are acclimated to N-limitation, the relationship between F_v/F_m and N-stress breaks down. This limits the utility of F_v/F_m as a measure of phytoplankton physiological status in the laboratory and the field.

Chapter 3

A new diagnostic tool using fluorescence for determining relative electron transport and non-photochemical quenching as a function of irradiance in phytoplankton cultures

3.1 Chapter overview

A new measurement system, amalgamating a PAM fluorometer and a light incubation chamber assembly, was used to determine the temporal changes in relative electron transport and non-photochemical quenching (NPQ) at different irradiance levels for nutrient-replete unialgal cultures of the neritic diatom, *Thalassiosira pseudonana*. Strong agreement with measurements determined from ^{14}C incubations and relative electron flow (from irradiance and a fluorescence-based quantum yield term, $\Delta F/F_m'$) was observed. Nutrient-replete cultures grown under 150, 350, and 1000 μmol m^{-2} s^{-1} showed significant changes in fluorescence parameters, such as the parameter of light saturation (E_{KF}), and the degree of NPQ as a function of growth irradiance. This new measurement tool may elucidate the effect of physiological stress conditions (i.e. supra-saturating irradiance, N-starvation and limitation, and temperature) on an algal population and provide a rapid

non-invasive measurement of relative photosynthetic efficiency and changes in quenching mechanisms.

3.2 Introduction

Photochemical processes (i.e. photosynthesis) compete with fluorescence and heat (dissipation processes) for the radiant energy absorbed by phytoplankton. Any changes in the relative fluxes for these pathways will affect the transfer of energy to photosynthesis and dissipation processes, including fluorescence (Butler 1978; Prézelin 1981; Krause and Weis 1991; Parkhill et al. 2001). Under stressed conditions, photosynthetic efficiency of an algal population is reduced due to alterations in the light harvesting complex and photosynthetic reaction centers and pathways; therefore changes in the physiological status of phytoplankton are reflected by changes in fluorescence measurements (Falkowski and Kolber 1993). Because fluorescence yield is roughly proportional to the amount of pigment, and light-induced changes of fluorescence can be related to photochemical efficiency, parameters derived from measurements of fluorescence can be used as indicators of algal biomass and physiological state and stress conditions (i.e. nutrients and temperature)(Kiefer 1973; Krause and Weis 1991; Chamberlin and Marra 1992; Falkowski and Raven 1997).

In aquatic science, fluorescence metrics have been used to estimate the maximal quantum yield for PSII using the proxy F_v/F_m (Cullen and Renger 1979; Prézelin and Ley

1980; Geider et al. 1993a) (List of Symbols xviii summarizes significant symbols). This is determined by measuring the minimal (F_o) and maximal (F_m) fluorescence for a dark-adapted sample. In the dark, when all the reaction centers are open, the primary acceptors are oxidized, the yield of photosynthetic processes is maximal and both fluorescence and heat dissipation is minimal; relative fluorescence yield can be measured with a modulated measuring beam which does not deliver enough photons to cause significant reduction of reaction centers. A saturation pulse of very bright light induces maximal fluorescence yield, F_m, by closing all the reaction centers; when reaction centers are closed, the yield of photochemical processes is zero and both fluorescence and heat dissipation are maximal. Variable fluorescence, F_v (= F_m - F_o) is determined from those measurements (Chapters 1 and 2).

Maximum quantum yield for PSII, F_v/F_m, has been proposed as a diagnostic for N-stress in both batch cultures subjected to N-starvation (Cleveland and Perry 1987) and nitrogen-limited cultures in steady-state (Kolber et al. 1988), as well as in the field (Falkowski et al. 1992; Geider et al. 1993b; Greene et al. 1994). These studies show that reduced F_v/F_m reflects N-stress; the metric is unaffected by light once dark adaptation of the sample has been accomplished. The accuracy of this parameter as a diagnostic tool for N-stress has been questioned (Cullen et al. 1992b; Olaizola et al. 1996; Parkhill et al. 2001). Olaizola et al. (1996), found no relationship between nutrient concentration and F_v/F_m in the North Atlantic Ocean, while Parkhill et al. (2001) showed that the relationship between N-stress and measurements of F_v/F_m broke down under acclimated steady-state growth conditions in the laboratory. Chapter 2 shows this result; fully

acclimated N-limited diatoms have a high F_v/F_m regardless of growth rate. Since F_v/F_m may not be a good indicator of physiological stress under all conditions, the search for another or complementary fluorescence metric should continue (Wood and Oliver 1995).

In this chapter I introduce a new fluorescence measurement system, PAMoTron, which interfaces a PAM fluorometer (Schreiber et al. 1986) and a light incubation chamber (Eppley 1968; Lewis and Smith 1983). The system allows for parallel incubations at 12 irradiance levels to resolve fluorescence parameters as a function of irradiance and time (e.g. NPQ, photochemical quenching, and the light saturation parameter determined by fluorescence, E_{KF}). The light saturation parameter is calculated from the relative electron transport rate (ETR*) determined from the light adapted fluorescence yield ($\Delta F/F_m'$), also called the Genty yield (GY), and the actinic irradiance (Genty et al. 1989; White and Critchley 1999). One sample in the light incubation assembly is kept in the dark to determine F_v/F_m. By allowing the determination of the temporal variations of the different fluorescence metrics, the new measurement system is potentially a useful tool to assess the physiological state of algae under a range of light conditions. The rate of change and amplitude of fluorescence metrics (E_{KF} and NPQ) may provide diagnostics for physiological stress. This new measurement system can also determine relative electron transport rates as a function of irradiance for comparison with carbon-based photosynthesis-irradiance estimates. Calculation and determination of the fluorescence metrics under different growth irradiances for nutrient-replete cultures are described and the advantages and limitations of this new system are discussed.

3.3 Background

3.3.1 Fluorescence

Fluorescence measurements have the advantage of being rapid, sensitive, and minimally invasive and have shown promise for determination of photosynthetic efficiency (Schreiber et al. 1986; Falkowski 1992), and, in turn, for describing the effects of physiological stress on photosynthetic performance of plants and phytoplankton (Genty et al. 1989; Geider et al. 1993a; Kolber and Falkowski 1993; Babin et al. 1996a). Earlier research in aquatic science was limited to conventional fluorometry, using herbicides such as DCMU, for determining the dark-adapted maximum quantum yield for photosystem II (F_v/F_m) (Prézelin et al. 1977; Samuelsson and Öquist 1977; Cullen and Renger 1979; Roy and Legendre 1979; Neale et al. 1989). This excludes important information on the kinetics and relative photosynthetic efficiency of the algal population under ambient light conditions. More recently, there have been an increasing number of experiments using active fluorescence techniques (Falkowski et al. 1986; Schreiber et al. 1986; Genty et al. 1989; Oquist and Chow 1992; Kolber and Falkowski 1993; Babin et al. 1996a; Flameling and Kromkamp 1998) to determine different parameters describing changes in fluorescence under various manipulations of irradiance. Active fluorometers, such as the PAM fluorometer, can estimate dark-adapted maximum quantum yield of PSII, F_v/F_m, and strong agreement exists between conventional fluorometers and active fluorometers (Geider et al. 1993a; Parkhill et al. 2001). Active fluorometers have the added capability to measure fluorescence under a range of background irradiance. The

rapid light curve technique investigates some of these fundamental relationships between irradiance, physiological stress and fluorescence (Schreiber et al. 1997; Ralph et al. 1999; White and Critchley 1999; Kühl et al. 2001). The limitations of such a system are that no temporal resolution at individual irradiances can be achieved and results are influenced by the choice of time-steps for the sequential shifts of irradiance. The proposed new measurement system allows parallel measurements of discrete samples at a given light field and determination of temporal changes for a sample not subjected to light step-sequence experimental design.

Amalgamation of an active fluorometer with other instruments is not novel and has already shown to be useful. Goh et al. (1999) combined the PAM fluorometer with a Zeiss epifluorescence microscope to elucidate physiological parameters (i.e. electron transfer rate, and the trans-thylakoid proton gradient) and provide biochemical and photochemical analysis at the cellular level. I show that the new measurement system (PAMoTron) provides representative measurements that allow the determination of a light saturation parameter and the amount of non-photochemical quenching for an algal population and that these may be useful diagnostics of algal physiological status.

3.3.2 Fluorescence, relative electron transport and its comparison to ^{14}C incubation measurements

Fluorescence parameters can be used as a proxy for photosynthetic efficiency allowing the estimation of relative photosynthesis as a function of irradiance (Genty et al.

1989). Fluorescence is used to examine the activity of the PSII reaction center, hence the non-cyclic photosynthetic electron transport system, because fluorescence originates principally from the chlorophyll *a* in PSII. Active fluorometers accomplish this by modulating fluorescence excitation. The "measuring beam" is rapidly switched on and off and the changes in the fluorescence signal are separated from the background. In this active fluorometry technique, fluorescence yield measurements under different irradiances can provide important fluorescence metrics, which are relative measures of photosynthetic efficiency. There are many types of active fluorometers, but the two most prevalent are the PAM fluorometer (Schreiber et al. 1986) and the Fast Repetition Rate Fluorometer (FRRF) (Falkowski et al. 1986). The difference between the two systems is that the PAM fluorometer uses a relatively long multiple turnover flash, saturating the Q_A, Q_B and plastoquinone pools, whereas the FRRF uses a single turnover flash, which only reduces the Q_A pool (Chapters 1 and 2). Although these techniques measure slightly different processes (Prasil 1998), it remains to be seen whether these differences are important for most ecological studies, especially those trying to resolve physiological stress.

Active fluorometry, and more precisely the PAM system, has received criticisms about its use in assessing the physiology of phytoplankton (Ting and Owens 1992; Büchel and Wilhelm 1993; Kolber et al. 1998). Büchel and Wilhelm (1993) have cited problems in resolving quenching analysis with dilute samples of unicellular algae. Ting and Owens (1992) have shown that the taxonomic composition of different algal classes can lead to misinterpretation of fluorescence results. Their results have also shown decreased

maximal fluorescence (F_m) at saturation pulse intensities because of non-photochemical quenching. The PAM fluorometer has recently overcome some of these problems by increasing sensitivity. It is now capable of measuring the fluorescence signal at chlorophyll levels comparable to those found in natural surface waters (i.e. 0.1 $\mu g\ L^{-1}$) (Schreiber and Bilger 1993). The other problems can be minimized by careful attention to methodology (i.e. consistent sampling protocols, increased times between saturating flashes). Problems such as cyclic flow around photosystem II giving elevated values for maximal fluorescence can be minimized by monitoring the intensity of the saturation pulse (Schreiber et al. 1995). The relationship between fluorescence-based measurements of light adapted quantum yield (Genty et al. 1989) under different irradiance levels and other measurements of photosynthetic efficiency remains unclear since no consensus has been reached about the relationships under all growth and sampling conditions (Flameling and Kromkamp 1998). The PAMoTron, being able to monitor fluorescence variations on relatively short time scales, might provide some answers to understanding the discrepancies between methodologies.

The most common method to determine photosynthesis-irradiance (P vs. E) curves in marine microalgae is through ^{14}C incubation experiments (Steemann-Nielsen 1952; Lewis and Smith 1983). This method measures the rate of incorporation of inorganic radioactive ^{14}C into acid-stable organic carbon as a function of irradiance (Lewis and Smith 1983; Falkowski and Raven 1997). The rationale for the ^{14}C-based tracer method is that the light dependent rate of incorporation of the radioactively labeled carbon into organic material is quantitatively proportional to that of non-radioactive

inorganic carbon. Over short periods of time, before a significant fraction of the organic carbon becomes labeled and ^{14}C is respired, the radio carbon method gives a reasonable approximation of gross photosynthetic rate (Geider 1992b; Falkowski and Raven 1997). The P vs. E curves provide an indication of the ability of algae to use the available light for photosynthesis. P vs. E curves have also been used extensively to explore acclimation and physiological stress in plant species (Eppley and Renger 1974; Terry et al. 1985; Herzig and Falkowski 1989; Cullen et al. 1992b; Henley 1993). This is generally accomplished by relating physiology to parameters of the P vs. E relationship (Jassby and Platt 1976). The advantages of this method are that it is fast, sensitive and relatively easy to use. However, the ^{14}C method has some problems such as toxicity and "bottle" artifacts (Eppley 1980; Geider 1992a; Falkowski and Raven 1997). Another criticism of the ^{14}C incubation method is that the initial measurements of incorporation are blind to respiratory losses, since the respired carbon is not radiolabeled (Geider et al. 1986). Longer incubations would represent net photosynthesis as opposed to gross photosynthesis (Morris 1981), and isotopic discrimination against the radioactive isotope during carbon fixation can be a source of error (Strickland and Parsons 1972). Another concern is that this method involves radioactive material. Although this method has come under some criticism, it remains the most common method for determination of photosynthetic rates of marine phytoplankton (Falkowski and Raven 1997; Cullen 2001).

Geel et al. (1997) observed a linear relationship between productivity measurements determined from oxygen evolution and fluorescence methods under light limiting photon fluxes, but non-linear behavior at light saturating irradiances. Deviations

from a linear relationship have also been observed in other published results (Falkowski et al. 1986; Rees et al. 1992; Flameling and Kromkamp 1998; Hartig et al. 1998). At higher irradiances, the electron transport rates were observed to be higher than the corresponding O_2 evolution or CO_2 assimilation. Several reasons for this lower O_2 evolution, in comparison to electron flow include cyclic flow around PSII (Hartig et al. 1998) and Mehler reaction (Neubauer and Schreiber 1989; Geel et al. 1997). Büchel and Wilhelm (1993) and Ting and Owens (1992) showed that the fluorescence signal may be influenced by light dependent processes including spillover and chlororespiration. Other reasons for differences may include electron partitioning mechanisms such as in nitrate reduction (Weger et al. 1988; Huppe and Turpin 1994; Lomas and Glibert 1999) or other electron sinks. Regardless of discrepancies between measurement systems, ^{14}C uptake and fluorescence have shown strong agreement (Kolber and Falkowski 1993; Boyd et al. 1997; Leipner et al. 1999) under set conditions; although there are consistent problems with measuring productivity (Suggett et al. 2001), the relative estimates between measurements systems can be correlated. The author's intent is not to determine real photosynthetic estimates, but to discover a rapid non-invasive diagnostic showing relative changes in photosynthesis as a function of irradiance in algal species as a potential tool for detecting physiological stress.

3.3.3 Fluorescence and non-photochemical quenching

Non-photochemical quenching (NPQ) is the increase in heat dissipation, relative to dark adapted state, that can protect a plant from light induced damage (Demmig-Adams

and Adams III 1992; Ruban and Horton 1995; Ruban et al. 2001). In terms of fluorescence, NPQ is more generally defined as the decrease of fluorescence at supra-saturating light intensities not due to photochemical processes. Such down-regulation of PSII photochemistry is achieved by increasing the heat dissipation in the light harvesting complexes. This heat dissipation decreases the quantum yield of PSII photochemistry as well as fluorescence and is thus called non-photochemical quenching (NPQ) (Govindjee 1995; Buschmann 1999). NPQ is induced by at least three processes: increases of the pH gradient at the thylakoid membrane (qE), state transitions (qT), and photoinhibition (qI). There is considerable interest in understanding the factors which regulate NPQ, what determines its rate and magnitude under different ambient light conditions, and what NPQ might reveal about the physiological status of phytoplankton.

In the natural environment, light intensity is variable on short time scales and the kinetics of the formation and relaxation of NPQ can be important; if the onset of NPQ lags behind an increase in light intensity, transient over-excitation may have photoinhibitory consequences (Buschmann 1999). Equally, if relaxation of NPQ lags behind a decrease in light intensity, the maintenance of excessive levels of energy dissipation will result in a loss of photosynthesis (Long et al. 1994). An increase in NPQ can be due to processes which protect the plant from photo-induced damage, or by the damage itself. For the purposes of this study, the processes which relax within minutes after the high-light stress is removed are regarded as photo-protective processes (qE, qT), while stress-induced NPQ extending over longer time scales (minutes to hours) will be called photoinhibition (qI). These photoprotective and photoinhibitory processes are

collectively called non-photochemical quenching and can be quantified by a parameter, qN, which reflects influences of the non-photochemical processes on the fluorescence emission during a transition from dark-adapted to light-adapted condition (Krause and Weis 1991; Demmig-Adams 1998).

The quenching coefficients qN and qP defined by Schreiber et al. (1986) require accurate determination of minimal fluorescence after a given state of pre-illumination (F_o') (Figure 3.1). In order to assess F_o', the actinic light must be turned off and the electron pool must be quickly reoxidized with the help of far red light, before the relaxation of the non-photochemical quenching occurs. For this study, and the new measurement system, this is impractical and has not been done. Therefore, instead of qN and qP, the fluorescence parameters NPQ (Bilger and Björkman 1990) and $\Delta F/F_m'$ (Genty et al. 1989) are presented, the calculation of which does not require knowledge of F_o'.

Fluorescence changes (F_m'-F_s) measured under ambient light and with saturation pulses contain essential information for quenching analysis, resulting in the assessment of the PSII quantum yield and energy status of the chloroplast (Genty et al. 1989). Any decrease in F_m' with respect to the original F_m reflects NPQ, whereas the difference F_m'-F_s reflects the capacity for photochemical quenching, which is a relative measure of open PSII reaction centers (Figure 3.1). Caution should be used when comparing non-photochemical quenching coefficients (qN and NPQ) because they describe the same fluorescence signal in a different way (Buschmann 1999). Non-photochemical quenching

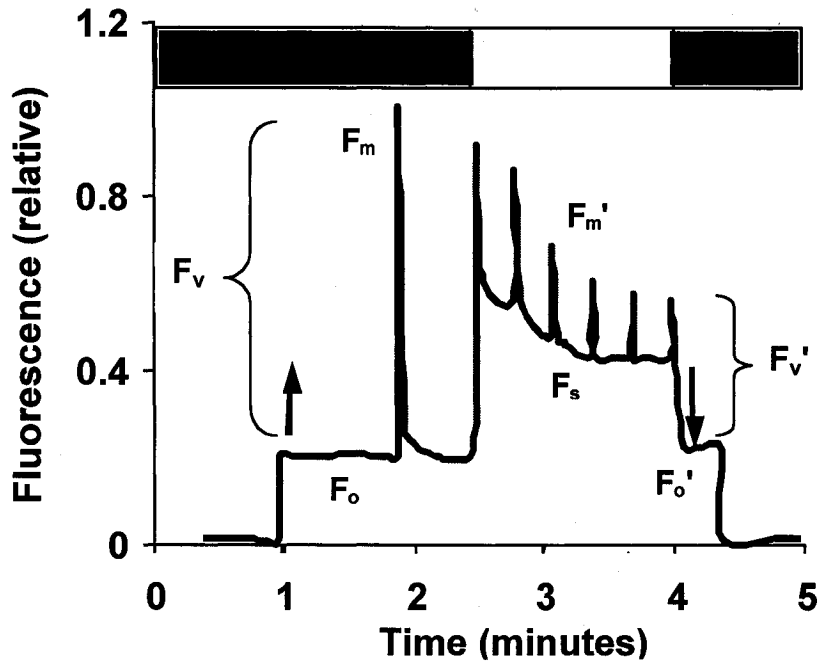

NPQ	$(F_m - F_m')/ F_m'$
qN	$(F_v - F_v')/F_v$
qP	$(F_m' - F_s)/ F_v'$

Figure 3.1 A schematic of fluorescence signals measured under dark (■) and ambient light (❑) conditions. The modulated measuring beam is turned on (🡅) and determination of minimal fluorescence (F_o) for a dark-adapted sample can be done. Subsequently, a saturation pulse, which closes all the reaction centers, allows determination of maximal fluorescence (F_m) under dark adaptation. From these two parameters variable fluorescence (F_v) can be determined ($F_v = F_m - F_o$). Under ambient light, fluorescence (F_s) and maximal fluorescence (F_m') can be determined. After the sampling period is complete the ambient light can be turned off (🡇) and determination of minimal fluorescence after ambient light exposure can be determined (F_o').

(NPQ) is derived from the Stern-Volmer equation based on a matrix or lake model of the antennae organization (Schreiber et al. 1995). Björkman and Demmig Adams (1995) report that, in higher plants, NPQ is linearly related to the excess radiation and the extent of NPQ is related to the formation of zeaxanthin. Under ambient light conditions, NPQ is also used as an indicator of excess radiant energy dissipation processes in the antennae complexes. On the other hand, qN, non-photochemical quenching of the variable fluorescence yield, requires accurate determination of initial fluorescence values under ambient light and will be confined to values between zero and one ($0 < qN < 1$). The accuracy of this measurement breaks down under high ambient light, and is reserved mainly for investigation under light-limiting conditions.

Non-photochemical quenching processes can be further subdivided into high energy state quenching (qE) and quenching due to state transitions (qT). High energy state quenching is due to rapid changes in photo-protective pigments in the light harvesting complex (LHC) (Demmig-Adams 1990; Horton et al. 1996; Schofield et al. 1998) involving the presence of the thylakoid proton-gradient. State transitions, qT, is the reversible phosphorylation of light harvesting proteins balancing the distribution of light energy between PSII and PSI at low light (Walters 1991); the process occurs on longer time scales of 5-15 minutes. Both processes occur on time scales that overlap and it is difficult to resolve their respective relaxation kinetics in plants. However, state transitions, contribute only a small portion to the quenching and is mostly observed at low light (Krause and Weis 1991). Therefore investigation into high-light quenching of NPQ on minute time-scales is largely attributed to qE (Horton and Hague 1988). The

relationship between the extent of qE and the rate of formation of NPQ is complex and poorly understood (Ruban and Horton 1995), although both are increased by increased irradiance (Demmig-Adams and Adams III 1992; Verhoeven et al. 1997).

3.3.4 NPQ and light

Under increased irradiance, more reaction centers become closed and steady-state fluorescence yield increases. Under excess light conditions, the photosynthetic apparatus can quench excited states in the antennae before damage can occur and a subsequent decrease in maximal fluorescence (F_m') is observed. This change is attributed to NPQ. Short-term responses of NPQ include photoprotective avoidance and dissipation mechanisms (qE and qT), although when these strategies fail under prolonged and or extreme stress, photoinhibition can occur (qI) (Gilmore and Govindjee 1999). Plants grown under low irradiance have reduced photoprotective capabilities and are more susceptible to photoinhibition of photosynthesis than plants grown under higher irradiance levels (Park et al. 1995). The enhanced susceptibility of "low-light" plants to excess irradiance has been attributed to various factors such as a larger antennae size, reduced photosynthetic rate, slower replacement of the D1 protein, and a reduced capacity for formation of zeaxanthin via the xanthophyll cycle (Demmig-Adams and Adams III 1992; Park et al. 1996; Schofield et al. 1998; Gilmore and Govindjee 1999; Niyogi 1999). Park et al. (1996) also showed different strategies may be employed depending on the growth irradiance. Low light grown plants relied on D1 protein

synthesis rather than non-radiative dissipative photoprotective mechanisms, because of their limited capacity for NPQ dissipation. In contrast, plants grown at high-light would have a greater capacity for both photochemical and non-photochemical dissipation along with the same intrinsic capacity for D1 protein synthesis and other photoprotective processes (Park et al. 1996). The change in rate and magnitude of fluorescence metrics should be a function of the ambient light conditions and the ability for an algal species to acclimate. The onset and rate of increase of NPQ, previously unavailable from conventional fluorometers, may provide information into the relative productivity of the algal species and prove to be a potential diagnostic of physiological stress.

3.4 Materials and methods

3.4.1 Measurement system

The PAMoTron is a diagnostic tool made by interfacing a light incubation chamber and a Pulse Amplitude Modulation (PAM) fluorometer (Schreiber et al. 1986) (Figure 3.2) to measure time-dependent changes in fluorescence parameters as a function of irradiance for 12 samples of phytoplankton incubated in parallel. The PAM101/102/103 system (Walz Effeltrich, Germany) utilizing the Photomultiplier Tube (PMT) accessory was used in conjunction with an incubation chamber with different irradiance levels. This new measurement tool provides temporal resolution by incorporating the incubation chambers of photosynthetrons (Lewis and Smith 1983) with

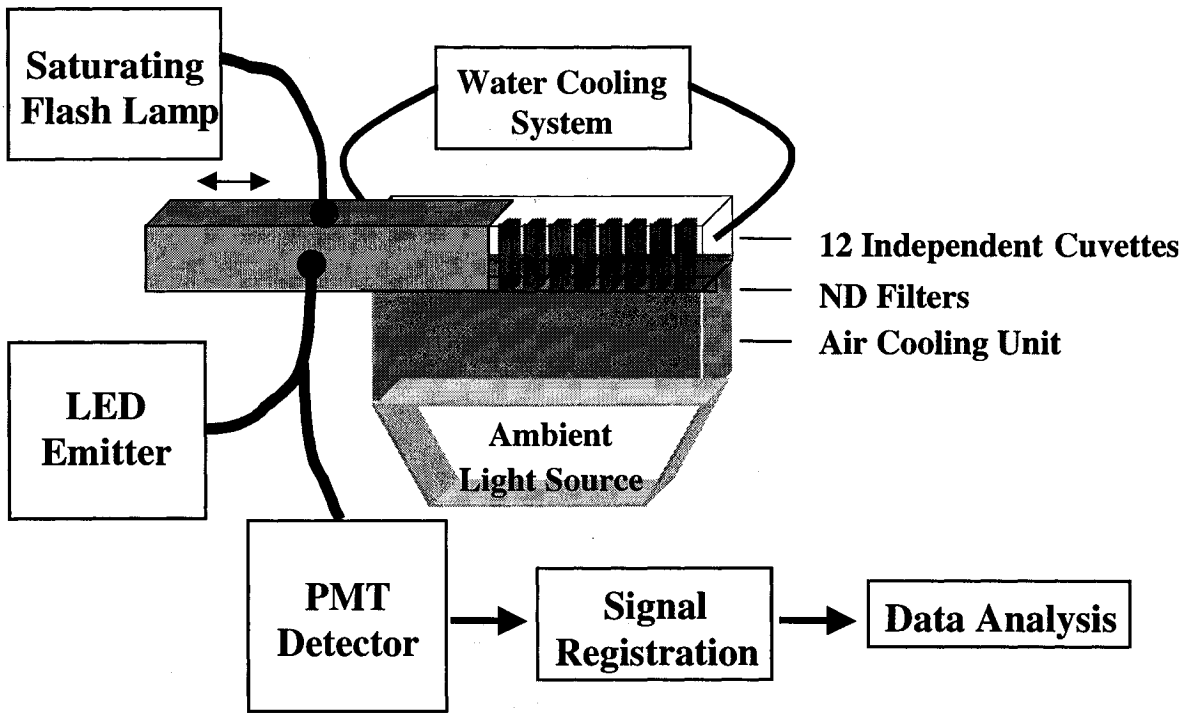

Figure 3.2 A schematic of a new fluorescence measurement system (PAMoTron), an amalgamation of an incubation light chamber and a Pulse Amplitude Modulation (PAM) fluorometer allowing parallel measurements of fluorescence parameters under a suite of irradiance levels. Culture sub-samples (4mL) are placed in a black anodized cuvette holding unit with a closed internal water cooling system housing 12 cuvettes. Each cuvette unit has a different ambient irradiance provided by a metal halide lamp (1000W) and attenuated by neutral density screening. A 90° black metal guard is long enough to cover all cuvettes while it is moved, allowing protection from stray ambient light and also ensures that the fiber-optic cable to the photomultiplier tube (PMT) and saturating flash lamp are at right angles. The metal guard has a guide with stoppers which allow for accurate and rapid changes from one sample to the next. A secondary cooling unit using a fan system provides further heat dissipation. A light shield (not shown) blocks out all ambient irradiance, which allows measurement of individual samples under dark-adapted conditions prior to exposure to their respective incubation irradiances. Once these initial readings are taken the light shield is removed. The signal from each sub-sample is propagated down a fibre-optic light guide and amplified by the PMT; it is then recorded for further data analysis. Sampling time for an individual sub-sample is 10 seconds. A run of 12 cuvettes requires 2 minutes and a sample is observed over a 20 minute period. The PAM system is run using a program generated from a Labview 4.0 software package.

fluorescence measurements on individual samples at pre-measured ambient irradiances. Twelve cuvettes fit inside the incubation chamber made from a temperature-controlled aluminum block. Ambient light is supplied from the bottom by a metal halide lamp (Phillips MH1000W) and the light is attenuated by different grades of neutral density Mylar filters at the base of the individual cuvette holders (Figure 3.2). The ambient light field was also spectrally altered using blue cellulose acetate screening (Lee Filters #202 - 1/2 control temperature blue). The incubation chamber irradiance levels ranged from 1 to 1000 μmol m^{-2} s^{-1} of photosynthetically available radiation as measured with a Biospherical Instruments Inc. (San Diego, CA) QSL-100 4π sensor. The samples exposed to the metal halide lamp were cooled with a two tiered system consisting of two fans for heat dispersion, and a flow through water bath system, which also served to house the cuvettes.

The unit that holds both fiber optic cables at the proper angle was connected to the aluminum block on runners so that the detector, LED, and saturating pulse move easily from sample to sample to record individual results at intervals of 10s (Figure 3.2). Two-way fiber optic cables were placed at a 90° angle to provide accurate determination of fluorescence under ambient light conditions (F_s), using a LED (λ = 650 nm), and maximal fluorescence under ambient light conditions (F_m') determined during a saturating pulse (Schott KL1500-E; E > 5000 μmol m^{-2} s^{-1} each of 600 ms duration). The LED pulses have low-light intensity (< 0.2 μmol m^{-2} s^{-1}) and have a 1μs duration at a frequency of 1.6 Khz or 100 Khz (Schreiber et al. 1986). The red radiation from the LED

passes through a short pass filter ($\lambda < 670$nm) before absorption by a sample. For the different ambient light sources chosen (1-1000 μmol m^{-2} s^{-1}), one of the cuvettes simulated the dark-adapted state (1 μmol m^{-2} s^{-1}) and was used for determination of F_v/F_m. A fiber optic cable to deliver saturating pulse was positioned at the top of the sample. The analog signal was digitized and recorded using a Labview 4.0 application (National Instruments, Austin, TX) designed by Pat Neale (SERC). Initial fluorescence (F_o and F_s) is an average of 300 points for the three seconds prior to the saturation pulse, while F_m is calculated as the highest running average (4 continuous points) during the saturation pulse.

The PAMoTron signal is determined initially for blank cuvettes using filtered (0.22μm) artificial seawater medium. Sub-samples of a dark adapted (>10 min) culture (4 mL aliquots) are then placed in the individual cuvettes for determination of F_o and F_m (Kolber and Falkowski 1993; Babin et al. 1996a). After initial dark-adapted sampling, the light shield is removed and the samples are exposed to different ambient light fields. Fluorescence under ambient light (F_s) is determined prior to the saturation pulse by the LED detector for a minimum of 5 seconds before the saturation pulse closes all the reaction centers for determination of maximum fluorescence under the ambient light condition (F_m'). This 10 second protocol is repeated on each of the 12 discrete samples (2 minute runs) for a 20 minute interval to observe changes in the fluorescence signal over time. Signals are exported from the Labview data files into a Microsoft Excel spreadsheet and are analyzed to provide relative measurements of electron transport and NPQ.

A mechanistic model using non-linear curve fitting (MATLAB program created by Richard Davis, Dalhousie University) was used to determine relative electron transport rate ($ETR_i^* = GY \bullet E$), and for the calculation of the parameter of light saturation (E_{KF}) (Equation 3.1).

$$ETR_i^* = ETR^*_{max}\,(1 - e^{(-E_i/E_{KF})}) \qquad 3.1$$

Maximum quantum yield for PSII (F_v/F_m) and non-photochemical quenching was also determined from the fluorescence parameters determined from discrete samples in 20 minute incubations with the new measurement system. The duration, intensity and time between saturation pulses were measured to ensure that the settings on the PAM fluorometer did not over or under saturate the sample leading to erroneous results (data not shown).

3.4.2 Culture growth conditions

Semi-continuous cultures of the neritic diatom, *Thalassiosira pseudonana*, Clone 3H, provided by the Provasoli-Guillard National Center for Culture of Marine Phytoplankton (CCMP 1015) were grown in triplicate at 150 (low-light), 350 (medium-light); and 1000 μmol m^{-2} s^{-1} (high-light) (Table 3.1). Cultures (2.5 L) were grown in 4 L Erlenmeyer flasks and were maintained through many generations to study acclimated growth, replete in all nutrients. Photosynthetically available radiation (PAR) was measured with a Biospherical Instruments Inc. QSL-100 4π sensor. Low-light cultures

Table 3.1 A summary of the experiments described in this chapter, with the initial nutrient concentrations, light levels, light:dark cycle, growth rates and duration of the individual experiments.

Type of Experiment	Initial N levels ($\mu mol\ L^{-1}$)	Irradiance ($\mu mol\ m^{-2}\ s^{-1}$)	Light :Dark Cycle (h:h)	μ (d^{-1})	Duration (d)
BALANCED GROWTH					
Semi-Continuous	880 (NH_4^+)	150	24:0	1.78	15
(N-replete)	880 (NO_3^-)	350	12:12	1.48	15
	880 (NO_3^-)	1000	12:12	1.82	21

were grown in continuous light, while medium and high-light cultures were grown on a 12:12 light:dark cycle. The designation of low, medium and high-light are labels introduced for reference only, since 150 μmol m^{-2} s^{-1} in some culture studies would represent a medium-high light intensity. Low and medium light cultures were grown using 40W Vita-Lite full spectrum fluorescent bulbs, and the desired irradiance was achieved using neutral density screening. High-light cultures were grown under 500 W portable halogen lights in a flow-through water bath with mirrored oven-glass assembly. This assembly was necessary to maximize irradiance and control excess heat from the lamp, and to shift the spectral quality of the light field more into the blue. Temperature was controlled at 20 ± 0.5°C. The nutrient-replete cultures were manually agitated and daily dilutions were made with f/2 media to maintain a low cell concentration. A detailed description of culture conditions and the reason for choosing experimental conditions have been previously reported (Parkhill et al. 2001). Nitrogen for nutrient-replete cultures was supplied as NH_4 for low-light cultures (880 μM) and NO_3 in medium and high-light cultures (880 μM).

3.4.3 Measurements

Cell concentrations, nitrogen (NO_3^- or NH_4^+) and chlorophyll concentrations, and F_v/F_m were sampled on a daily basis, 3 h into the light period (10:00h), to determine if constant growth rates were achieved (calculation of growth rate is described in section 2.4.3). Daily dilutions of approximately 5:1 (new medium:culture) ratio, were done to ensure the concentration did not exceed pre-determined chlorophyll concentrations (150

mg chl m^{-3}). Cultures having low chlorophyll concentrations were not diluted. Chlorophyll *a*, corrected for phaeopigments (Strickland and Parsons 1972), was measured using a Turner Designs fluorometer (10-005 R) calibrated with pure chlorophyll *a* (Sigma Chemical Co.). Duplicate volumes of 1 mL each were filtered on Whatman GF/F filters and extracted in 10 mL of 90% acetone in the dark at –15°C for at least 24 hours. Cell size and concentration were determined on triplicate samples after dilution on a Coulter Multisizer II Particle Analyzer calibrated with latex beads. Concentrations of NO_3^- (and ammonium concentration for low-light grown cultures) were determined from filtered (0.22 μm) samples of culture medium by using a Technicon II Autoanalyzer (Grasshoff et al. 1976) to ensure the cultures were not N-limited. Fluorescence was measured using a Turner Designs (Sunnyvale, CA) fluorometer (10-005R), on triplicate 30 minute dark-adapted 10 mL samples, before and 30 seconds after the addition of 50 μL of 3mM DCMU in ethanol. Neutral screening (cellulose acetate, 60% transmission) was placed around the cuvettes for cultures under low light to ensure that the initial measuring beam did not close reaction centers, and overestimate F_o (Parkhill et al. 2001).

Once constant exponential growth was observed and a constant maximal specific growth rate (μ_{max}) was determined, the routine sampling as well as PAMoTron measurements and ^{14}C incubations were done. PAMoTron measurements have been previously described (Section 3.4.1). The bicarbonate uptake experiments (^{14}C incubations), were measured in a photosynthetron (Lewis and Smith 1983) with 24 light intensities from 0-2000 $\mu molm^{-2} s^{-1}$. The incubation procedure followed that of

MacIntyre and Cullen (1995). Samples were incubated for 30 minutes and then carbon incorporation was stopped with 250 µl of 50% HCl, which removes all non-incorporated inorganic carbon, as verified by time-zero samples. The samples were counted by a Beckman LS 3801 scintillation counter after addition of 5 mL Ready Safe Scintillation Cocktail (Beckman, Fullerton, CA).

Triplicate P vs. E curves were normalized to chlorophyll and corrected for time zero. Dissolved inorganic carbon (DIC) was determined using a Li-Cor 6262 CO_2/ H_2O Infrared detector. Curves were estimated by fitting experimental data points to an exponential function (Gallegos and Platt 1982) using MATLAB (version 5.2) (Equation 3.2).

$$P_i^B = P_m^B(1 - e^{(-E_i/E_K)}) \qquad 3.2$$

Maximum photosynthetic capacity, normalized to chlorophyll ($P^B{}_m$) and the parameter of light saturation (E_K) were determined from the P vs. E curve for comparison with the complementary measurement (E_{KF}) done with the new fluorescence measurement system (Equation 3.1). PAMoTron measurements were run concurrently on the same sub-samples as the ^{14}C incubations to minimize sampling error and diurnal fluctuations.

3.4.4 Statistics

To determine steady state and routine measures, analysis of variance (ANOVA) involving repeated measures analysis was performed in the statistical package SAS

(Statistical Analysis Software Version 8, SAS Institute Inc. Cary NC). To determine the statistical significance of different parameters, linear regression analysis was performed using Minitab statistical analysis software Version 1.3 (Minitab Inc, State College PA). If a significant linear regression was observed, ANOVA using the general linear models procedure in SAS was conducted to determine where the differences existed. Tukey-Kramer least square means test was used to determine differences between means. The selected alpha error rate was $P > 0.05$. For determination of F vs. E and P vs. E curves, non-linear regressions were done using MATLAB (5.2) non-linear fit routine and 95% confidence intervals were determined for E_{KF} and ETR^*_{max} (and E_K and P^B_{max} for ^{14}C incubations) using the nlparci routine (code written by Yannick Huot, Dalhousie University).

3.5 Results

3.5.1 Routine sampling

Routine sampling was conducted to ensure that acclimated growth was achieved in the cultures investigated (Figure 3.3). Nutrient-replete cultures for each of the different pre-conditioned light levels grew exponentially and all indicators showed that the growth was limited solely by growth irradiance (Figure 3.3). Constant algal physiological parameters such as growth rate, fluorescence chlorophyll^{-1}, and high and consistent F_v/F_m provide evidence that the cultures were acclimated (Figure 3.3). Other variable factors

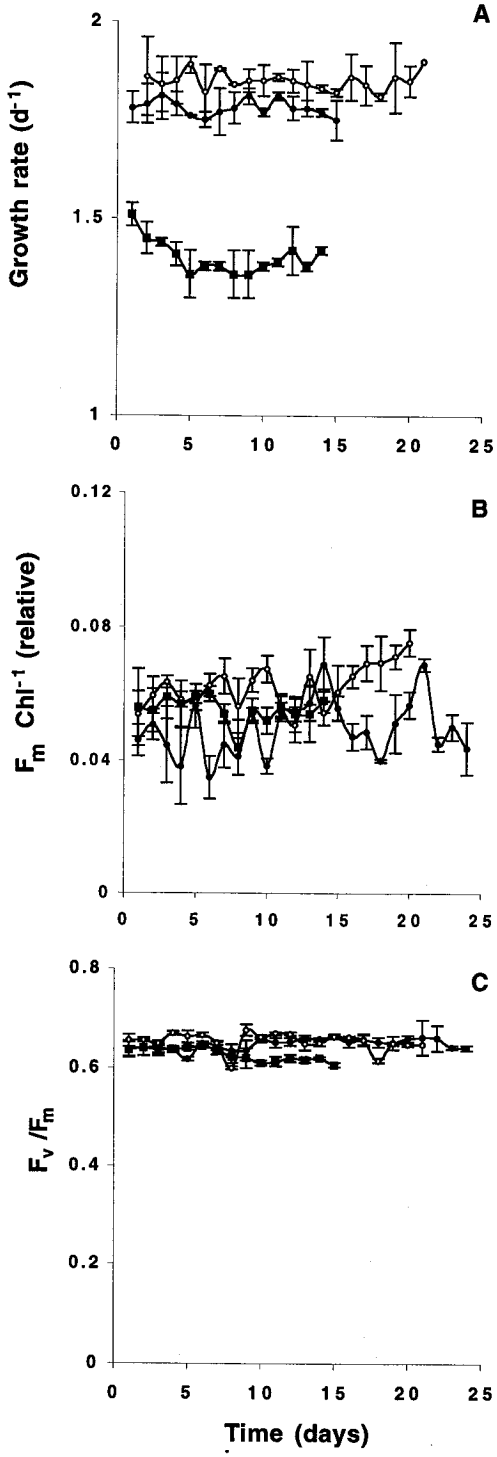

Figure 3.3 Daily routine measurements of replete cultures grown under three different irradiance levels (150 (●), 350 (■) and 1000 μmol m^{-2} s^{-1}(○)) provides evidence of steady-state exponential growth and irradiance limitation of growth. (A) Growth rate was determined by daily dilutions and provides evidence that cultures grown under higher irradiance levels had higher growth rates. (B) Measurements of a fluorescence parameter normalized to chlorophyll provides evidence of little physiological change over time. (C) F_v/F_m, an indicator of nutrient starvation, was high and constant for all light levels investigated, indicating nutrient replete growth conditions.

were also monitored to ensure nutrient-replete conditions including nitrate concentration (> 50 μmol $NO_3^- L^{-1}$).

3.5.2 Determination of blanks

Once the criteria for the desired growth conditions had been met, I investigated fluorescence parameters from sub-samples of individual cultures using the new measurement system. The measurement of fluorescence requires a correction for the signal from filtered medium. Variability between sampling cuvettes was observed by running blank samples in the measurement system, and are attributed to variability between cuvettes, since the blanks were not a function of ambient irradiance level (Figure 3.4A). These differences were not significant (< 5%) when compared to the signals observed from culture samples (Figure 3.4B), but all the reported results are corrected for their respective blank nonetheless. No changes in the fluorescence signals of the blanks were observed when the saturation lamp was turned on indicating that the measurement system does not contribute to any variable fluorescence within discrete samples.

3.5.3 Measurement of fluorescence parameters vs. irradiance

Duplicate measures of >10 minute dark-adapted samples provided the initial and maximal fluorescence (F_o and F_m) for discrete subsamples of a culture (Figure 3.4B). Once the light shield was removed, the haphazard pre-determined ambient irradiance selection

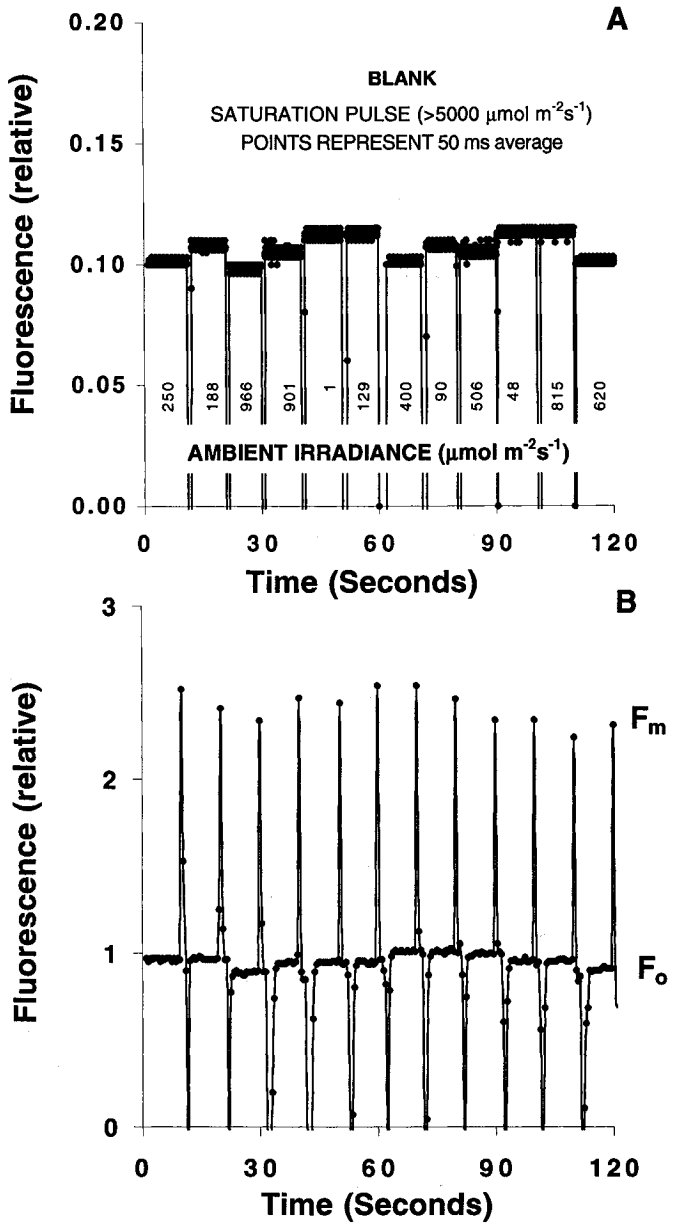

Figure 3.4 Fluorescence signal measured by PAMoTron. (A) Fluorescence signal of F_o and F_m for 12 blank subsamples of 0.22 µm filtered artificial media under ambient light conditions with the delivery of a 600 ms saturation pulse (>5000 µmol m^{-2} s^{-1}) at the end of the monitoring interval for each respective cuvette. F_m is not different from F_o. The monitoring interval of an individual sample is 10 s. Following completion of the saturation pulse, measurement moves to the next sample. No changes in the fluorescence signal are apparent within the blank subsamples. Gaps in the signal represent the change of the subsample being monitored. Ambient irradiance level (µmol m^{-2} s^{-1}) is reported for each sample investigated. (B) Measurement of F_o and F_m is done prior to exposure to the different incubation irradiance levels to allow for dark-adapted fluorescence parameters to be determined. For clarity, graph points represent 500 ms averages. Values are recorded in an Excel spreadsheet for determination of different fluorescence metrics.

provided data on F_s and F_m' for 2 minute intervals per sub-sample (Figure 3.5A). These raw data were then organized as a function of irradiance (Figure 3.5B). A 20 minute incubation provided 10 curves of F_s and F_m' as a function of irradiance (Figure 3.6). The data showed some variability (±10%), with the larger changes as a function of time and higher irradiance levels. Changes from the dark-adapted values were rapid and not well resolved with the 2-4 minute interval (Figure 3.7). A decrease in both F_s and F_m' was observed as a function of light intensity. As the light stress continued, a decrease in F_s and F_m' was observed over time, although over 80% of the change was observed in the first 4 minutes (Figure 3.7). For this reason, F_s and F_m' were integrated over the 20 minute incubation period for determination of the Genty yield (Genty et al. 1989)(Figure 3.6, 3.7).

3.5.4 Comparison of fluorescence based ETR with ^{14}C assimilation rates

Measurements of the fluorescence parameters (F_o, F_m, F_s, F_m') can allow determination of the probability of photochemical quenching, or Genty yield ((F_m'-F_s) /F_m') (Figure 3.7). The photochemical quenching parameter (Figure 3.7) multiplied by the irradiance is a measurement of the relative electron transport rate (ETR*) (Figure 3.8). Comparison of the relative electron transport curve with the structure of the P vs. E curves determined by ^{14}C incubations showed that they were qualitatively similar and both were well defined with an exponential function (Equations 3.1 and 3.2, Figure 3.8B, Appendix A). Both curves are fit to the same model and there is not enough evidence to

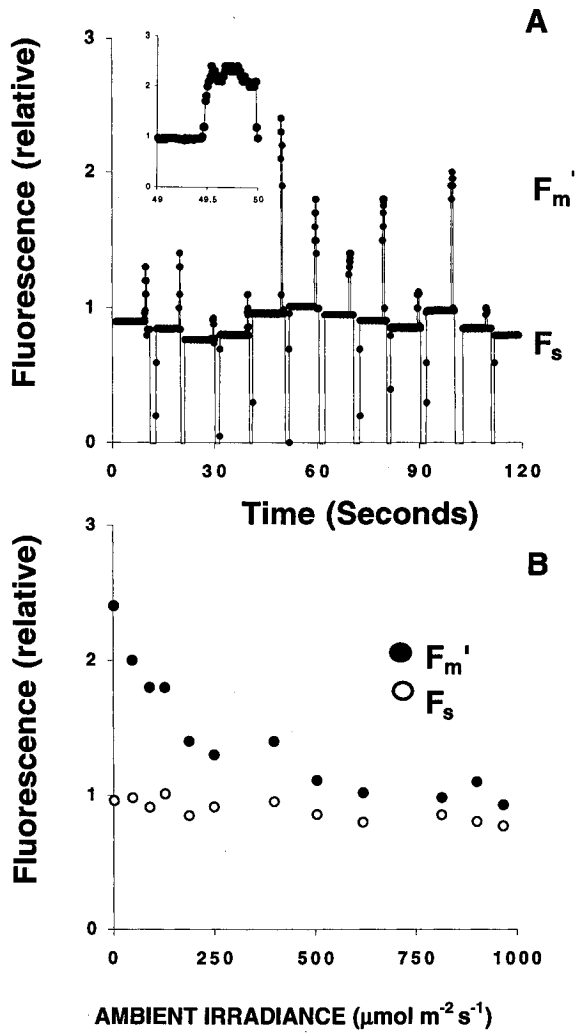

Figure 3.5 (A) Measurement of F_s and F_m' of a representative sample in the 12 respective cuvettes. F_m' can be observed as the rapid change in the fluorescence signal within individual samples when the saturation pulse is turned on. Each sample is under a different ambient irradiance and are monitored in parallel every two minutes. For clarity, graph points represent an average of 50 ms. The inset shows the increased fluorescence signal during a saturation pulse at a higher resolution (points represent 10 ms average). (B) F_m' and F_s is plotted as a function of irradiance for each 2 minute interval. The data in A are fluorescence signals from the 6-8 minute time interval.

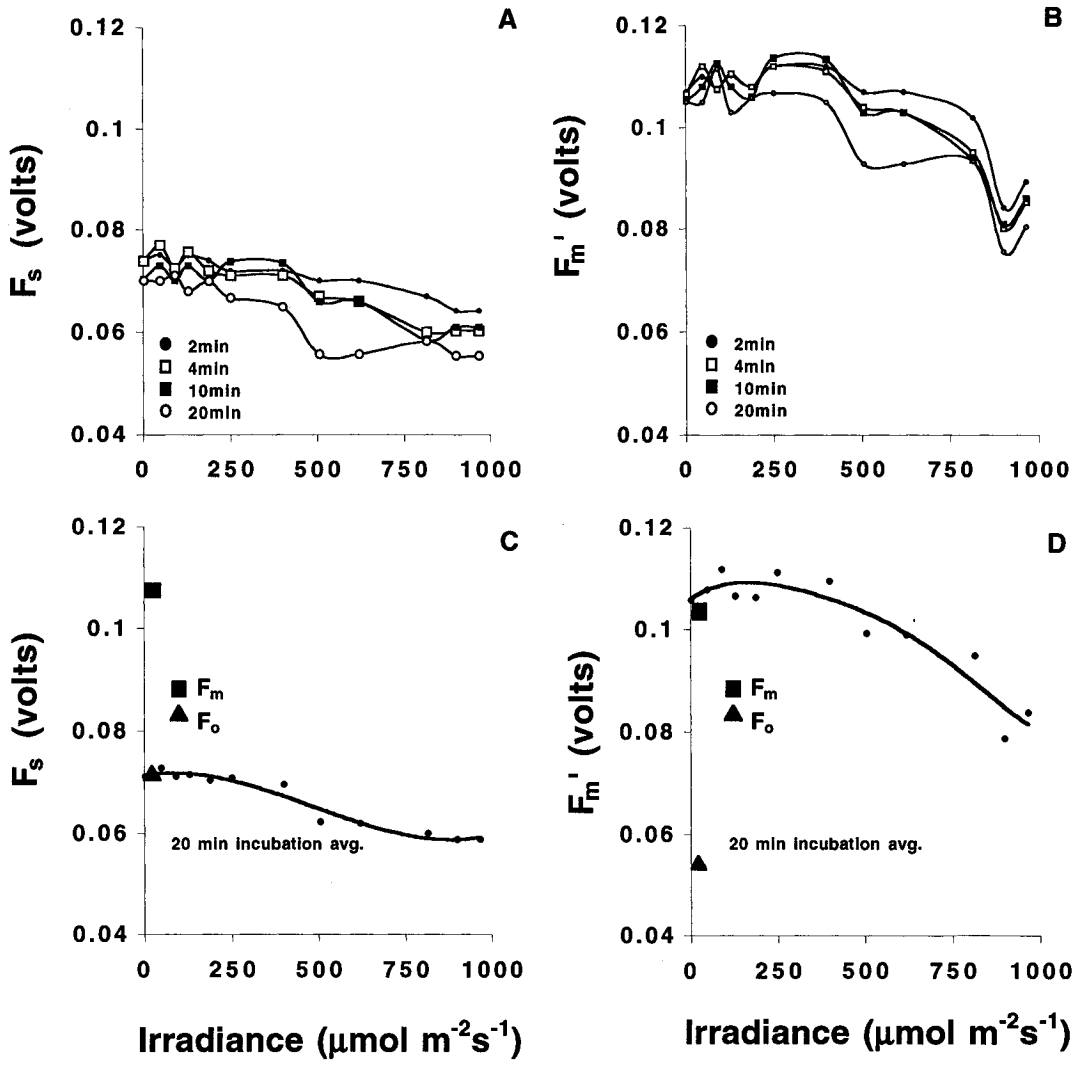

Figure 3.6 Fluorescence signals as a function of irradiance measured on a nutrient-replete culture grown under 350 µmol m^{-2} s^{-1}. (A) Fluorescence under ambient light conditions (F_s) and (B) maximal fluorescence under ambient light (F_m') was determined at 2 minute intervals for 20 minutes. Four representative time intervals of the 10 curves are shown for comparison. These numbers can be integrated over the time period to provide 20 minute incubation averages of (C) F_s and (D) F_m' which can be used for determination of photochemical and non-photochemical quenching parameters. For reference, dark-adapted initial F_m (■) and F_o (▲) are shown at 0 irradiance.

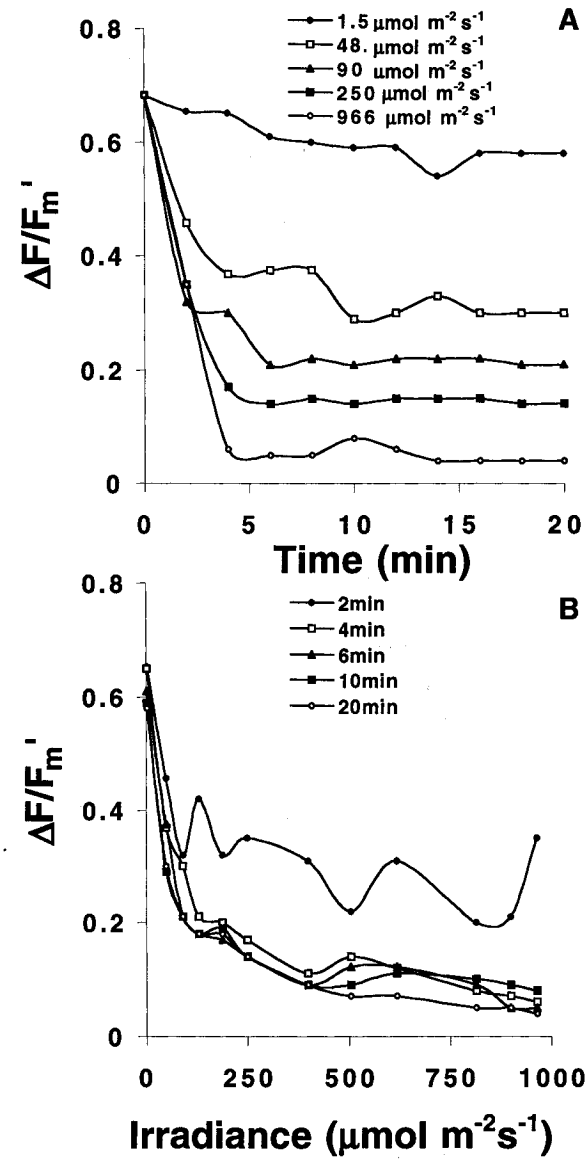

Figure 3.7 Photochemical quenching determined from fluorescence measurements as a function of time and ambient light field for a replete culture grown under 350 µmol m^{-2} s^{-1}. (A) A decrease of the relative photochemical quenching ($\Delta F/F_m'$) is observed under increasing irradiance and the onset of this decrease occurs on short time scales (<4 minutes). A representative five of the 12 different irradiances investigated are shown. The graphical representation is of the 6 minute time interval and lines are point to point and are used strictly for clarity. (B) The same photochemical quenching parameter ($\Delta F/F_m'$) is shown as a function of ambient irradiance. Variability in the curve is observed due to the rapid onset of non-photochemical quenching and the time delays observed in some samples due to the haphazard order of irradiance in the 12 independent samples.

state that the curves are different, or if they are different it is of no practical significance (Figure 3.8B). A limitation of the test of differences is the small sample size (n = 9). Agreement between methodologies is observed when photosynthetic rates (P^B_i) and relative electron transport rates (ETR^*_i) from the modeled curves of individual cultures are compared at light-saturated (500 µmol m^{-2} s^{-1}) and light-limited levels (50 µmol m^{-2} s^{-1}) (Figure 4.4). Also, a linear relationship between the two independent measurements of the parameter of saturation (E_K and E_{KF}) was observed (E_{KF} = 0.74 E_K + 81.7; R^2= 0.71, n = 18). Linear regression was done in Minitab version 8, while the curve fits were done in MATLAB using non-linear least squares models. Increasing the number of parameters, such as an inhibition (i.e. B) or an intercept term (P_o), had little effect on the correlation of the curves, and the high correlation coefficients from the curves (P vs. E R^2 = 0.91, F vs. E R^2 = 0.93; n = 9) provides evidence that the data is accurately represented by equations 3.1 and 3.2.

3.5.5 E_{KF} and E_K as a function of growth irradiance

Comparison over the different growth irradiances shows strong agreement between E_{KF} and E_K measurements and that the measurement is dependent on growth irradiance (Figure 3.9). As growth irradiance increased, an increase in E_{KF} and E_K was observed. Triplicate averages of E_{KF} and E_K for 150 µmol m^{-2} s^{-1} growth irradiance were 195 ± 42 and 138 ± 71 (µmol m^{-2} s^{-1}, ± SD) respectively; E_{KF} and E_K at 350 µmol m^{-2} s^{-1}

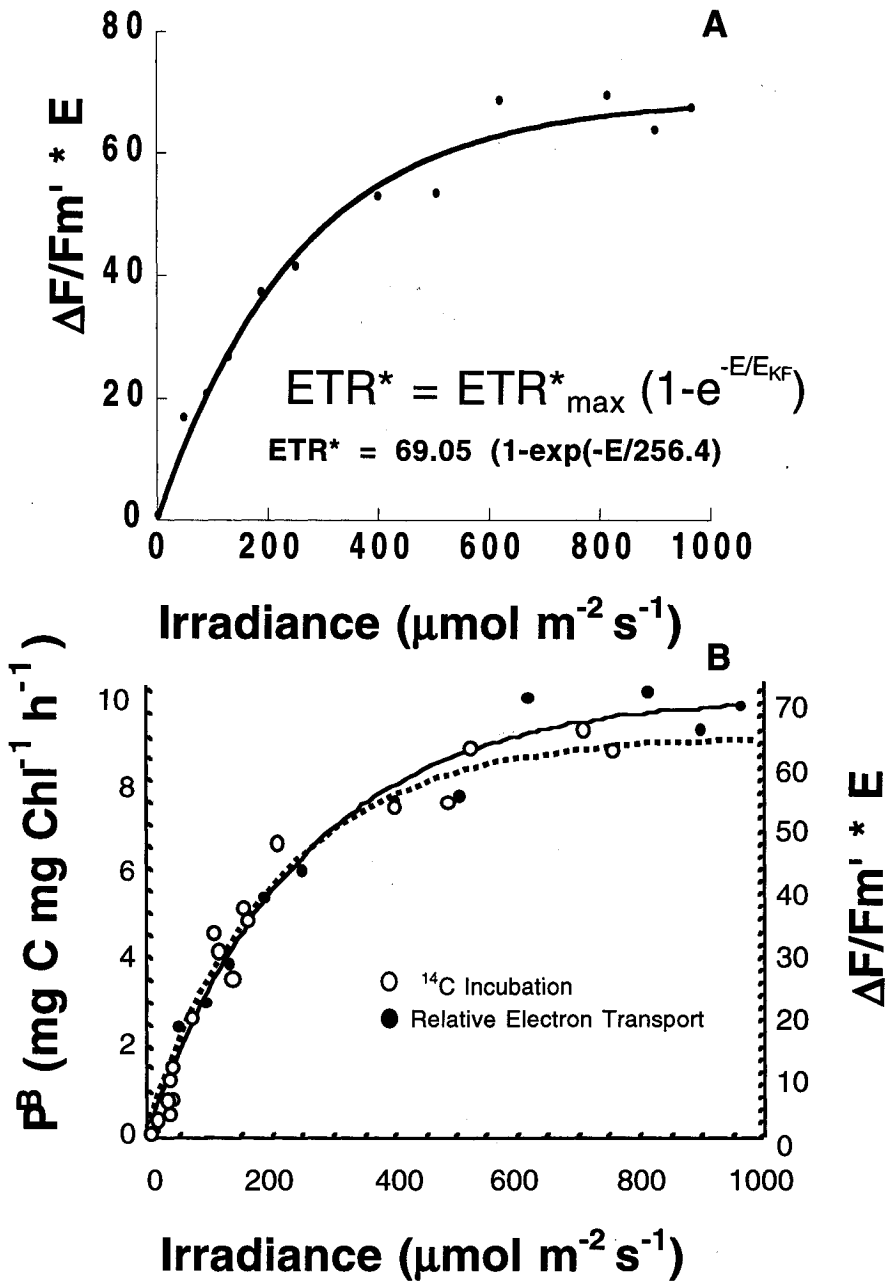

Figure 3.8 (A) The integrated photochemical quenching term (Genty Yield) multiplied by the ambient irradiance provides a relative effective electron transport (ETR*), which is a function of irradiance. The 20 minute integrated value is for a replete culture grown at 350 μmol m^{-2} s^{-1}. Equation of the trendline is inset. (B) Comparison of the two independent systems shows that the relative electron transport estimate is correlated to saturation of production as determined from ^{14}C incubation experiments. Trendlines for both ^{14}C incubation (·····) and relative electron transport (—) are provided for clarity. A table with correlation coefficients for all curves is provided in appendix B.

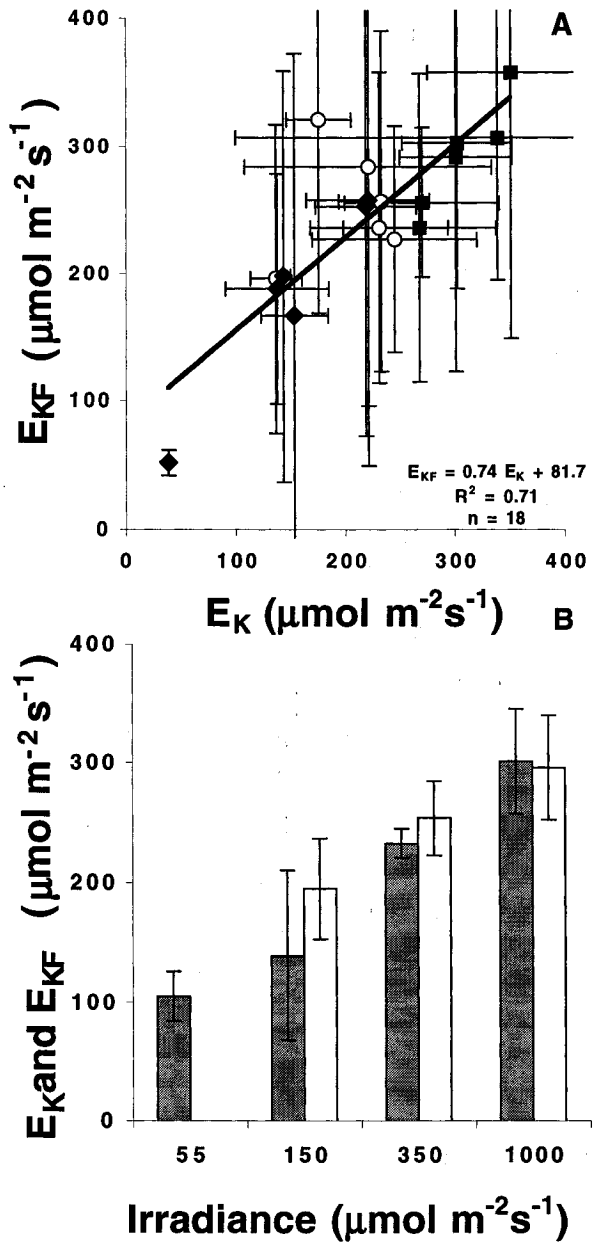

Figure 3.9 Parameter of light saturation (E_K) determined from two different measurement systems (^{14}C incubation experiments and PAMoTron) shows strong agreement over the different light levels investigated (◆ 150, O 350, and ■ 1000 µmol $m^{-2}s^{-1}$). Points represent paired determinations of the saturation irradiance for photosynthesis determined from ^{14}C uptake (E_K) and variable fluorescence as a function of irradiance (E_{KF}) for 18 experiments (duplicate determinations for triplicate cultures at three irradiance levels for growth +/- 95% confidence limits for the estimate). (B) Averaged E_K ▨ and E_{KF} □ for different growth treatments is a function of growth irradiance. Means ± SD of triplicate samples measured in duplicate. E_K for 55 µmol $m^{-2}s^{-1}$ is shown for reference (Cullen unpublished).

were 253 ± 31 and 232 ± 12 (μmol m^{-2} s^{-1}, ± SD), and for 1000 μmol m^{-2} s^{-1} E_{KF} and E_K was 296 ± 44 and 301 ± 44 (μmol m^{-2} s^{-1}, ± SD) (Figure 3.9B). One-way ANOVA to test differences between the three growth irradiances was done using the general linear models procedure in SAS. When significant effects were observed, the Tukey-Kramer least square means test was used to determine differences between means. The selected alpha error rate was $P > 0.05$. Significant differences between 150 μmol m^{-2} s^{-1}, 350 μmol m^{-2} s^{-1} and 1000 μmol m^{-2} s^{-1} are observed ($P < 0.001$, $n = 3$) (Figure 3.9B).

3.5.6 NPQ and growth irradiance

Non-photochemical quenching increases as a function of ambient irradiance (Figure 3.10). High energy state transitions (qE) were observed on rapid time scales of 4 minutes or less and appear to be the dominant role in quenching compared to state transitions and inhibition (qT and qI) for incubation periods of ~ 20 minutes (Figure 3.7). Changes consistent with qT and qI were observed on time scales of 6 to 20 minutes for the samples under high ambient irradiance (Figure 3.7). Although the rate of NPQ onset could not be determined due to instrument constraints on the sampling rate of each culture, the maximum value for the different growth irradiances investigated was determined. Triplicate samples fit to a mechanistic model using non-linear curve fitting (MATLAB program created by Richard Davis (Dalhousie University) providing average NPQ curves

for the 3 growth irradiances investigated. Non–photochemical quenching was determined at the 20 minute incubation interval as a function of irradiance.

$$NPQ_i = NPQ_{\max}(1 - e^{(-E_i / E_{K\text{-}NPQ})}) \qquad 3.3$$

From this exponential function maximal non-photochemical quenching (NPQ_{max}) and the parameter for light saturation for non-photochemical quenching ($E_{K\text{-}NPQ}$) were determined. Non-photochemical quenching curves for 150, 350, and 1000 μmol m^{-2} s^{-1} were 1.62*(1-exp(E/ 236.7)), 1.59*(1-exp(E/ 277.1)) and 1.79*(1-exp(E/ 232.6)) respectively ($R^2 > 0.98$, $n = 3$). Maximum non-photochemical quenching (NPQ_{max}) comparisons of 350 and 1000 μmol m^{-2} s^{-1} showed significant differences ($P < 0.05$, $n = 3$), although no differences between 150 and 350 μmol m^{-2} s^{-1} were observed (Figure 3.10, Appendix B).

3.6 Discussion

3.6.1 Blanks and time-zero variability

Variability between sample cuvettes was observed, although it was too small to be significant for the analysis (< 5% deviation compared to average sample signal). Differences were attributed to cuvette imperfections and sampling error. Cuvette imperfections were corrected for by subtracting individual blank values from the discrete samples. Initial fluorescence readings of dark adapted samples showed no differences in F_o and F_m respectively ($P < 0.10$, $n = 12$). The initial F_v/F_m values were similar when

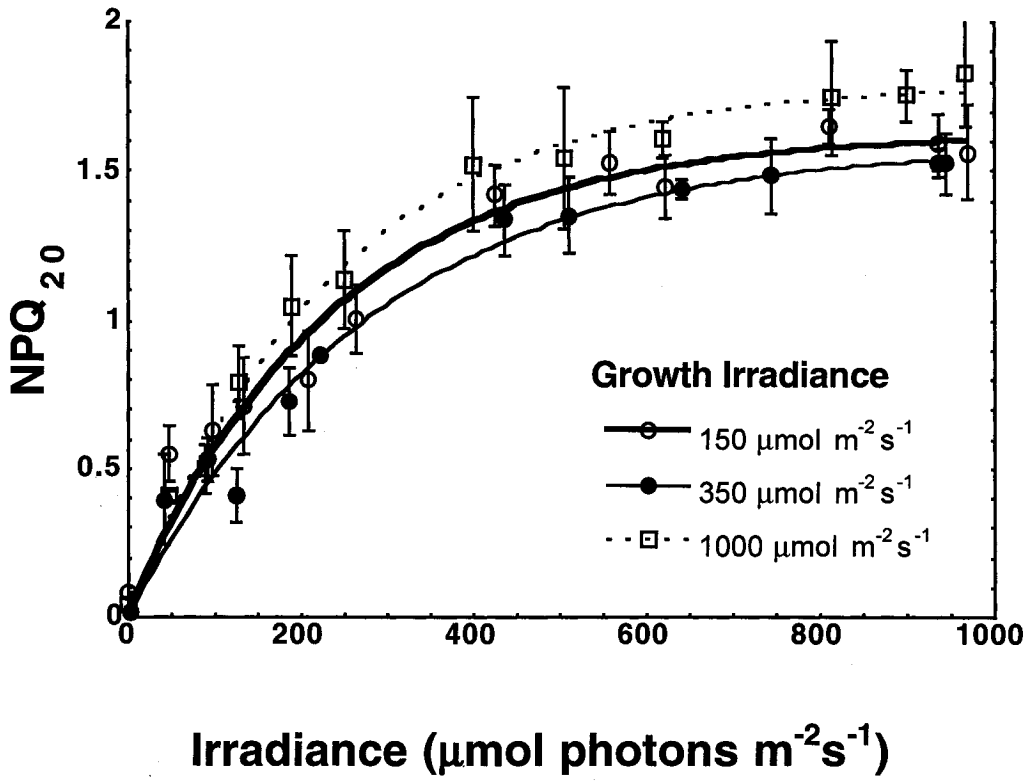

Figure 3.10 Determination of non-photochemical quenching (NPQ_{20}) determined at the 20 minute incubation interval as a function of irradiance for nutrient replete cultures grown under 150, 350 and 1000 µmol $m^{-2}s^{-1}$. NPQ was calculated using maximal fluorescence under dark and ambient light $((F_m-F_m')/F_m')$ for 20 minute incubations. Means ± SD for triplicate cultures. Parameters from individual curves are provided in Appendix B.

comparison between cuvettes was done, providing evidence that initial samples conditions and physiological state for individual cuvettes were comparable.

3.6.2 Fluorescence measurements

The new measurement system showed the high energy state quenching (qE) on fast time scales (< 4minutes) appeared to be the dominant process of non-photochemical quenching in the samples investigated (Figure 3.7). This is consistent with what has been described in the literature (Horton et al. 1994; Ruban and Horton 1995; Muller et al. 2001; Ruban et al. 2001). State transitions (qT) appear to be minor on time scales of 5-20 minutes, although there is also a problem of confounding the effects of state transitions with photoinhibition (qI) which were not resolved in this study. The different quenching mechanisms can be resolved by conducting relaxation kinetics experiments to see how much of the non-photochemical quenching is reversible on short time scales (minutes to hours) (Ruban et al. 2001). Temporal resolution of the fluorescence metrics could not be determined on short time scales (<2 minutes), therefore ETR was integrated over the 20 minute incubation period. Future versions of this new measurement system may resolve fast fluorescence kinetics (<2 minutes), however, the current version which measures samples averaged over a set time period still provides a better representation of the physiological status than an incubated sample with no temporal resolution.

Changes in electron transport rate (ETR) as a function of irradiance have been measured in some studies (White and Critchley 1999; Barranguet and Kromkamp 2000;

Kühl et al. 2001), but the kinetics of the short time scales (< 2minutes) and light pre-conditioning as the instrument imposes successive increases in ambient irradiance have not been resolved. The fluorescence measurements from these studies had subsamples altered through artificially increasing light field and thereby losing the temporal component of the changes in the fluorescence properties, as well as physiologically relevant data. Sequential changes confound temporal and irradiance-dependent changes in the fluorescence proxy of photosynthetic pathways and makes a potential determination of photosynthesis at any one irradiance ambiguous. There is an implicit assumption when quantifying ETR that the algal population has not been exposed to stress prior to the start of the experiment; quenching is calculated using a reference F_m to be compared to all the subsamples. When pseudo-replicates are run on the same sample through time, while changing the conditions, this assumption is violated. A more reasonable approach is to have independent samples at the desired irradiance levels and monitor them independently through time. The PAMoTron provides data from independent sub-samples and allows direct comparison of samples trained in different ambient light conditions.

3.6.3 E_K and E_{KF} comparison

The light saturation parameter (E_{KF}), a fluorescence metric determined from the relative ETR, shows promise as an indicator of physiological status. The results show that decreases in E_{KF} occur under lower growth irradiance for the nutrient-replete growth conditions investigated (Fig 3.9). The parameter E_K is not a static number (Falkowski

1980; Demers et al. 1991; Falkowski et al. 1994) and should show differences due to growth irradiance, but also as a function of temperature and nutrient availability (Falkowski 1992). Since E_K will be altered by changes in absorption cross section and should be relative to the maximum rate of electron transport, physiological stress influencing the maximum quantum yield of photosynthesis should be manifested in a higher E_K.

For this study on a unialgal diatom culture grown under nutrient-replete conditions at three different light intensities, there was strong agreement ($R^2 = 0.71$, $n = 18$) between the parameter of light saturation determined by the new measurement system and the conventional ^{14}C incubation method (Figure 3.9). It should be noted that my experiments investigated only one species and therefore identification of genetic constraints or interspecies differences should be further investigated. Any time a new measurement system is incorporated in scientific investigations, it is important to ground truth it with systems which investigate similar processes. The strong correlation between the two independent measurement systems provide evidence that the new measurement system accurately reflects changes in physiological parameters when culture conditions (i.e. growth irradiance) are altered.

3.6.4 E_K and E_{KF} and growth irradiance

The parameter of light saturation determined from fluorescence metrics (E_{KF}) and ^{14}C fixation experiments (E_K) increased with increased growth irradiance (Figure 3.9). This

is consistent with observations described in the literature (Geider et al. 1996; Johnson 2001). Johnson (2001) shows lower intrinsic efficiencies of light utilization, therefore increased parameters of light saturation under increased growth irradiance. Cultures can photo-acclimate and can partition energy into different strategies to maximize growth (Geider et al. 1996). Under increased irradiance, a photo-protective strategy would be incorporated involving reduced light harvesting centers and increased protective pigments (i.e. pigments of the xanthophyll cycle). Also, since cultures would be under excess light at high growth irradiances the requirement to harvest light at lower irradiances would be less important for achieving maximal growth rates. This may cause the observed shift of increased E_K and E_{KF} under increased growth irradiance. Values of E_K and E_{KF} for all growth irradiances were significantly different, although smaller differences were observed between 150 μmol m^{-2} s^{-1} and 350 μmol m^{-2} s^{-1}. This discrepancy may be attributed to differences in light cycles, with the lower light level under a 24 hour light cycle. A culture grown under a 24 hour light cycle of a lower growth irradiance would have an increased amount of absorbed irradiance compared to a culture grown under a 12:12 light dark cycle of the same irradiance, perhaps resulting in an increase in E_K and E_{KF}.

3.6.5 NPQ and growth irradiance

When excitation energy is in excess of that required to reduce the photosynthetic electron chain (photochemical quenching), and cannot be dissipated safely, the excess irradiance can cause photodamage to the photosynthetic apparatus even at low irradiance.

Changes in PSII photochemistry in light-adapted algal species (i.e. increased NPQ) can be seen as regulatory responses to down-regulate the quantum yield of PSII electron transport (Havaux et al. 1991; Pospisil 1997).

The higher light level (1000 μmol m^{-2} s^{-1}) was significantly different and showed increased NPQ compared to the two other growth irradiances (Figure 3.10, $P < 0.10$, $n = 6$). Although the results show a significant difference, the differences are marginal and the changes between growth irradiances small and may not be ecologically relevant. Regardless, this finding of increased NPQ at high light in comparison to low light is consistent with the literature (Demmig-Adams and Adams III 1992; Horton et al. 1996; Park et al. 1996). Park et al. (1996) showed that cultures grown on high-light have a greater capacity for both photochemical and non-photochemical dissipation of absorbed energy and have the same intrinsic capacity for D1 synthesis, a mechanism employed by low-light cultures to regulate excess light. Therefore high-light cultures can employ the photoprotective strategies and mechanisms reducing their susceptibility to photo-damage. The principal role of NPQ is to maintain a balance between maximizing the efficiency of photosynthesis at low light and minimizing the damage to the photosynthetic apparatus under excess light conditions by directly quenching excited states in the antennae before damage occurs (Owens 1994). Therefore, when cultures are grown under high growth irradiance, they can employ different physiological strategies including reduced chlorophyll concentrations, lower intrinsic efficiencies of light utilization (≈ increased E_K), and a higher capacity for thermally dissipating excess light energy (increased NPQ). My results are consistent with these strategies (Figure 3.9, 3.10). Acclimation at high

growth irradiance shows increased capacity for thermal dissipation of excess energy and increased NPQ. This is beneficial in avoiding damage due to the absorption of excess light energy and advantageous under excess light energy and under physiological stress.

A complication of the investigation of the effects of NPQ under different growth irradiances is that my low-light cultures (150 μmol m^{-2} s^{-1}) were grown with a 24 hour light period, which shows comparable findings to the medium light level (350 μmol m^{-2} s^{-1}) on a 12:12 light cycle. I believe this is the reason that no significant difference was observed between the 150 μmol m^{-2} s^{-1} (24 h) and 350 μmol m^{-2} s^{-1} (12:12 light cycle) grown cultures ($p > 0.10$, $n = 3$). Further investigation not only into the intensity, but also the duration of the light period is warranted to elucidate these differences. There may be some advantage for persistent light activation. If NPQ does not fully revert over the night period, then it could rapidly form photo-protective processes upon illumination giving elevated levels of NPQ. Maxwell (1994) showed zeaxanthin pools persist during the dark period under constant daily light activation, giving the selective advantage for the subsequent light period (Ruban and Horton 1995).

3.6.6 Advantages and limitations of the measurement system

The proposed fluorescence measurement system has advantages and limitations for algal research. The main advantage of the new measurement system is the potential to assess changes in relative electron transport rates as well as NPQ mechanisms using fluorescence on physiologically relevant time scales. Photo-acclimation and

photoinhibition studies range from 10 minutes to days, resolving qI (photoinhibitory processes) (Olaizola and Yamamoto 1994; Ting and Owens 1994; White and Critchley 1999), while the ability for the cell to react on the minute time scale still remains unresolved. This new measurement system allows for resolution of fluorescence metrics on time scales which are physiologically representative of changes in algal populations (hours-days). The instrument is non-invasive, easy to use, and allows determination of electron flow in relatively real time. Unlike other measurements systems such as rapid light curves from the MINI-PAM, the PAMoTron allows parallel fluorescence measurements as opposed to sequence sampling that allows for the culture to fully acclimate to a predetermined light level. Rapid light curves show changes in electron transport rates when a series of increasing shifts in irradiance levels were applied to the sample. The disadvantage of this system is that the photosynthetic apparatus is affected by the light conditions when the measurements are taken in sequence. Therefore, light steps (100-2200 $\mu mol\ m^{-2}\ s^{-1}$) during a 90 second recording time may alter levels of electron transport rates at higher irradiance levels in a manner that may be a function of preconditioning. Another limitation of the rapid light curve technique is the inability for determination of fluorescence kinetics at any one light level because the light conditioning is not imposed on discrete samples. The PAMoTron removes any biases that could be caused by placing a sample in increasing irradiance levels over tens of minutes. This approach allows the observation of photosynthetic fluorescence adjustments to a range of light levels, not a sequence, so time dependence at each light level can be resolved (Figure 3.7).

The parallel measurements from the new system allow accurate determination of fluorescence metrics vs. irradiance and important kinetics previously unavailable to dark-adapted measurements. An active fluorometer can monitor fluorescence characteristics under ambient light conditions; however, measuring fluorescence yields at different irradiance levels at the same time would require either a number of active fluorometers or one system whereby individual samples are observed at different irradiances through a temporal sequence of neutral density filters (Cullen et al. 1997; White and Critchley 1999). Having numerous active fluorometers is impractical, but making measurements over time is necessary to resolve important temporal components of non-photochemical quenching. Temporal variability in fluorescence metrics can reveal the physiological status of the cell, which shows fundamental relationships with nutritional status (Chapter 4). The PAMoTron allows for measurement of fluorescence parameters on the minutes time-scale, while eliminating the compound effects of pseudo-replicating samples through sequentially changed multiple irradiance levels.

The PAMoTron does have limitations. It is unable to resolve important kinetics on the second to minute time scale. The current system configuration does not allow resolution below 5 minutes and the measurement of discrete samples of a haphazard arrangement will cause fluctuations within short-term measurements of the incubation experiments (Figure 3.7B). These fluctuations are attributed to photoprotective and photoinhibitory processes in the light harvesting complex (LHC) and the reaction centers and may hold key answers to the effect of physiological stress on the photosynthetic

apparatus. Rate estimates on these short time scales with the current configuration of the measurement system can not be done.

Also, fluorescence measurements are relative values and the applicability to an unknown population with variable photosynthetic strategies (i.e. PSII:PSI ratios, accessory pigments, and physiological adaptations) is difficult. Correct determination of the F_m and F_o values (i.e. after complete dark adaptation and reversion of NPQ) is essential because all changes of fluorescence measurements made during the incubation period representing quenching mechanisms are compared to these reference levels.

The sensitivity of the instrument for applicability in the field needs to be improved. Initial trials on natural populations in a mesotrophic basin (Bedford Basin, NS, Canada) have provided results close to, or below, detection limits. Blanks and cuvette anomalies play an increasing role in the accurate determination of a reliable, repeatable fluorescence metric (Figure 3.4). Future designs should provide increased sensitivity. Changes in the spectral quality of the light field within and between different measurement systems and their effects on algal physiology were not determined. The effects were minimized by trying to mimic oceanic conditions using blue cellulose acetate and a metal halide light source, but comparison with other measurements should account for the differences in spectral quality among instruments (Harrison et al. 1985; Babin et al. 1996b). Gilbert et al. (2000) warned that instrument setup might yield measurements from distinctly different sections of the photosynthetic machinery giving erroneous or unrepeatable results within the same instrument. These differences would be compounded by comparison between different instruments in assessing productivity from different

measures of the non-cyclic electron flow. The instrument could also increase the number of subsamples at different irradiances tested. Twelve independent measurements are enough to determine parameters from the curve (Zimmermann et al. 1987), although more data would provide increased confidence in metrics being resolved.

Although the new measurement system does have some limitations, it provides reasonable estimates of relative changes in electron transport and strong agreement between the fluorescence metric E_{KF} and E_K determined by ^{14}C incubations. It also allows estimates of NPQ in 2 minute intervals or determination of values after any length of time when steady-state is reached.

3.7 Summary and conclusions

In summary, I have described a novel measurement system using 12 sub-samples under 12 different irradiance levels which allows for F vs. E curves to be measured in parallel every 2 minutes. This system is the amalgamation of a Pulse Amplitude Modulation fluorometer and a light incubation chamber providing fluorescence metrics under a suite of irradiances. These F vs. E curves work on the same premise as Rapid Light Curves (White and Critchley 1999) although the system allows for distinct incubation chambers and does not expose the sample to sequential changes in the light field. This avoids the problems of time step and pre-conditioning which occurs in the Rapid Light Curve technique. The advantage of the new measurement system is that it

provides parallel measurement as opposed to sequence, shows strong agreement with conventional measurements, is non-invasive, easy to use, and allows determination of relative electron rates in almost real time. The limitations include the inability to resolve qE rates shorter than 5 minutes, the fluorescence measurements are relative values, so absolute fluorescence yields cannot be calculated, and application to unknown populations with variable photosynthetic strategies (i.e. PSII:PSI, accessory pigments, physiological adaptations) is difficult, and the sensitivity of the current design needs to be improved.

The 20 minute integrated Genty yield parameter was multiplied by the incubation irradiance to determine the relative electron transport rate and plotted as a function of irradiance. It is well established that the saturation irradiance level (E_K) is a function of growth irradiance and physiological stress. I introduce a new determination of this saturation parameter by fluorescence (E_{KF}) which showed comparable results to E_K determined by ^{14}C incubations, therefore, E_{KF} can be used as a proxy for E_K in studies of physiological stress. E_{KF} is determined from the ETR* integrated over a 20 minute trial from the PAMoTron measurements and was a function of growth irradiance for nutrient-replete cultures.

Non-photochemical quenching (NPQ_{20}) determined from 20 minute incubations was dependent on growth irradiance and pre-conditioning for nutrient-replete cultures. NPQ_{20} increases as a function of growth irradiance and incubation irradiance for nutrient-replete cultures. This novel measurement system provides fluorescence metrics such as E_{KF} and NPQ_{max}, both appear to be sensitive to the physiological state of an algal

population, therefore rapid diagnostics of physiological stress and relative photosynthetic rates may be developed. This is extremely important for phytoplankton assessment of the oceans and as the amalgamation of current systems and new technology emerges, the investigation into the validity and accuracy of the proposed systems and their measurements will be required.

Chapter 4

Non-photochemical quenching and relative electron transport rate parameters as diagnostics of nutrient stress

4.1 Chapter overview

A new measurement system was used to determine parameters of photosynthetic electron transport rates and non-photochemical quenching (NPQ) as a function of irradiance in a neritic diatom, *Thalassiosira pseudonana*, under different nutritional conditions. Nutrient-replete, N-starved and acclimated N-limited cultures were used to investigate fluorescence-based parameters as potential diagnostics of N-stress. Investigations were conducted under two different growth irradiances (350 and 1000 μmol m^{-2} s^{-1}). The parameter of light saturation (E_{KF}; μmol m^{-2} s^{-1}) determined from the relative electron transport rates, and NPQ_{max} (determined from an exponential function fit to NPQ vs. E after 20 minute incubations) were both sensitive to N-limited and N-starved conditions, and were a function of growth irradiance: NPQ_{max} and E_{KF} increased with growth irradiance. While under increased N-stress, NPQ_{max} increased and E_{KF} decreased.

A higher ratio of photoprotective pigments to chlorophyll under N-limitation supports these findings. Furthermore, photosynthetic electron transport rates as a function of irradiance from the new measurement system showed strong correlation with conventional ^{14}C incubation experiments. Another fluorescence metric, maximum relative electron transport (ETR^*_{max}), showed strong correlation with maximal photosynthetic rate, normalized to chlorophyll, determined from ^{14}C incubation experiments (P^B_{max}). Maximum relative electron transport was a function of growth irradiance, although it was insensitive to N-stress. The proposed fluorescence metrics, NPQ_{max} and E_{KF}, were a diagnostic of N-stress when growth irradiance was the same. Consequently, the applicability of this new technique in the field is currently unclear.

4.2 Introduction

In this chapter, a new measurement system, a modulated fluorometer interfaced with a light incubation assembly (PAMoTron-Chapter 3) was used to investigate fluorescence metrics as a function of N-stress. In particular I focused on the parameter of light saturation and maximum relative electron transport rate, E_{KF} and ETR^*_{max}, determined from the relative electron transport rate, and NPQ_{max} determined from maximal fluorescence in supersaturating irradiance as compared to dark-adapted conditions, as potential metrics of N-stress. Cultures under nutrient-replete, N-limited, and N-starved conditions were investigated and the basic relationships between these fluorescence metrics and N-stress are reported.

Due to the limitations of this fluorescence method (detailed in section 3.3.2), it was not the intent of this study to develop a measurement system that can accurately determine absolute rates of photosynthesis as a function of irradiance, but to use fluorescence as a function of irradiance as a tool for determining acclimation of different phytoplankton to their environment. Although fluorescence measurements may sometimes provide a useful measure of photosynthetic performance of plants (Genty et al. 1989; Hartig et al. 1998), their real strength arguably lies in giving insight into the ability of an algal population to tolerate environmental stress and the extent to which those stresses have altered the photosynthetic apparatus.

4.3 Background

4.3.1 Fluorescence and non-photochemical quenching

If an algal cell is unable to dissipate energy absorbed by photosynthetic pigments, excess absorbed photons lead to damage resulting in photoinhibition. Photoinhibition, the loss of photochemical activity, can be detected in variable fluorescence (Prasil et al. 1992; Vass and Styring 1992). To avoid permanent photodamage, an algal cell has protective mechanisms that dissipate excess energy as heat (Krause and Weis 1991; Ibelings et al. 1994; Long et al. 1994). These types of quenching mechanisms are called non-photochemical quenching (NPQ). The general process of NPQ is a succession of different processes developing in time. One component of the NPQ is termed the energy dependent quenching (qE). It is induced by the acidification of the thylakoid lumen,

dependent on the presence of photoprotective pigments of the xanthophyll cycle (Horton et al. 1996). Energy dependent quenching occurs on time scales of seconds and can be reversed, once the light induced stress is removed. Another quenching mechanism is state transitions, qT, and involves the uncoupling of the light harvesting complex (LHC) from photosystem II (PSII). In plants, this process occurs on a 5-20 minute time scale (Laisk and Oja 2000; Muller et al. 2001). Laisk and Oja (2000) assert that state transitions (qT) are the most difficult to quantify because of the compounding effects with photoinhibition (qI), the final quenching mechanism which causes photodamage. The qT and inhibition on longer time scales (qI) would overlap, making it difficult to interpret the time-dependence of quenching (Horton et al. 1994; Laisk and Oja 2000). NPQ can be associated with photodegradation of reaction centers (Neale and Richerson 1987) photoprotective pigment cycling (i.e. xanthophyll cycle) (Demers et al. 1991; Olaizola and Yamamoto 1994; Uhrmacher et al. 1995; Schofield et al. 1998) transmembrane electrochemical potentials, state transitions and cyclic flow around PSI and PSII (Falkowski et al. 1986; Schreiber et al. 1995; Falkowski and Raven 1997). These protective processes affect the rate and amount of photochemistry and should be reflected in fluorescence metrics.

Previous methods employed by Cullen et al. (1996), Falkowski and Kolber (1993), Schreiber et al. (1995) and White and Critchley (1999) show the influence of non-photochemical quenching (NPQ) on fluorescence measurements as a function of irradiance, although the temporal changes in fluorescence measurements as a function of irradiance still needs investigation. Initial studies utilizing the non-actinic (unable to

induce photochemical reactions and close reaction centers) measuring beam in the PAM fluorometer (F_s) shows that under experimentally increased irradiance, NPQ would complicate the inverse relationship between fluorescence and photosynthesis (Schreiber et al. 1995). Since NPQ is a function of excess light, and N-stressed conditions would reduce the ability to utilize light, a relationship between N-stressed conditions and NPQ as a function of irradiance should exist.

4.3.2 Fluorescence and nutrient stress

It is important to understand the distinction between types of N-stress. Nutrient stress refers to both N-limitation and N-starvation. Nutrient limitation refers to balanced, steady-state N-limited growth, where cellular components have acclimated to a reduced nutrient supply, whereas N-starvation refers to unbalanced growth during which the availability of a limiting nutrient decreases relative to cellular demand (Shuter 1979; Eppley 1981; Cullen et al. 1992b). For further clarification see Section 2.3.2. In this chapter, "nutrient stress" refers solely to "nitrogen-stress" and the terms are used interchangeably within the text, since nitrogen was the only nutrient investigated in my experiments.

The physiological state of microalgae is different in cultures grown under N-stressed and nutrient-replete conditions (Falkowski and Raven 1997). By quantifying physiological shifts under N-stress, diagnostics may be developed for robust relationships between fluorescence metrics and N-stress. Chloroplasts and proteins rich

in nitrogen, are more susceptible to N-stress because they turn over rapidly in response to the particularly large swings in redox potential (Turpin 1991). However, both proteins with normally high levels of turnover such as reaction center proteins D1, D2, and CP43 as well as slower turnover, non–reaction center proteins such as ribulose-1,5-bisphosphate carboxylase/oxygenase (Rubisco) are sensitive to N-stress (Falkowski et al. 1989; Beardall et al. 1991; Vasilikiotis and Melis 1994). Because it alters the production of necessary proteins, N-stress leads to altered photosynthetic functionality. For example, reaction center proteins, which are crucial to the efficient use of absorbed light energy, can become damaged under N-stress which can lead to marked reductions in PSII conversion efficiencies and lead to overall increase in the functional size of PSII antennae (Cleveland and Perry 1987; Geider et al. 1998). In addition to these direct effects other components and processes of photochemistry are affected by N-stress. For example, pigment concentrations are dramatically altered under N-stress including chlorosis as well as the relative increase in non-photosynthetic pigments (Sosik and Mitchell 1991; Latasa and Berdalet 1994). In turn, these changes in pigmentation can affect absorption properties (Sosik and Mitchell 1991; Geider et al. 1993a).

From studies of the effects of N-stress on protein turnover and expression, it is not surprising that photosynthetic rates and efficiencies are significantly reduced under N-stress (Cleveland and Perry 1987; Sosik and Mitchell 1991; Geider et al. 1993a). These reductions are characterized by decreases in the magnitude and altered structure of photosynthesis vs. irradiance curves, determined from ^{14}C incubation experiments, and specifically result in reduced P^{B}_{max} and quantum efficiencies. However the effect of N-

stress, and more specifically N-limitation, has been difficult to resolve (Cullen et al. 1992b).

At low irradiances, a depressed fluorescence yield would be the result of photochemical quenching (open reaction centers), while at supersaturating irradiances (when most reaction centers are closed) the fluorescence yield is reduced by NPQ. The effect that N-stress has on this fluorescence yield is not well understood, but it is clear that determining the changes in non-photochemical quenching (NPQ) under varying levels of irradiance is essential for resolving the relationship between fluorescence and physiological stress. Babin et al. (1996a) attributes reduced solar induced chlorophyll fluorescence yield to NPQ, stating that the relative importance of NPQ is altered by photodamage from excessive light, intracellular accumulation of non-photosynthetic pigments and N-limitation. Babin et al.(1996a) stated that N-limitation would decrease the functional reaction centers in high irradiance causing a decrease in fluorescence yield. Letelier et al. (1997) presented a contradictory argument, suggesting that increased fluorescence yield occurred under N-limitation because the probability that photochemical reactions would occur was reduced. However nutrients were never measured in their study and limitation was assumed from calculations of water column vertical fluxes of nutrients. If the fluorescence yield is influenced by NPQ and is a function of N-limitation, then the threshold of transition should reflect the photo-physiological status of the cell. Also, since NPQ is time dependent, the temporal resolution of an algal cell's ability to "protect" itself should also reflect reduced photosynthetic efficiency under less favorable conditions. Letelier et al. (1997) discussed the importance of temporal variability in

natural fluorescence and its relationship with chlorophyll concentration and hypothesize that it could prove to be a useful tool for indicating N-limitation. Further support by Genty et al. (1989) showed departure from the linear relationship between photochemical quenching and quantum yield of non-cyclic electron flow when light intensity was increased. Exploring the role of N-limitation in this departure by temporal resolution of the NPQ and fluorescence yield will show the algal cell's ability to cope with increased irradiance, through physiological shifts such as photoprotective pigment pool "cycling" (i.e. xanthophyll) (Demmig et al. 1987; Schubert et al. 1994; Schofield et al. 1998).

If the measurement of F_v/F_m is inadequate to resolve the effects of N-stress for all growth conditions (Parkhill et al. 2001) and cannot serve as a diagnostic for N-stress under varying, ambient irradiance levels, then more sensitive methodologies and sampling tools are necessary. Dark adaptation may oversimplify the effects of NPQ and the role of fluorescence as an indicator of N-stress in phytoplankton physiology. The ability to resolve NPQ and fluorescence yield under varying irradiance levels for different nutritional regimes in real time is the goal of this work and will contribute to insight into the physiological state of algal species, and may provide a tool for determining N-stress in the natural environment.

4.3.3 Effects of preconditioning and growth irradiance

All estimations of NPQ are strictly relative to some dark-adapted point (Chapter 3; Figure 3.1). For this reason, it is necessary to design experiments in such a way that a

dark-adapted reference point, F_m, can be estimated. This may be a major limitation for using this fluorescence metric in the field, since a sufficiently long dark period (> 10 minutes) would be required before determination of fluorescence metrics can be done. Although, relative fluorescence metrics (i.e. F_v/F_m) for dark-adapted samples have the advantage of not requiring calculation of absolute fluorescence yield and therefore allowing comparison between different natural assemblages.

Light history (i.e. growth irradiance) of acclimated cultures plays an important role in determining the fluorescence signature of the culture investigated. Cultures grown at high light accumulate non-photosynthetic pigments and therefore an increased NPQ potential (Demers et al. 1991; Demmig-Adams and Adams III 1992; Casper-Lindley and Björkman 1998). For example, photoacclimation to high-light can increase photosynthetic capacity (P^B_{max}) and decrease PSII functional cross-sectional area and photosynthetic unit size (Falkowski et al. 1981; Kolber et al. 1988). High growth irradiance has also been shown to dramatically reduce light utilization and quantum efficiency relative to low-light grown populations while not significantly affecting the maximal quantum yield of PSII (F_v/F_m) (Kolber et al. 1988; Marra et al. 2000). Photosynthetic unit turnover rates can also be influenced by growth irradiance (Falkowski et al. 1981; Dubinsky et al. 1986; Behrenfeld et al. 1998).

Changes in abundance and ratios of pigments can determine the amount of absorbed light energy and the relative proportions that this light will be dissipated (heat, fluorescence, or photochemistry). A change in chlorophyll $cell^{-1}$ is a function of growth irradiance, whereby low-light adapted cells increase their pigment concentrations to

increase light absorption, while high-light cultures may increase the relative proportions of photoprotective pigments such as carotenoids (Demmig-Adams 1990; Owens 1994; Geider et al. 1998). Two different irradiance levels were investigated to examine the effects of photoacclimation on the ratio and abundance of both photosynthetic and photoprotective pigments.

The new measurement system determines fluorescence metrics under ambient light and allows calculation of E_{KF}, ETR^*_{max}, and NPQ_{max} as diagnostics for N-stress conditions. E_{KF} is the parameter of light saturation determined from relative electron transport curves, while ETR^*_{max} represents the maximal assimilation rate at saturating irradiance, and NPQ_{max} is the maximal rate of non-photochemical quenching indicating the relative down regulation of PSII photochemistry by increased heat dissipation, a photoprotective strategy, therefore these parameters should reflect the physiological healthiness of the algal population. Investigation of nutrient-replete, N-limited, and N-starved growth conditions under 2 different growth irradiances (350 $\mu mol\ m^{-2}\ s^{-1}$ and 1000 $\mu mol\ m^{-2}\ s^{-1}$) allowed fundamental relationships between fluorescence and nutrient and light stress to be determined.

4.4 Materials and methods

4.4.1 Culture conditions

The culture conditions and methods have been previously described in sections 2.4.1, 2.4.2, and 3.4.2. Although the methods remain predominately unchanged they are

included below for the convenience of the reader.

Semi-continuous, continuous and batch type experiments were performed on unialgal cultures of a neritic diatom, *Thalassiosira pseudonana.* Triplicate cultures grown under 350 μmol m^{-2} s^{-1} and duplicate cultures under 1000 μmol m^{-2} s^{-1} were sampled daily in triplicate (3 hours into the light period) for cell counts, nutrient concentration, and chlorophyll concentration, dilution rates and fluorescence (Table 4.1). I monitored these parameters to determine when a culture had met the predetermined criteria for the desired growth condition (i.e. continuous cultures showed N-limited steady-state growth rates for at least 10 generations within 10%) (Chapter 2, Figure 4.1). Growth irradiance level for the 350 μmol m^{-2} s^{-1} grown cultures was achieved using 40W Vita-lite full spectrum fluorescent bulbs, while 1000 μmol m^{-2} s^{-1} growth irradiance culture conditions used 500W portable halogen lights in a flow through water bath, mirrored oven glass assembly (Chapter 3). Photosynthetically Available Radiation (PAR) was measured with a Biospherical Instruments Inc. QSL-100 4π sensor. Temperature was controlled at 20.0 ± 0.5°C. All cultures were continuously mixed with magnetic stirrers and aerated with sterile air.

Nutrient-replete cultures were grown at the two different growth irradiances and were diluted approximately 5:1 daily to maintain relatively low cell concentrations and to obtain a constant exponential, maximal irradiance-limited growth rate. Continuous cultures had a constant predetermined inflow rate (Table 4.1) of N-deficient (50 μmol l^{-1}) F/2

Table 4.1 A summary of all the experiments performed, with the initial nutrient concentrations, light levels, growth rates, maximal growth rates and duration of the individual experiments. Cultures were grown under 12:12 light dark cycles.

Type of Experiment	Initial N levels ($\mu mol\ L^{-1}$)	Irradiance ($\mu mol\ m^{-2}\ s^{-1}$)	μ (d^{-1})	μ_{max} (d^{-1})	Duration (d)
BALANCED GROWTH					
Semi-Continuous	880 (NO_3^-)	350	1.48	1.48	15
(N-replete)	880 (NO_3^-)	1000	1.82	1.82	21
Cyclostat	50 (NO_3^-)	350	1.20	1.48	34
(N-limited)	50 (NO_3^-)	350	0.80	1.48	35
	50 (NO_3^-)	350	0.40	1.48	35
	50 (NO_3^-)	350	0.40	1.48	35
Cyclostat	50 (NO_3^-)	1000	1.45	1.82	32
(N-limited)	50 (NO_3^-)	1000	1.1	1.82	32
	50 (NO_3^-)	1000	0.75	1.82	38
	50 (NO_3^-)	1000	0.36	1.82	38
UNBALANCED GROWTH					
Batch- N-Starvation	< 50 (NO_3^-)	350	Variable	1.48	7
	< 50 (NO_3^-)	1000	Variable	1.82	7

medium (Guillard and Ryther 1962). Cultures (2.1 L) were grown in 2.5L polycarbonate bottles. Culture medium inflow was through silicone tubing using a Masterflex peristaltic pump, with all sub-samples withdrawn from the growth chamber using sterile syringes. For batch culture experiments, nitrogen starvation was imposed by stopping flow of the medium in N-limited continuous cultures causing unbalanced growth. The cultures were monitored and sampling was conducted when the cells were in late starvation.

4.4.2 Measurements

Cell concentration was measured after dilution on a Coulter Multisizer Particle analyzer (Coulter Electronics of Canada, LTD., Burlington, Ontario, Canada) calibrated with latex beads. Nitrate concentrations were determined from filtered samples of culture medium by a Technicon Autoanalyzer (Technicon Co, Tarrytown, NY Grasshoff et al. 1976). Chlorophyll *a* concentration corrected for phaeopigments was measured using a Turner Designs (Sunnyvale CA) fluorometer (100005R) calibrated with pure chl a (Sigma Chemical Co, St Louis, MO). Volumes of 1mL were filtered on Whatman GF/F filters (Whatman Inc., Clifton, NJ) and extracted in 10mL of 90% acetone in the dark at –15°C for at least 24 hours. Dilution rates were used to determine growth rates (Equation 2.5, Chapter 2). Fluorescence measurements were taken from dark-adapted (30 minutes) samples for determination of maximal quantum yield of PSII (F_v/F_m) using a Turner Designs fluorometer and DCMU methodology. No neutral density screening was used in

the Turner Designs fluorometer because growth irradiances (350 μmol m^{-2} s^{-1} and 1000 μmol m^{-2} s^{-1}) were sufficiently high.

Once the desired growth condition (nutrient-replete, N-limited, N-starved) was achieved, the new measurement system (PAMoTron) (Chapter 3) and ^{14}C incubation experiments were used to determine electron transport rates and photosynthesis vs. irradiance curves respectively. The PAMoTron was used to measure fluorescence parameters under 12 ambient light conditions to allow determination of relative electron transport ($ETR^* = \Delta F/F_m' * E$) and non-photochemical quenching (NPQ_{20}: $(F_m-F_m')/F_m'$) over a 20 minute incubation. An exponential function was fit to relative electron transport (ETR^*_i) as a function of irradiance (E_i) to determine maximal relative electron transport (ETR^*_{max}) and the parameter of light saturation (E_{KF}) (Equation 4.1), using the protocol for the fluorescence measurement system as described in Chapter 3.

$$ETR_i^* = ETR^*_{\max}(1-e^{(-E_i/E_{KF})}) \qquad 4.1$$

NPQ_{20i} were plotted as a function of irradiance (E_i) and an exponential function was fit to the data. Maximal non-photochemical quenching (NPQ_{max}) and the parameter of light saturation for NPQ ($E_{K\text{-}NPQ}$) were determined from this non-linear curve fit (Equation 4.2).

$$NPQ_{20i} = NPQ_{\max}(1-e^{(-E_i/E_{K-NPQ})}) \qquad 4.2$$

The carbon fixation incubation studies (P vs. E curves) were also fit to an exponential function and the maximal photosynthetic rate (P^B_{max}) and parameter of light saturation from carbon uptake (E_K) were determined (Equation 4.3).

$$P_i^B = P_m^B(1 - e^{(-E_i/E_K)}) \qquad 4.3$$

Triplicate samples (25mL) were filtered on GF/F filters and frozen in liquid nitrogen for pigment analysis by high performance liquid chromatography (HPLC) at the same time as the ^{14}C incubation experiments and the PAMoTron measurements. Pigments were analyzed following the method of Head and Horne (1993). Of the main carotenoids found in the samples, fucoxanthin, 19-hexanoyloxyfucoxanthin and zeaxanthin are treated as photosynthetic pigments, while diatoxanthin and diadinoxanthin are treated as photoprotective pigments. Because of the rapid epoxidation of the xanthophyll cycle, I combined concentrations of diadinoxanthin and diatoxanthin for analysis.

4.4.3 Statistics

To determine steady state and routine measures, analysis of variance (ANOVA) involving repeated measures analysis was performed in the statistical package SAS® (Statistical Analysis Software Version 8, SAS Institute Inc. Cary NC). To determine the statistical significance of different parameters, linear regression analysis was performed using Minitab statistical analysis software Version 1.3 (Minitab Inc, State College PA). If a significant linear regression was observed, ANOVA using the general linear models

procedure in SAS was conducted to determine where the differences existed. Tukey-Kramer least square means test was used to determine differences between means. The selected alpha error rate was $P > 0.05$. For determination of F vs. E, P vs. E, and NPQ_{20} vs. E curves, non-linear regressions were done using MATLAB (5.2) non-linear fit routine and 95% confidence intervals were determined for E_K, E_{KF}, $E_{K\text{-}NPQ}$, P^B_{max} ETR^*_{max}, and NPQ_{max} using the nlparci routine (code written by Yannick Huot, Dalhousie University).. Correlation between F vs. E and P vs. E curves for individual samples was done by comparing values at light-saturating (500 µmol m^{-2} s^{-1}) and light-limiting (50 µmol m^{-2} s^{-1}) conditions.

4.5 Results

4.5.1 Culture conditions

Continuous cultures at 350 µmol m^{-2} s^{-1} and 1000 µmol m^{-2} s^{-1} growth irradiance under multiple N-limited growth rates each showed nearly constant physiological parameters when monitored for a minimum of 10 generations prior to sampling (Figure 4.1). Experiment durations for N-limited cultures were a minimum of 30 days to ensure that the cyclostat cultures had achieved balanced steady-state growth. As expected, chlorophyll $cell^{-1}$ decreased as a function of N-limited growth rate for both irradiance levels, and maximal quantum yield of PSII (F_v/F_m) remained maximal (~ 0.65) and constant throughout the N-limited experiments (Figure 4.1). Sampling of balanced N-limited

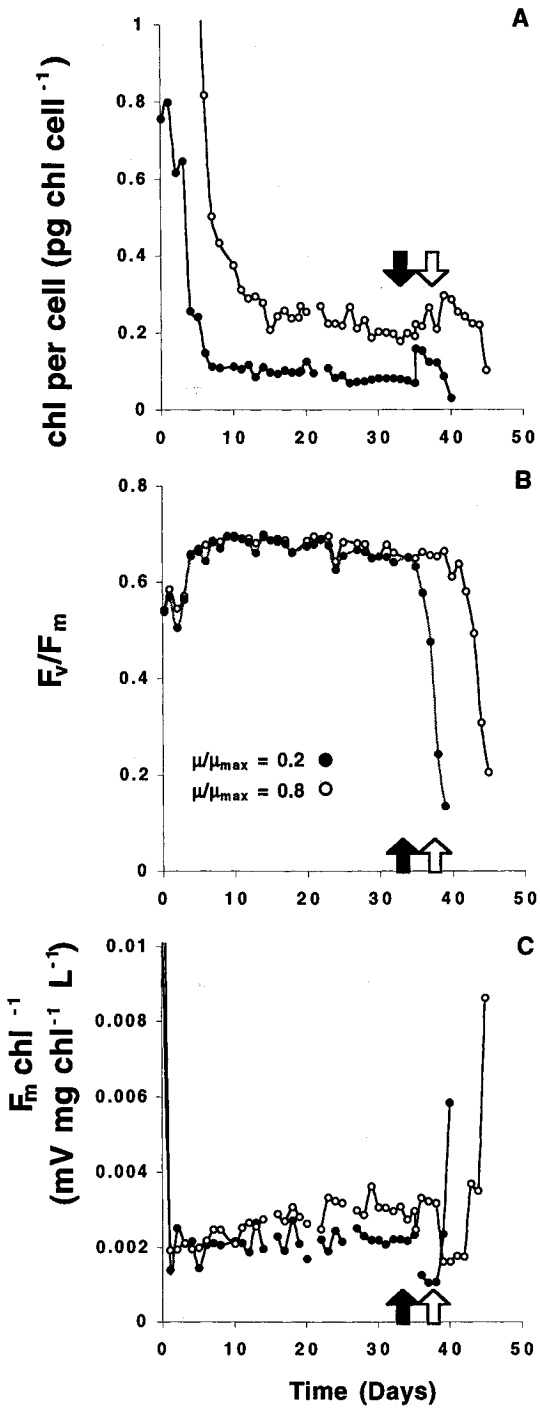

Figure 4.1 Physiological parameters of *Thalassiosira pseudonana* as a function of time for determining balanced and unbalanced growth conditions. Representative low N-limited growth rates (●) and high nutrient-limited growth rates (O) grown under 1000 μmol m^{-2} s^{-1}. General parameters for N-limited cultures grown under 350 μmol m^{-2} s^{-1} are previously reported (Chapter 2 - Figure 2.7). Parameters shown as a function of time include changes in (A) Chl per cell , (B) F_v/F_m, and (C) F_m per unit chl. Sampling of acclimated cultures occured 1-3 days prior to initiation of the starvation experiment. The start of the nutrient starvation experiments are shown as ⬆ and ⇧ for the low and high N-limited growth rate cultures respectively.

growth conditions was done one or two days prior to the start of N-starvation experiments shown in Figure 4.1. Other parameters such as cell concentration, nutrient concentration, and growth rate showed similar trends of physiological regulation and balanced growth (data not shown). Repeated measures analysis in SAS® (Statistical Analysis Software Version 8, SAS Institute Inc. Cary NC) showed that the cultures did not vary significantly from day to day for F_v/F_m and chl cell^{-1} ($P > 0.05$, $n = 3$) (Figure 4.1).

Nutrient starvation experiments were performed by stopping the constant inflow of nutrients to the N-limited cultures. This caused an abrupt change in the physiological parameters and disruption to the algal cells by unbalanced growth. The proxy for photosynthetic efficiency, F_v/F_m, reflects this change in growth conditions (Figure 4.1). The nutrient-replete cultures show constant exponential irradiance-limited growth, and the criteria for determining nutrient-replete growth conditions are previously reported in Chapter 3.

4.5.2 ETR and ^{14}C fixation

Fluorescence vs. irradiance (F vs. E) curves generated from the Genty yield and incubation irradiance from a new measurement system showed similar shapes to the photosynthesis vs. irradiance (P vs. E) curves generated from the ^{14}C fixation experiments (Figure 4.2, 4.3). The non-linear model, shown in equations 4.1 and 4.2, was used for both sets of data and fit the data well (Appendix A: P vs. E $R^2 = 0.92$, $n = 33$; F vs. E $R^2 =$

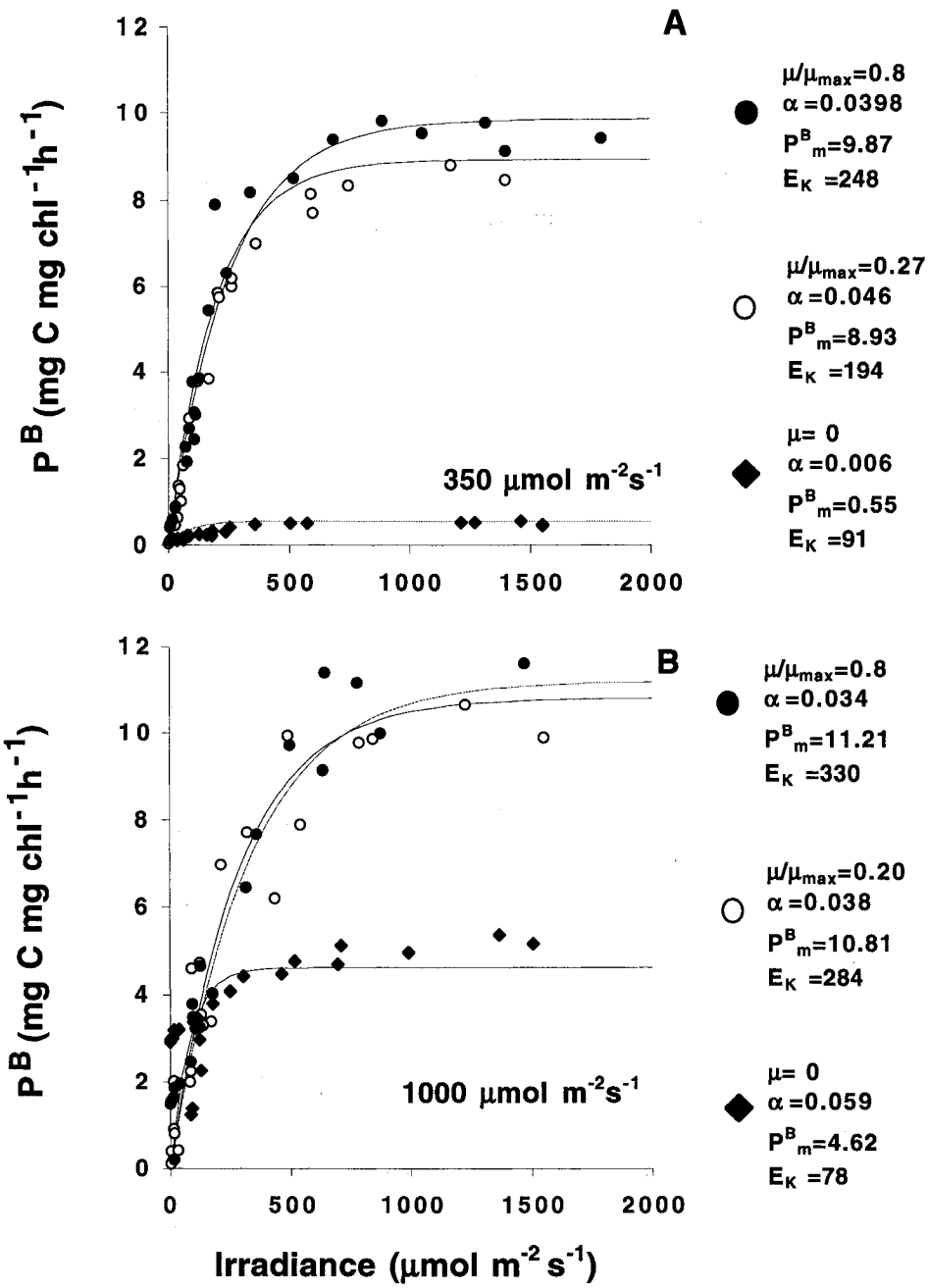

Figure 4.2 Photosynthesis vs. irradiance curves determined from ^{14}C incubation experiments for N-limited and N-starved cultures of *Thalassiosira pseudonana* grown under irradiance of (A) 350 µmol $m^{-2} s^{-1}$ and (B) 1000 µmol $m^{-2} s^{-1}$. Representative curves from ● high N-limited growth rate, O low N-limited growth rate, and ◆ N-starved cultures. N-starvation is represented as a growth rate (µ) = 0. Parameters reported include relative growth rate (µ/ μ_{max}, d^{-1}), initial slope (α, gC $gChl^{-1}$ h^{-1} (µmol $m^{-2} s^{-1})^{-1}$), maximum photosynthetic rate normalized to chl (P^B_{max}, gC $gChl^{-1}$ h^{-1}) and the parameter of light saturation (E_K, µmol $m^{-2} s^{-1}$). Parameters for all curves are provided in Appendix A and B.

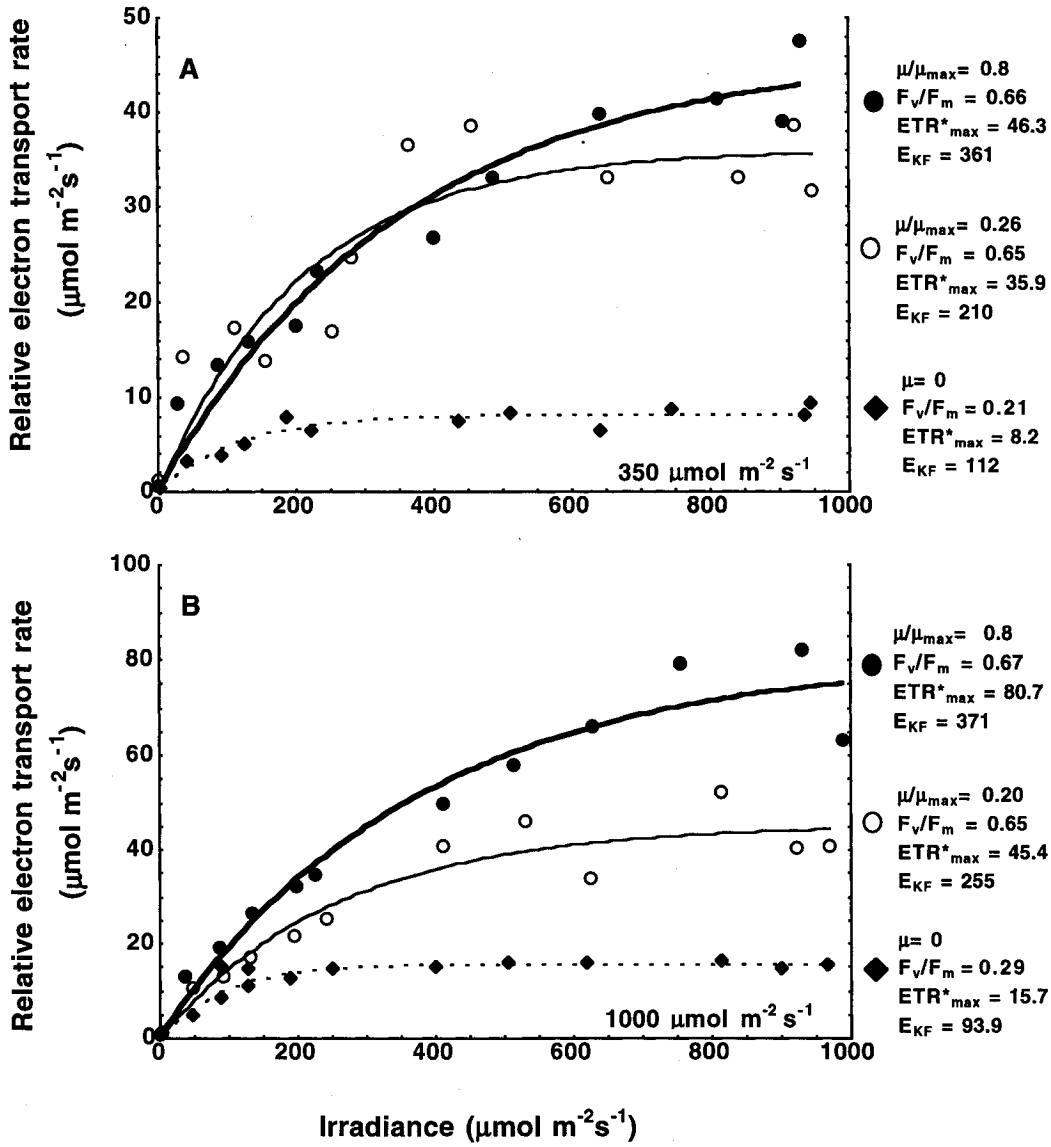

Figure 4.3 Relative electron transport rates determined by the Genty yield ($\Delta F/F_m'$) integrated over 20 minutes multiplied by the irradiance as a function of irradiance for ● high N-limited growth rate, ○ low N-limited growth rate, and ◆ N-starved cultures grown at irradiance of (A) 350 and (B)1000 μmol m^{-2} s^{-1}. Parameters reported include relative growth rate (μ/μ_{max}, d^{-1}), fluorescence based maximum quantum yield for PSII (F_v/F_m, dimensionless), maximum relative electron transport rate (ETR^*_{max}, μmol m^{-2} s^{-1}) and the parameter of light saturation (E_{KF}, μmol m^{-2} s^{-1}). Parameters from all curves are provided in Appendix A.

0.92, $n = 34$) provides evidence that the data is accurately represented by equations 4.1 and 4.2. Increasing the number of parameters (i.e. y-intercept or inhibition term) in the non-linear least squares models had little effect on the correlation of the curves. The relationship between P vs. E. and F vs. E was further investigated by comparing results at light-saturated (500 μmol m^{-2} s^{-1}) and light-limited irradiances (50 μmol m^{-2} s^{-1}), where data from both light levels showed significant correlation ($R^2 = .49$, n =30 and $R^2 = .47$, n = 30 respectively) (Figure 4.4).

4.5.3 E_K and N-Stress

The parameter of light saturation, E_{KF}, determined from relative electron transport rates, not only showed a strong correlation with E_K from ^{14}C fixation experiments, it also showed that E_{KF} was a function of N-limited growth rates and growth irradiance (Figure 4.5). Similar to the P vs. E curves, the relative electron transport rates show a shift (i.e. lower E_K and E_{KF}) under both N-limited and N-starved conditions for both irradiance levels investigated (Figure 4.5). Relative electron transport rates ($\Delta F/F_m' * E$) showed a dramatic decrease under severe N-starved conditions (Figure 4.3). A decrease in E_{KF} as a function of N-limited growth rate was observed under two different growth irradiances (350 μmol m^{-2} s^{-1} $E_{KF} = 45.4\ \mu/\mu max + 208.8$; $R^2 = 0.40$, $n = 6$, $P < 0.05$; and 1000 μmol m^{-2} s^{-1} $E_{KF} = 130.8\ \mu/\mu max + 183.4$; $R^2 = 0.52$, $n = 6$, $P < 0.05$). A similar decrease was observed in E_K as a function of N-limited growth rate (350μmol m^{-2} s^{-1} $E_K = 85.1\ \mu/\mu max$

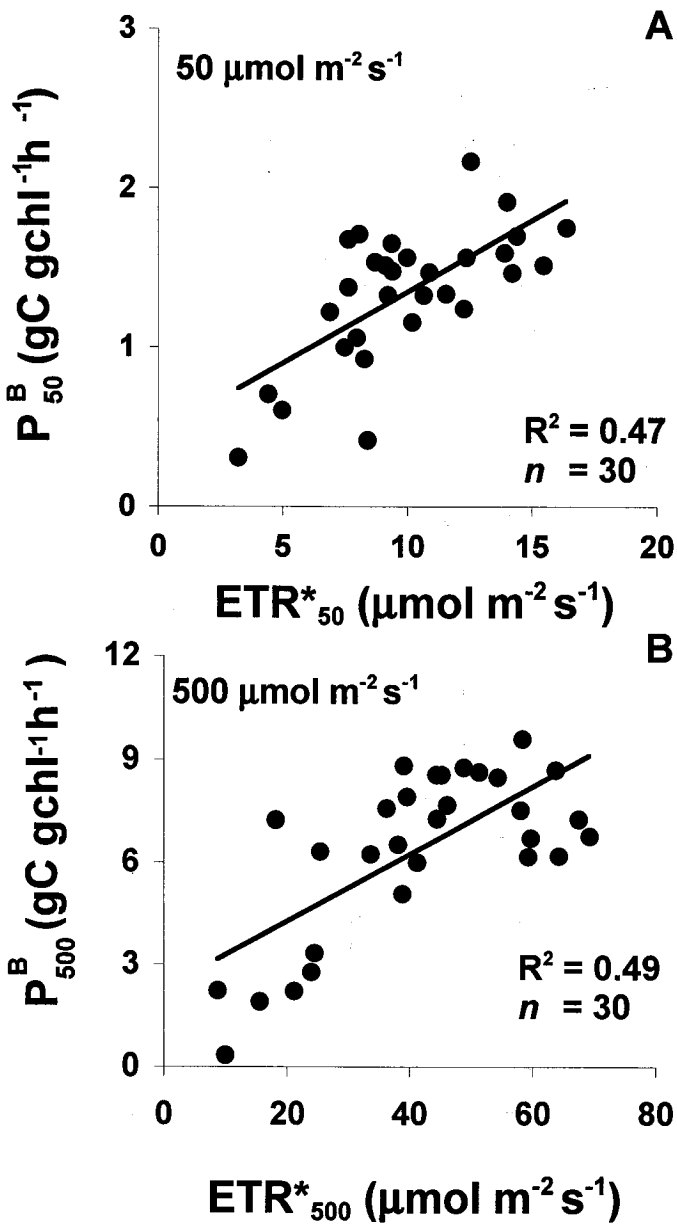

Figure 4.4 The relationship between photosynthesis from ^{14}C incubation experiments (P^B_i) and relative electron transport (ETR^*_i) at (A) light-limited (50 µmol m^{-2} s^{-1}) and (B) light-saturated (500 µmol m^{-2} s^{-1}) levels for cultures grown under nutrient-replete, N-limited, and N-starved conditions (n = 30).

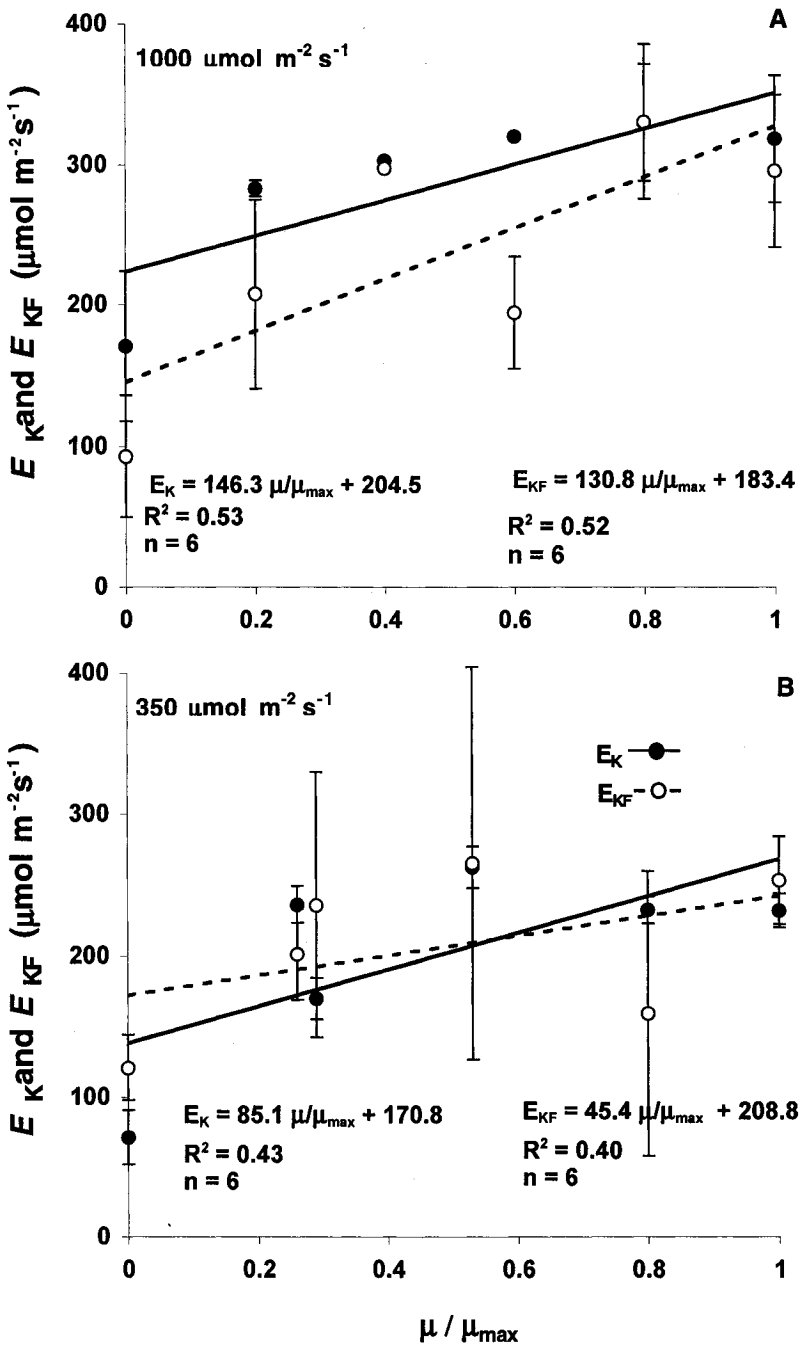

Figure 4.5 The parameters of light saturation (E_K and E_{KF}) determined from ^{14}C incubation and fluorescence metrics for *Thalassiosira pseudonana* grown at (A) 1000 µmol $m^{-2}s^{-1}$ and (B) 350 µmol $m^{-2}s^{-1}$ for N-replete and N-limited and N-starved cultures. Error bars represent standard deviation for duplicate (A) and triplicate (B) cultures. N-starved cultures are shown on the Y axis where $\mu = 0$.

+ 170.8; $R^2 = 0.43$, $n = 6$, $P < 0.05$; and 1000 μmol m^{-2} s^{-1} E_K = 146.3 μ/μmax + 204.5; R^2 = 0.53, $n = 6$, $P < 0.05$) (Figure 4.5). The effects of N-limited growth rate on E_{KF} and E_K were determined by linear regression. Once a relationship had been established, analysis of variance (ANOVA) using a general linear model procedure was conducted to show the effect of N-stressed growth rate, and irradiance on E_{KF} and E_K. Under N-starvation, a more pronounced reduction for E_K and E_{KF} was observed when compared to N-limited trend lines for both light levels investigated (Figure 4.5).

Conversely, P^B_{max} and ETR^*_{max} for acclimated N-limited cells were relatively invariant regardless of N-limited growth rate for the different light levels investigated (Figure 4.6). Although, P^B_{max} and ETR^*_{max} were both sensitive to growth irradiance with lower values observed at lower growth irradiances (Figure 4.7A, B). There was significant agreement between the P^B_{max} and ETR^*_{max} observed ($ETR^*_{max} = 4.89\ P^B_{max} + 10.04$; n = 24; $R^2 = 0.63$) (Figure 4.7C).

4.5.4 NPQ and N-Stress

As light energy increases, photo-protective quenching mechanisms dissipate the excess light as heat causing an increase in NPQ_{max} as a function of the ambient irradiance (Figure 4.8). Maximum non-photochemical quenching also increased as a function of N-stress of the same growth irradiance for continuous cultures and showed differences in NPQ_{max} between different growth irradiances (Figure 4.9). The high-light (1000 μmol m^{-2} s^{-1}) cultures had increased NPQ_{max} values compared with cultures grown under irradiance

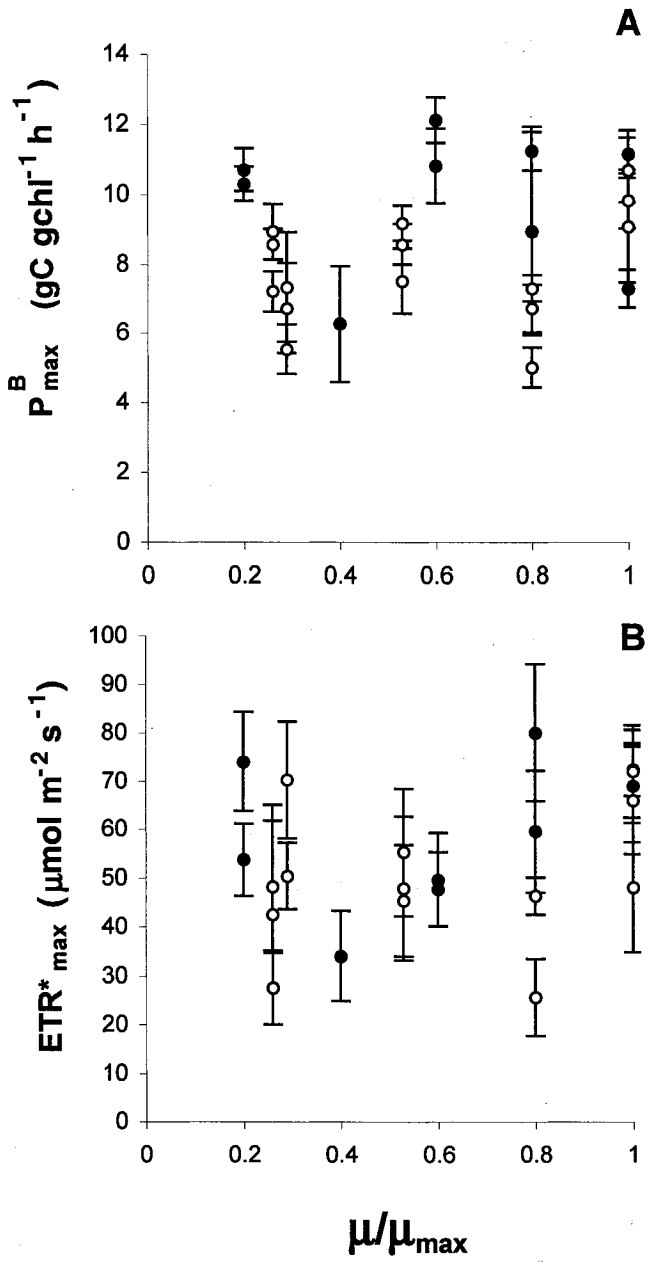

Figure 4.6 (A) Maximal photosynthetic rate normalized to chlorophyll (P^B_{max}) determined from ^{14}C incubation experiments and the (B) Relative electron transport maximum (ETR^*_{max}) determined from fluorescence metrics ((F_m'-F_s)/F_m') * E generated from the PAMoTron for *T. pseudonana* at (○) 350 µmol m^{-2} s^{-1} and (●) 1000 µmol m^{-2} s^{-1} for N-replete and N-limited cultures. Error bars represent a 95% confidence interval for the maximum values obtained in a non-linear curve fit.

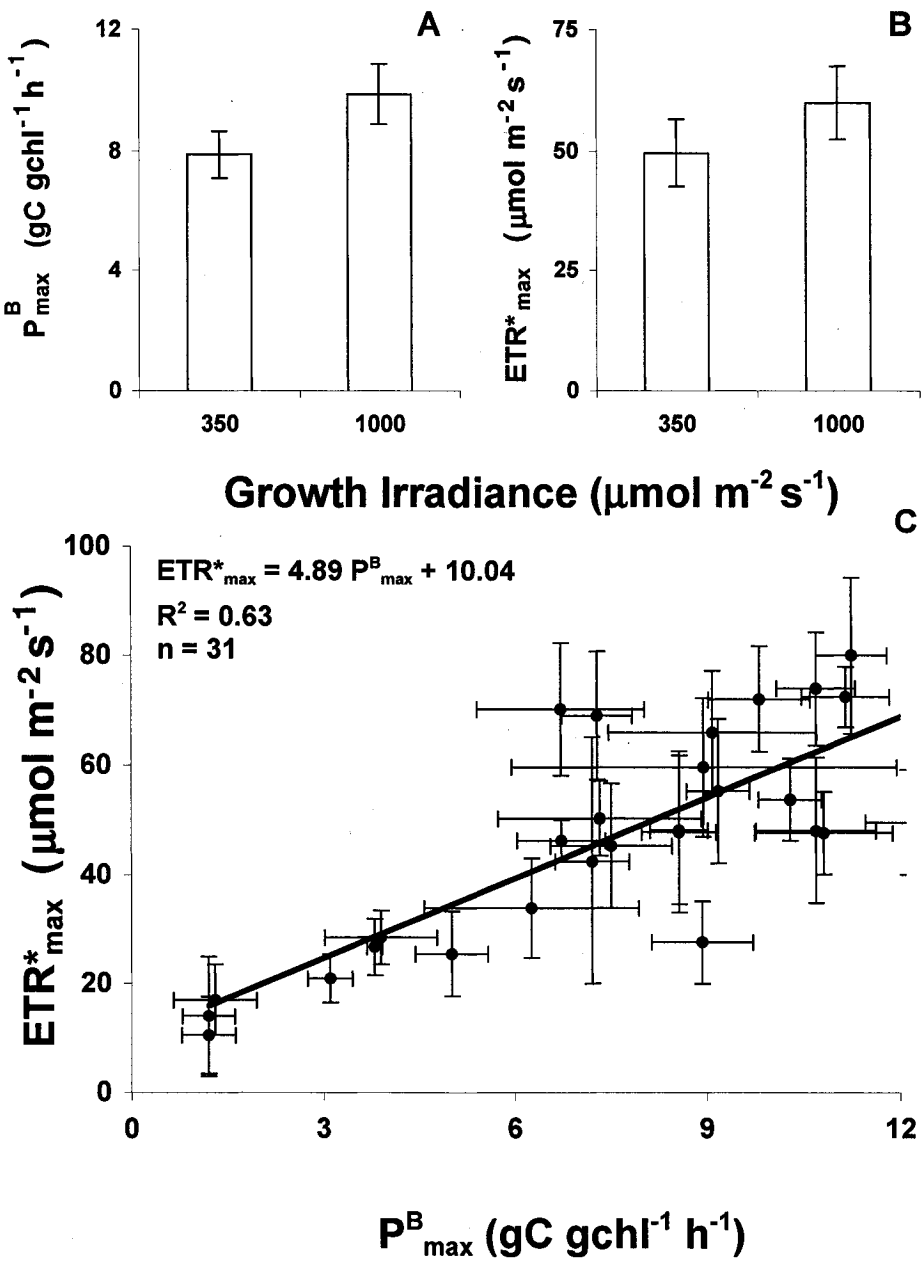

Figure 4.7 (A) The average maximum photosynthetic rate normalized to chlorophyll (P^B_{max}) and the (B) average maximum relative electron transport (ETR^*_{max}) for both growth irradiances investigated (350 µmol m^{-2} s^{-1} and 1000 µmol m^{-2} s^{-1}) for N-replete and N-limited cultures. Means ± SE for triplicate cultures grown at 350 µmol m^{-2} s^{-1} and duplicate cultures grown at 1000 µmol m^{-2} s^{-1}. (C) The relationship between P^B_{max} and ETR^*_{max} for N-replete, N-limited and N-starved cultures. The equation (ETR^*_{max} = 4.89 P^B_{max} + 10.04) and trendline represent a linear regression of the data and error bars represent a 95% confidence interval for the maximum values obtained in a non-linear curve fit.

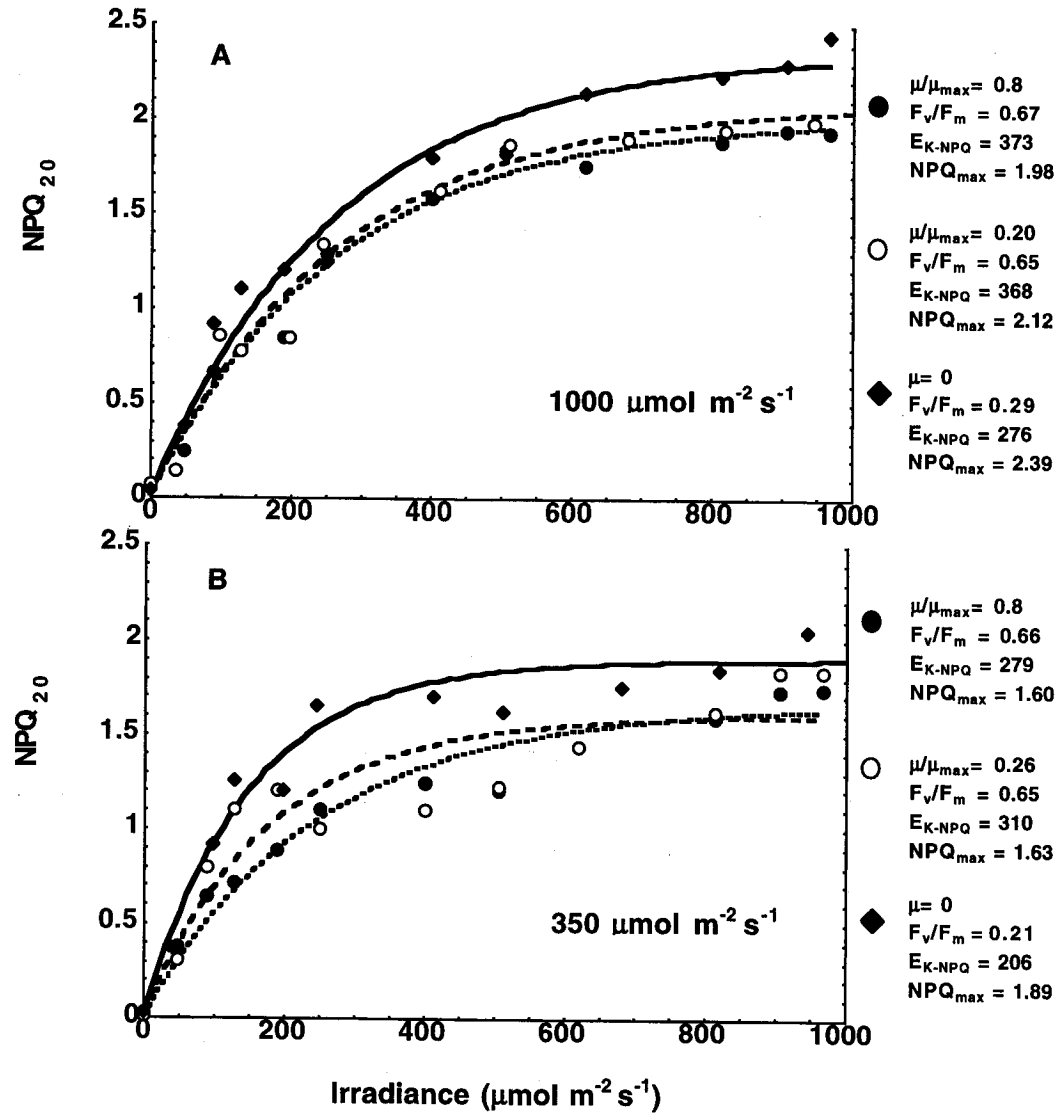

Figure 4.8 NPQ_{20} (F_m-F_m'/ F_m') as a function of irradiance after 20 minute incubations for N-limited and N-starved cultures of *Thalassiosira pseudonana* grown under irradiance of (A) 1000 µmol $m^{-2}s^{-1}$ and (B) 350 µmol $m^{-2}s^{-1}$. Representative curves from ● high N-limited growth rate, O low N-limited growth rate, and ◆ N-starved cultures are shown.

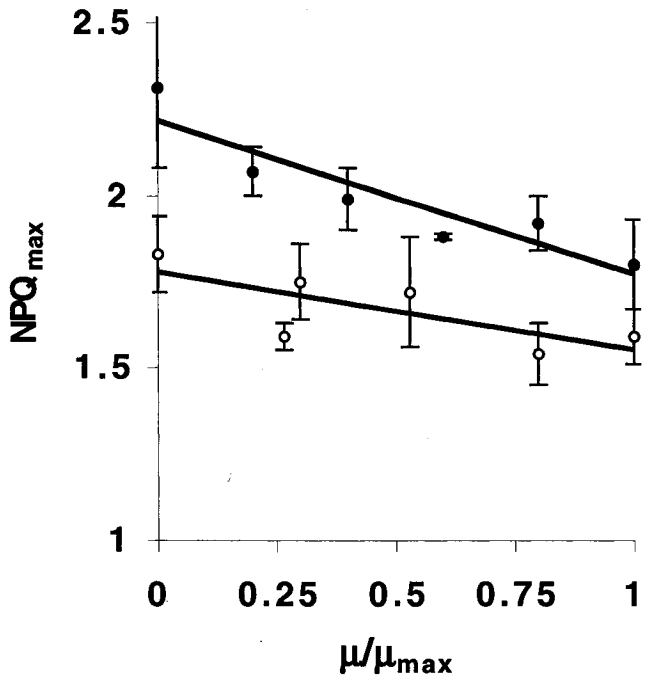

Figure 4.9 NPQ_{max} determined from an exponential function (Equation 4.2) fit to NPQ data from a 20 minute incubated sample as a function of relative growth rate for N-limited and N-starved cultures. Trendline represents the relationship for N-limited cultures grown at irradiance of (O) 350 μmol $m^{-2} s^{-1}$ and (●) 1000 μmol $m^{-2} s^{-1}$. N-Starved cultures are represented as a relative growth rate (μ/μ_{max}) = 0. Means ± SD from averaged measurements for triplicate cultures grown at 350 μmol $m^{-2} s^{-1}$ and duplicate cultures grown at 1000 μmol $m^{-2} s^{-1}$.

of 350 μmol m^{-2} s^{-1}. Differences in curves were observed using non-linear curve fitting (Figure 4.8). A relationship between NPQ_{max} and N-limited growth rate was observed for both growth irradiances (350 μmol m^{-2} s^{-1}, NPQ_{max}= 1.78 - 0.226 μ/μ_{max}, R^2 = 0.55, n = 6, $P < 0.05$; 1000 μmol m^{-2} s^{-1}, NPQ_{max} = 2.22 - 0.444 μ/μ_{max}, R^2 = 0.85, n = 6, $P < 0.05$), and although the correlation was weak between NPQ_{max} and N-limitation at 350μmol m^{-2} s^{-1}, the relationship was still significant (Figure 4.9). The effects of N-limited growth rate on NPQ_{max} were determined by linear regression and then ANOVA was done to determine where the differences within the N-limited cultures existed. The NPQ_{max}/ N-stress relationship was most evident when N-starvation and N-limitation were compared ($P > 0.05$) (Figure 4.9). The NPQ rate cannot be accurately determined for very short time scales (< 2 minutes) for the PAMoTron and therefore the influence of growth irradiance and N-stress on the NPQ rate could not be resolved. For this study, 20 minute incubation averages were used for determination of relative electron transport rates, and the 20 minute maximal fluorescence under supersaturating irradiance (F_m') was used for determination of maximum non-photochemical quenching (NPQ_{max}).

4.5.5 Photo-protective pigments

Pigment analysis by HPLC showed that the xanthophyll cycling pigments such as diadinoxanthin and diatoxanthin, important in energy dependent quenching, varied with N-stress and growth irradiance for cultures at 350 μmol m^{-2} s^{-1}. Cultures with lower

growth irradiance exhibited increased xanthophyll pigment abundance per cell ((diadinoxanthin (DD) + diatoxanthin (DT)) $cell^{-1}$) than the high growth irradiance, (Figure 4.10). As N-limited growth rates decreased the (DD + DT) $cell^{-1}$ decreased for the 350 μmol m^{-2} s^{-1}growth irradiance ((DD + DT) $cell^{-1}$ = 0.0257 μ + 0.0105, R^2 = 0.47, n = 15, P < 0.01), while the (DD + DT) $cell^{-1}$ for 1000 μmol m^{-2} s^{-1} remained constant ((DD + DT) $cell^{-1}$ = 0.0008 μ + 0.0094, R^2 = 0.02, n = 10, P > 0.1) (Figure 4.10a). Pigment ratios (DD +DT : chl) for cultures at both growth irradiances investigated were remarkably constant. Also, as N-limited growth rates decreased the (DD + DT) chl^{-1} remained constant for the 350 μmol m^{-2} s^{-1}growth irradiance ((DD + DT) chl^{-1} = 0.048 μ + 0.419, R^2 = 0.01, n = 15, P > 0.1), while the (DD + DT) chl^{-1} for 1000 μmol m^{-2} s^{-1} increased slightly ((DD + DT) $cell^{-1}$ = 0.434 μ + 0.739, R^2 = 0.84, n = 10, P < 0.001) (Figure 4.10b). During N-starvation, the ratio of photoprotective carotenoids (DD + DT) increased compared to the nitrogen-rich chlorophyll for both growth irradiances tested (Figure 4.10).

4.6 Discussion

4.6.1 ETR and ^{14}C fixation

Relative electron transport rates, determined from Genty yields and irradiance, can give a relative measure of the rate of noncyclic electron transport, and are therefore an indicator of relative photosynthesis. A strong correlation between the ETR* and the

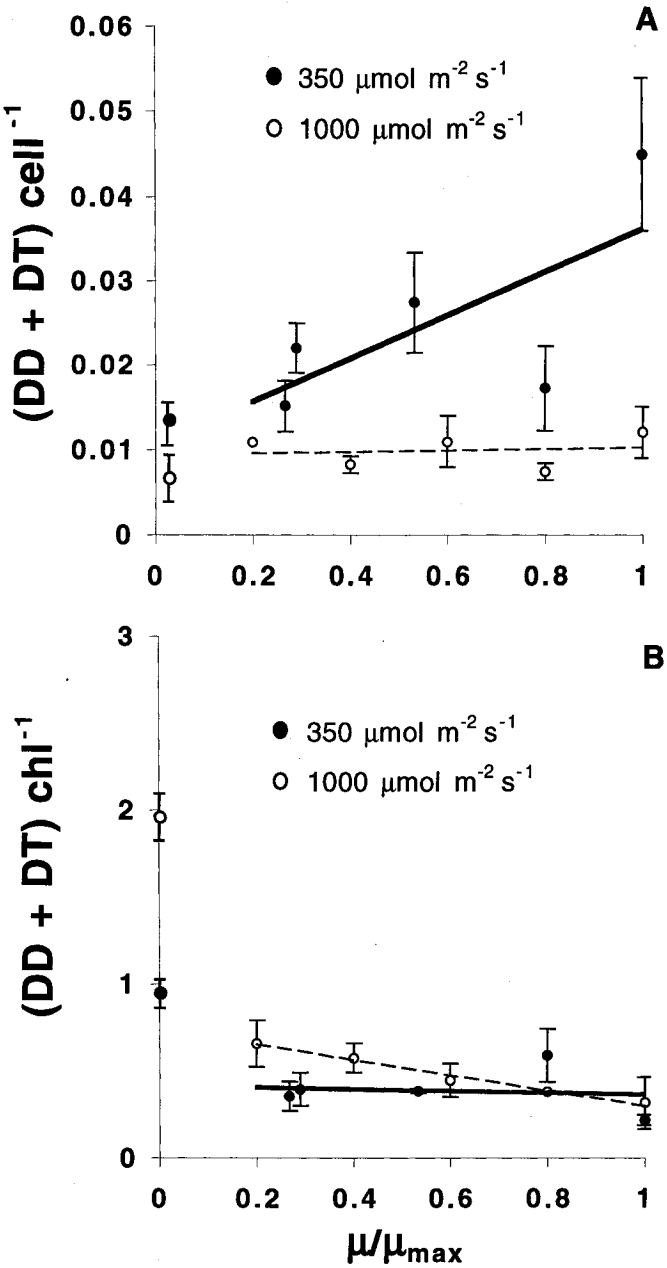

Figure 4.10 The sum of diadinoxanthin (DD) and diatoxanthin (DT) normalized (A) per cell and (B) to chl *a* concentration for N-limited, N-starved ($\mu/\mu_{max} = 0$) and N-replete ($\mu/\mu_{max} = 1$) relative growth rates at two different irradiances (O 350 µmol m^{-2} s^{-1} and ● 1000 µmol m^{-2} s^{-1}) for *Thalassiosira pseudonana.* Means ± SD from averaged measurements for triplicate cultures grown at 350 µmol m^{-2} s^{-1} and duplicate cultures grown at 1000 µmol m^{-2} s^{-1}.

efficiency of carbon fixation as a function of irradiance has been observed (Chapter 3 Genty et al. 1989; Hartig et al. 1998), however a discrepancy may occur under certain stressed conditions (Flameling and Kromkamp 1998; Fryer et al. 1998). Contrary to these findings, Henley (1993) states that the structure of P vs. E curve does not adequately document change in photophysiology and that since the calculation of E_K implicitly assumes P vs. E structure to be bi-linear and disregards convexity it can not be a sensitive measure of algal physiology. In my results I show contradictory evidence to Henley's (1993) results and present consistent relative structure of P vs. E as a function of N-stress. This consistent curve shape was also observed in F vs. E curves as a function of N-stress.

4.6.2 E_K and growth irradiance

My findings showed lower E_K and E_{KF} for the cultures grown under lower light levels (Figure 3.9, 4.5). Under increased growth irradiance, photoprotective strategies would be used to maximize growth rates. Strategies used by high irradiance cultures include reduction of pigments and increasing relative pigment ratios of carotenoids to chlorophyll (Kana and Gilbert 1987a; Ting and Owens 1994; MacIntyre et al. 2002). The overall decrease in cellular pigment concentration is due to a reduction in the number of PSI and PSII reaction centers, providing the capacity to dissipate excess absorbed energy at the light harvesting complex (MacIntyre et al. 2002). Furthermore, cultures grown at high light would not need to harvest light at low irradiance levels to achieve maximal

growth rates and therefore would not need to have a low parameter of light saturation (E_K) (Geider et al. 1996).

Conversely, acclimation to high light appears to be expressed not solely as increased relative photosynthetic capacity but rather as increased capacity for thermal dissipation of excess energy, which would prove beneficial in avoiding damage due to the absorption of excess light energy. My findings also support Johnson's (2001) findings of plants growing at high light intensity having reduced chlorophyll concentrations, lower intrinsic efficiencies of light utilization (i.e. higher E_K), and a higher capacity for thermally dissipating excess light energy (i.e. increased NPQ). When the relative influences of N-stressed growth rates and growth irradiance are compared, growth irradiance is the dominant parameter in determining E_K and E_{KF}.

4.6.3 E_K and N-stress

Changes in the relative curve structure (E_K or E_{KF}) under N-limitation and N-starvation supports the finding that E_K is a measure of physiological stress under controlled laboratory conditions, when the light history is known. A decrease in the N-limited growth rate caused a corresponding decrease in the E_K or E_{KF} for both growth irradiances investigated. This relationship, although significant, would be difficult to determine in the field, where varying light regimes, N-stressed conditions and multiple species persist. Nonetheless, the reported findings of changes in E_K and E_{KF} are consistent with the literature on N-stressed conditions, which shows that as cultures become more

N-stressed the efficiency to do photochemistry per unit chl is increased causing a subsequent decrease in the parameter of light saturation (Cleveland and Perry 1987; Babin et al. 1996a). Further support of a reduced E_{KF} under N-stress is provided by the pigment analysis which shows a reduction of chlorophyll per cell, while the photoprotective pigments become more dominant in comparison to cellular chlorophyll concentrations under N-stress (Figure 4.10). This could indicate that the light harvesting complexes would service fewer available reaction centers causing a reduction in the parameter of light saturation (Demers et al. 1991; Falkowski 1992). A key parameter for determining E_K and E_{KF} is the maximal rate of photosynthesis normalized to chlorophyll, or P^B_{max} and ETR^*_{max} respectively. Consistent P^B_{max} were observed for all N-limited growth rates for both light levels investigated, although, P^B_{max} and the magnitude of relative electron transport rates ($\Delta F/F_m' * E$) showed a dramatic decrease under severe N-starved conditions. Herzig and Falkowski (1989) also showed that P^B_{max} was insensitive to N-limitation, although this is contradictory to other reported findings (Thomas and Dodson 1972; Glover 1980; Kolber et al. 1988; Chalup and Laws 1990). Cullen et al. (1992b) reviewed the literature and found no clear consensus on using P^B_{max} as an indicator of N-limitation. Ensuring that cultures had achieved balanced, acclimated growth conditions may account for some of the discrepancies between reported experiments. The decrease in these parameters under N-starved conditions are most likely driven by processes such as Rubisco availability effecting turnover times or pigmentation, since both measurements show a strong correlation (Figure 4.2 and 4.3). Although, decreased ETR*, and subsequent lowering of E_{KF}, under N-stress can indicate a large proportion of inactive

PSII reaction centers due to oxidation or degradation of D1 protein (Anderson et al. 1997). Severely reduced pigment concentrations in reaction centers would also diminish these parameters, which would be consistent with reduced chlorophyll content for algal populations exposed to N-limitation or starvation (Falkowski 1992).

4.6.4 NPQ and growth irradiance

The principal role of NPQ is to maintain a balance between maximizing the efficiency of photosynthesis at low light and minimizing the damage to the photosynthetic apparatus under excess light conditions by directly quenching excited states in the antennae before damage occurs (Owens 1994). Therefore, cultures grown under high light would benefit more from NPQ processes. High-light grown cultures have a greater capacity for both photochemical and non-photochemical dissipation of absorbed energy (Demmig-Adams and Adams III 1992). High-light cultures can employ more photoprotective strategies and mechanisms reducing their susceptibility to photo-damage. My findings are supported by the literature that high-light grown cultures are more capable of non-photochemical dissipation of excess energy in comparison to low-light grown cultures (Neubauer and Schreiber 1989; Demmig-Adams and Adams III 1992; Geider et al. 1997; Muller et al. 2001; Kashino et al. 2002).

It is important to note that changes in NPQ are relative to the dark-adapted state. Therefore, a minimum time to allow NPQ to revert in the dark-adapted cultures prior to experiments is required (>10 min). The same increase in heat dissipation will appear as a

smaller increase in quenching in the case where the reference point has higher initial quenching. This means that direct comparison with N-starved conditions and between starved and limited conditions, as well as preconditioned light histories can lead to ambiguous results if attention is not paid to preconditioning.. Further investigation into these relationships is required.

4.6.5 NPQ and N-stress

Nutrient stress, both starvation and limitation, results in increased NPQ_{max} (Figure 4.9), and may be a critical component in the regulation of photosynthetic light harvesting, especially under unfavorable nutrient regimes (Niyogi 1999; Demmig-Adams and Adams 2000; Li et al. 2000), and increases in NPQ_{max} are consistent with reduced photochemical yield (Bungard et al. 1997; Verhoeven et al. 1997). This increase in relative NPQ capacity is also supported by the increase in photoprotective pigments (diadinoxanthin (DD) and diatoxanthin (DT)) to chlorophyll a pigment ratio under N-starvation although under limitation the (DD + DT)/chl *a* ratio remains relatively constant (Figure 4.10). This invariable ratio is consistent with acclimation to its new nutrient regime and balanced growth (Geider et al. 1998). Changes in overall pigment abundance are observed as a function of N-stress regardless of growth irradiance and N-stressed conditions (i.e. limited or starved). Increased NPQ_{max} in N-stressed cultures may be due to increased effective cross sections causing photoinhibition to occur at lower irradiance levels and losses to selective reaction center proteins decrease the ability of cells to repair damage. The

relative small changes in (DD +DT) /chl *a* ratio under increased N-stress and growth irradiance is consistent with the literature (Kana and Gilbert 1987a; MacIntyre et al. 2002). The increased NPQ_{max} for starved cultures observed may have been caused by decreases in chlorophyll and subsequent loss of PSII reaction centers or by disruption of the thylakoid membrane proton gradient required for photochemical processes (Falkowski 1992; Gilmore and Govindjee 1999; MacIntyre et al. 2002).

4.7 Summary and conclusions

In summary, E_K and E_{KF} showed strong agreement under all growth conditions and were found to be sensitive measures of N-stressed conditions and/or growth irradiance. This relationship is difficult to assess in nature because effects of irradiance and nutrients cannot be easily distinguished. Therefore the utility of this diagnostic in the field is tenuous, at best.

Maximum non-photochemical quenching (NPQ_{max}) was a sensitive diagnostic of N-stress, although the relationship was much more apparent under N-starved than under N-limited growth conditions. This parameter was also a function of both incubation and growth irradiance. Results from pigment analysis show increased photoprotective pigments when compared to chlorophyll which supports the finding of increased NPQ_{max} under N-stress.

Finally, this research highlights the importance of growth irradiance in determining both photochemical and non-photochemical parameters and emphasizes the scrutiny that

should be placed on growth conditions and preconditioning in future research. The limited utility of this new measurement in the field should be emphasized, since the response under different controlled conditions, produced only small changes in E_{KF} and NPQ_{max}. With unknowns such as natural species composition, light history, or effects of diurnal variability, and, since the growth irradiance contributes more to changes in fluorescence metrics than N-stressed growth conditions, the benefit of the new measurement system to determine nutrient status of algal populations would be called into question. However, when parameters are closely monitored and carefully controlled the new measurement system can be used as a diagnostic of N-stress.

Chapter 5

General summary and future directions

5.1 General summary and conclusions

Basic relationships between nutrition and active fluorescence metrics need to be investigated. Two independent fluorescence measurement systems, PAM fluorometry (active) and DCMU methodology (conventional), showed a strong 1:1 correlation when the DCMU method was corrected for over-excitation of minimal fluorescence for cultures grown under low-light. These independent systems were used to investigate the use of fluorescence-based maximal quantum yields for photosystem II (F_v/F_m) as a sensitive indicator of N-stress. My findings showed that under nutrient-replete growth conditions, F_v/F_m for the neritic diatom *Thalassiosira pseudonana* (3H) is high and independent of growth irradiance, while during N-starvation F_v/F_m declines and is correlated to time without nutrients. This is consistent with the current literature. Also, when N-starvation was imposed on acclimated N-limited cultures, the onset of the decline of F_v/F_m was a function of preconditioned N-limited growth rate, although the subsequent rate of decline of F_v/F_m was independent of preconditioned N-limited growth rates. This suggests that F_v/F_m is more susceptible to perturbations in nutrient supply for phytoplankton with

lower N-limited growth rates. In contrast to published results, F_v/F_m remained high and constant (~ 0.65) for the acclimated steady-state cultures at different nitrogen-limited growth rates, independent of growth irradiance. This result should be verified for a range of species isolated from different environments. These results show that fluorescence-based maximal quantum yield for photosystem II is not a robust diagnostic for all N-stressed conditions. It is a sensitive indicator of N-stress during unbalanced growth, but when phytoplankton are acclimated to N-limitation, the relationship between F_v/F_m and N-stress breaks down. This limits the utility of F_v/F_m as a measure of phytoplankton physiological status in the laboratory and the field. Therefore, I developed a measurement system that can be used to complement F_v/F_m measurements and possibly provide a more sensitive approach in determining physiological status of algal species under N-stressed conditions.

With active fluorometers, fluorescence measurements can now be measured under ambient irradiance allowing for previously unavailable metrics. Parameters such as the relative electron transport rate and the rate and amount of non-photochemical quenching have shown promise for being a proxy of the physiological state of phytoplankton

A novel measurement system using 12 independent sub-samples under 12 different irradiance levels allows for F vs. E curves to be determined in parallel every 2 minutes at the respective irradiance levels. This system is the amalgamation of a Pulse Amplitude Modulation fluorometer and a light incubation chamber providing fluorescence metrics under a suite of irradiances. These F vs. E curves work on the same premise as Rapid Light Curves (Schreiber et al. 1997; Ralph et al. 1999; White and Critchley 1999;

Kühl et al. 2001) although the system allows for distinct incubation chambers, not exposing the sample to sequential changes in the light field. This would avoid the problems of time step and pre-conditioning which would occur in the RLC samples.

The new measurement system presented in this thesis has advantages and limitations which are discussed in detail in Chapter 3. Advantages include parallel measurement as opposed to sequential, strong agreement with conventional measurements, resolution of important kinetics unavailable to dark adapted fluorescence metrics, and a non-invasive, easy to use, determination of electron flow in relatively real time. Limitations of the current measurement system include the inability to resolve qE and other photochemical and non photochemical kinetics, limited sensitivity, and retrieval of fluorescence metrics only as relative values. Also, the applicability to unknown populations with variable photosynthetic strategies (i.e. PSII:PSI, accessory pigments, physiological adaptations) is difficult.

The new measurement system provides a Genty yield for each irradiance every 2 minutes which were integrated over a 20 minute time interval. The integrated value was multiplied by the incubation irradiance to determine the relative electron transport rate and plotted as a function of irradiance. Comparison of the resulting F vs. E curves with P vs. E curves determined from ^{14}C incubation experiments shows promise for fluorescence as a proxy for photosynthetic rate determination. It is well established that the saturation irradiance level (E_K) is a function of growth irradiance, temperature, and N-stress. I introduce a new determination of this saturation parameter by fluorescence (E_{KF}) which showed results which compared well to the conventional method of ^{14}C incubations. E_K

and E_{KF} showed strong agreement for nutrient-replete cultures under three different light histories. Another fluorescence metric, maximum non-photochemical quenching (NPQ_{max}), increased as a function of growth irradiance.

Fluorescence metrics, E_{KF} and NPQ_{max} were found to vary as functions of N-stressed conditions and/or growth irradiance. This relationship is difficult to assess unless monitored under strict laboratory conditions, where one of these conditions is controlled. Therefore the utility of this diagnostic in the field is tenuous at best.

The parameter of light saturation, E_{KF}, decreased under conditions of N-stress, and was most apparent under conditions of N-starvation. This is supported by the reduction in chl $cell^{-1}$, which is essential in the reaction center for harvesting light. More light harvesting complex proteins servicing fewer available reaction center proteins would reduce E_{KF}. Although, differences were more pronounced between growth irradiance than N-stressed conditions.

Maximum non-photochemical quenching (NPQ_{max}) as measured with the new fluorometric system was also responsive to N-stress, although the relationship was much more apparent under N-starved conditions than for N-limited growth cultures. This parameter was also a function of both incubation and growth irradiance. Results from pigment analysis show increased photoprotective pigments relative to chlorophyll, corresponding to increased NPQ_{max} under N-stress.

Finally, this research highlights the importance of growth irradiance in determining both the photochemical and non-photochemical parameters and emphasizes the scrutiny that should be placed on growth conditions and preconditioning in future research. The

limited utility of this new measurement in the field should be emphasized, since the response under different controlled conditions, produced only small changes in E_{KF} and NPQ_{max}. With unknowns such as species of the natural population, light history, or effects of diurnal variability, and since, the growth irradiance contributes more to changes in fluorescence metrics than N-stressed growth conditions, the benefit of the new measurement system to determine nutrient status of algal populations is questionable. Although, when parameters are closely monitored and carefully controlled this new measurement system can be used as a diagnostic of N-stress.

5.2 Future work

The research done for this thesis fits well into a growing body of evidence that fluorescence can be a rapid and sensitive indicator of physiological stress, although the metrics still need further investigation. With modifications of the current system, increased sensitivity will allow this system to measure fluorescence metrics in the field. The system could also decrease the time required to generate F vs. E curves allowing for determination of the kinetics, thus providing further fluorescence diagnostics which could be used as indicators of stressed conditions. Investigation of different species as well as natural assemblages, since different species employ different light harvesting mechanisms and strategies (i.e. PSI:PSII ratios, accessory pigments, and algal size) is also required. Also by investigating the de-excitation timescale, determination of the type of NPQ may also be determined.

Once the sensitivity is improved, this new measurement system should be able to assess different physiological stresses such as temperature or essential nutrients besides nitrogen (i.e. P, Fe and Si) and provide fluorescence metrics, such as E_{KF}, which can be used as proxies for productivity estimates. Since E_K is important in most optical primary productivity models (Behrenfeld and Falkowski 1997), this new measurement system may produce a rapid, non-invasive measurement that closely reflects this metric, providing an alternative to a laborious measurement using radio isotopes. Furthermore, F vs. E vs. time determinations could be used to construct better time-dependent primary productivity models.

Amalgamation of the current system with other instruments may also provide avenues for investigation. For example, if this new measurement system utilized a Fast Repetition Rate Fluorometer (FRRF) instead of a PAM system it would allow simultaneous determination of functional absorption cross sections and connectivity parameters, previously unavailable from the current system. In the future, measurement systems, similar to the one reported in this thesis, will identify and quantify the basic relationships between nutrition, fluorescence, irradiance and productivity with a high resolution allowing for fluorescence to be used as a diagnostic of nutrient stress.

Appendix A Summary table of E_K and E_{KF} for nutrient-replete (μ/μ_{max} = 1), N-limited, and N-starved (μ/μ_{max} = 0) cultures grown at 350 and 1000 μmol m^{-2} s^{-1}, as well as nutrient-replete cultures grown at 150 μmol m^{-2} s^{-1}. Confidence Intervals (95%) within curves, and means and standard deviations between curves is shown. P vs. E R^2 and F vs E R^2 values based on n = 24 and n = 12 respectively.

Irradiance	Relative Growth rate	E_K	E_K	E_K	E_K	PvsE	E_{KF}	E_{KF}	E_{KF}	E_{KF}	FvsE
μmol m^{-2} s^{-1}	μ/ μmax	μmol m^{-2} s^{-1}	95% CI	mean	SD	R^2	μmol m^{-2} s^{-1}	95% CI	mean	SD	R^2
1000	1	351.0	151.0	319.0	45.4	0.97	358.0	118.0	295.9	54.6	0.98
	1	267.0	139.0			0.93	255.7	283.0			0.99
	1	339.0	162.0			0.86	274.0	189.0			0.97
1000	0.8	360.0	208.0	330.5	41.7	0.94	370.1	339.0	331.1	55.1	0.98
	0.8	301.0	103.0			0.98	292.1	314.0			0.96
1000	0.6	320.1	105.0	320.1	0.0	0.98	166.2	247.0	194.3	39.8	0.90
	0.6	320.1	166.0			0.95	222.5	217.0			0.96
1000	0.4	58.4*	1080*	303.0	0.0	0.88	94.5	283.0	297.5	0.0	0.78
	0.4	303.0	26.9			0.29*	297.5	418.0			0.94
1000	0.2	279.0	114.0	283.0	5.7	0.97	160.1	218.0	207.7	67.4	0.89
	0.2	287.0	87.0			0.98	255.4	246.0			0.96
1000	0	145.8	208.0	161.5	53.2	0.88	136.0	167.0	93.0	43.1	0.94
	0	599*	630*			0.85	75.7	53.2			0.98
	0	231.7	115.0			0.80	63.3	72.5			0.94
350	1	220.8	224.0	232.2	12.1	0.73	240.0	782.0	253.5	31.0	0.94
	1	230.9	126.0			0.90	231.5	243.0			0.99
	1	244.9	150.0			0.90	289.0	295.0			0.86
350	0.8	249.1	162.0	232.8	9.5	0.88	92.7	123.0	159.0	100.9	0.93
	0.8	221.9	142.0			0.88	*	*			*
	0.8	227.3	74.2			0.98	225.3	297.0			0.98
350	0.53	246.5	88.3	262.9	14.6	0.97	271.2	453.0	265.6	138.8	0.88
	0.53	265.8	106.0			0.97	248.7	620.0			0.95
	0.53	276.3	155.0			0.93	277.0	324.0			0.94
350	0.29	195.3	255.0	169.7	14.4	0.78	200.8	670.0	236.0	93.7	0.92
	0.29	199.7	176.0			0.79	339.8	412.0			0.94
	0.29	114.0	61.7			0.72	167.4	412.0			0.66
350	0.26	179.8	67.3	236.5	12.9	0.98	206.1	630.0	201.0	32.4	0.92
	0.26	264.6	130.0			0.97	201.3	239.0			0.94
	0.26	265.0	106.0			0.98	195.6	265.0			0.93
350	0	102.0	27.7	71.4	19.3	0.99	123.0	122.0	121.1	22.9	0.96
	0	86.8	24.7			0.99	106.0	141.0			0.93
	0	50.7	27.0			0.89	135.0	191.0			0.93
150	1	99.5	115.4	138.9	55.7	0.99	219.0	251.0	194.8	39.0	0.91
	1	34.8*	456.0			0.99	215.5	413.0			0.93
	1	178.3	212.0			0.96	149.8	312.0			0.81

* Excluded from analysis.

Appendix B Summary table of P^B_{max} and ETR^*_{max} for nutrient-replete (μ/μ_{max} = 1), N-limited, and N-starved (μ/μ_{max} = 0) cultures grown at 350 and 1000 µmol m^{-2} s^{-1}, as well as nutrient-replete cultures grown at 150 µmol m^{-2} s^{-1}.Confidence Intervals (95%) within curves, and means and standard deviations between curves is shown. P vs. E R^2 and F vs E R^2 values based on n = 24 and n = 12

Irradiance	Relative	P^B_{max}	P^B_{max}	P^B_{max}	P^B_{max}	ETR^*_{max}	ETR^*_{max}	ETR^*_{max}	ETR^*_{max}	PvsE	FvsE
µmol m^{-2} s^{-1}	µ/ µmax	gC $gChl^{-1}$ h^{-1}	95% CI	mean	SD	µmol m^{-2} s^{-1}	95% CI	mean	SD	R^2	R^2
1000	1	11.2	1.4	9.4	2.0	72.1	23.3	70.2	1.7	0.97	0.98
	1	7.3	1.1			69.1	10.9			0.93	0.99
	1	9.8	1.1			69.3	16.2			0.86	0.97
1000	0.8	9.0	2.1	9.9	1.3	80.7	25.2	70.1	14.9	0.94	0.98
	0.8	10.8	1.1			59.6	28.5			0.98	0.96
1000	0.6	10.8	1.3	10.8	0.0	47.6	19.1	48.6	1.5	0.98	0.90
	0.6	10.8	2.1			49.7	15.0			0.95	0.96
1000	0.4	6.3	3.4	6.3	0.0	33.9	18.4	53.9	28.3	0.88	0.78
	0.4	42.4*	51.6*			73.9	37.5			0.29*	0.94
1000	0.2	10.4	1.2	10.5	0.2	53.7	20.0	49.6	5.8	0.97	0.89
	0.2	10.7	1.0			45.4	14.9			0.98	0.96
1000	0	3.3	1.41	3.3	1.3	26.3	14.7	16.8	16.1	0.88	0.94
	0	4.6	5.83			8.3	2.9			0.85	0.98
	0	2.1	0.55			15.9	8.7			0.80	0.94
350	1	10.7	3.2	9.9	0.8	66.7	42.4	62.3	12.6	0.73	0.94
	1	9.8	1.6			72.1	19.1			0.90	0.99
	1	9.1	1.9			48.1	26.4			0.90	0.86
350	0.8	7.3	1.4	6.4	1.2	25.6	7.5	35.9	14.7	0.88	0.93
	0.8	5.0	1.1			*	*			0.88	*
	0.8	6.7	0.8			46.3	15.7			0.98	0.98
350	0.53	7.5	1.0	8.4	0.8	45.3	26.3	59.5	16.7	0.97	0.88
	0.53	8.6	1.2			78.0	49.4			0.97	0.95
	0.53	9.2	1.9			55.3	22.7			0.93	0.94
350	0.29	6.7	3.2	6.5	0.9	70.2	51.0	46.6	25.7	0.78	0.92
	0.29	5.5	1.4			50.4	13.6			0.79	0.94
	0.29	7.3	1.2			19.2	24.2			0.72	0.66
350	0.26	7.2	0.9	8.2	0.9	76.1	47.1	54.6	19.1	0.98	0.92
	0.26	8.9	1.6			39.6	15.2			0.97	0.94
	0.26	8.6	1.2			48.2	14.4			0.98	0.93
350	0	2.8	0.3	1.8	1.4	26.3	14.7	16.8	9.0	0.99	0.96
	0	2.3	0.3			15.9	8.7			0.99	0.93
	0	0.2	0.0			8.3	2.9			0.89	0.93
150	1	1.6	0.6	2.0	0.7	44.1	12.3	36.5	8.0	0.99	0.91
	1	0.61*	4.2*			37.3	8.6			0.99	0.93
	1	2.5	0.9			28.2	29.3			0.96	0.81

* Excluded from analysis.

Appendix C Summary table of $E_{K\text{-}NPQ}$ and NPQ_{max} for nutrient-replete, N-limited and N-starved cultures grown under 350 and 1000 μmol m^{-2} s^{-1}, as well as nutrient-replete cultures grown at 150 μmol m^{-2} s^{-1}. Confidence Intervals (95%) within curves, and means and standard deviations between curves is shown. Parameters were determined from NPQ vs E curves after a 20 minute incubation and the data fit to an exponential function. NPQ vs E R^2 values based on n = 12.

Irradiance	Relative Growth rate	$E_{K\text{-}NPQ}$	$E_{K\text{-}NPQ}$	$E_{K\text{-}NPQ}$	$E_{K\text{-}NPQ}$	NPQ_{max}	NPQ_{max}	NPQ_{max}	NPQ_{max}	NPQ vs. E R^2
μmol m^{-2} s^{-1}	μ/μ_{max}	μmol m^{-2} s^{-1}	95% CI	mean	SD		95% CI	mean	SD	
1000	1	232.4	115.0	233.61	29.06	1.73	0.28	1.80	0.13	0.99
	1	263.3	172.0			1.95	0.44			0.98
	1	205.2	134.0			1.71	0.32			0.97
1000	0.8	373.0	265.0	377.60	6.51	1.86	0.36	1.92	0.08	0.98
	0.8	382.2	313.0			1.98	0.55			0.98
1000	0.6	2132*	553.0	223.41	37.34	1.89	0.69	1.88	0.01	0.99
	0.6	249.8	188.0			1.87	0.38			0.98
1000	0.4	197.0	109.0	263.99	67.49	1.93	0.47	1.99	0.09	0.99
	0.4	263.0	180.0			2.05	0.29			0.98
1000	0.2	332.0	205.0	325.91	45.58	2.02	0.47	2.07	0.07	0.99
	0.2	368.2	214.0			2.12	0.51			0.99
1000	0	277.6	134.0	281.21	22.21	2.56	0.42	2.31	0.23	0.99
	0	261.0	249.0			2.11	0.66			0.96
	0	305.0	267.0			2.26	0.72			0.97
350	1	282.8	111.0	277.36	6.16	1.50	0.21	1.59	0.08	0.99
	1	278.7	216.0			1.64	0.45			0.97
	1	270.7	182.0			1.65	0.39			0.98
350	0.8	303.4	220.0	307.55	30.49	1.45	0.39	1.54	0.09	0.99
	0.8	339.9	220.0			1.57	0.41			0.99
	0.8	279.4	169.0			1.61	0.35			0.97
350	0.53	308.9	256.0	347.01	64.38	1.59	0.49	1.72	0.16	0.97
	0.53	421.3	348.0			1.89	0.69			0.97
	0.53	310.8	276.0			1.67	0.55			0.98
350	0.29	299.6	221.0	299.24	2.51	1.88	0.51	1.75	0.11	0.98
	0.29	301.6	180.0			1.69	0.37			0.96
	0.29	296.6	255.0			1.69	0.53			0.99
350	0.26	385.8	161.0	317.07	65.68	1.57	0.29	1.59	0.04	0.97
	0.26	310.4	230.0			1.63	0.47			0.97
	0.26	255.0	260.0			1.56	0.56			0.93
350	0	227.6	146.0	191.91	41.77	2.01	0.39	1.85	0.16	0.98
	0	202.2	150.0			1.69	0.35			0.98
	0	146.0	82.0			1.85	0.24			0.99
150	1	203.0	162.0	238.90	37.27	1.53	0.35	1.63	0.11	0.97
	1	236.3	162.0			1.74	0.37			0.98
	1	277.4	282.0			1.62	0.56			0.96

References

Anderson, J. M., Y. I. Park, and W. S. Chow. 1997. Photoinactivation and photoprotection of photosystem II in nature. Physiologia Plantarum **100:** 214-223.

Babin, M., A. Morel, H. Claustre, A. Bricaud, Z. Kolber, and P. G. Falkowski. 1996a. Nitrogen- and irradiance-dependent variations of the maximum quantum yield of carbon fixation in eutrophic, mesotrophic and oligotrophic marine systems. Deep-Sea Research I **43:** 1241-1272.

Babin, M., A. Morel, and B. Gentili. 1996b. Remote sensing of sea surface Sun-induced chlorophyll fluorescence: consequences of natural variations in the optical characteristics of phytoplankton and the quantum yield of chlorophyll *a* fluorescence. International Journal of Remote Sensing **17:** 2417-2448.

Bannister, T. T., and E. A. Laws. 1980. Modeling phytoplankton carbon metabolism, p. 243-248. *In* P. G. Falkowski [ed.], Primary Productivity in the Sea. Plenum.

Barber, J. 1992. Photosystems: Structure, Function and Molecular Biology. Elsevier Science.

Barranguet, C., and J. Kromkamp. 2000. Estimating production rates from photosynthetic electron transport in estuarine micro-phytobenthos. Marine Ecology Progress Series **204:** 39-52.

Beardall, J., S. Roberts, and J. Millhouse. 1991. Effects of nitrogen limitation and uptake of inorganic carbon and specific activity of ribulose-1,5-bisphosphate carboxylase/oxygenase in green microalgae. Canadian Journal of Botany **69:** 1146-1150.

Beardall, J., E. Young, and S. Roberts. 2001. Approaches for determining phytoplankton nutrient limitation. Aquatic Science **63:** 44-69.

Behrenfeld, M. J., and P. G. Falkowski. 1997. A consumer's guide to phytoplankton productivity models. Limnology and Oceanography **42:** 1479-1491.

Behrenfeld, M. J., O. Prasil, Z. S. Kolber, M. Babin, and P. G. Falkowski. 1998. Compensatory changes in Photosystem II electron turnover rates protect photosynthesis from photoinhibition. Photosynthesis Research **58:** 259-268.

Berman-Frank, I., and Z. Dubinsky. 1999. Balanced growth in aquatic plants: Myths or reality? Bioscience **49:** 29-37.

Bilger, W., and O. Björkman. 1990. Role of the xanthophyll cycle in photoprotection elucidated by measurements of light-induced absorbance changes, fluorescence and photosynthesis in leaves of *Hedera canariensis*. Photosynthesis Research **25:** 173-185.

Boyd, P. W., J. Aiken, and Z. Kolber. 1997. Comparison of radiocarbon and fluorescence based (pump and probe) measurements of phytoplankton photosynthetic characteristics in the Northeast Atlantic Ocean. Marine Ecology Progress Series **149:** 215-226.

Büchel, C., and W. C. Wilhelm. 1993. In vivo analysis of slow chlorophyll fluorescence induction kinetics in algae: progress, problems and perspective. Photochemistry and Photobiology **58:** 137-148.

Bungard, R. A., D. McNeil, and J. D. Morton. 1997. Effects of nitrogen on the photosynthetic apparatus of *Clematis vitalba* grown at several irradiances. Australian Journal of Plant Physiology **24:** 205-214.

Buschmann, C. 1999. Photochemical and non-photochemical quenching coefficients of the chlorophyll fluorescence: Comparison of variation and limits. Photosynthetica **37:** 217-224.

Butler, W. L. 1978. Energy distribution in the photochemical apparatus of photosynthesis. Annual Reviews of Plant Physiology **29:** 345-378.

Butler, W. L., and M. Kitajima. 1975. Fluorescence quenching in photosystem II of chloroplasts. Biochimica Biophysica Acta **376:** 116-125.

Casper-Lindley, C., and O. Björkman. 1998. Fluorescence quenching in four unicellular algae with different light harvesting and xanthophyll-cycle pigments. Photosynthesis Research **56:** 277-289.

Chalup, M. S., and E. A. Laws. 1990. A test of the assumptions and predictions of recent microalgal growth models with the marine phytoplankter *Pavlova lutheri*. Limnology and Oceanography **35:** 583-596.

Chamberlin, S., and J. Marra. 1992. Estimation of photosynthetic rate from measurements of natural fluorescence: analysis of the effects of light and temperature. Deep-Sea Research **39:** 1695-1706.

Clayton, R. K. 1980. Photosynthesis Physical mechanisms and chemical patterns. Cambridge University Press.

Cleveland, J. S., and M. J. Perry. 1987. Quantum yield, relative specific absorption and fluorescence in nitrogen-limited *Chaetoceros gracilis*. Marine Biology **94:** 489-497.

Cullen, J. 2001. Plankton: Primary production methods. *In* J. Steele, S. Thorpe and K. Turekian [eds.], Encyclopedia of Ocean Sciences. Academic Science.

Cullen, J. J., Á. M. Ciotti, R. F. Davis, and P. J. Neale. 1997. The relationship between near-surface chlorophyll and solar-stimulated fluorescence: biological effects. Ocean Optics XIII, Proc. SPIE **2963:** 272-277.

Cullen, J. J., M. R. Lewis, C. O. Davis, and R. T. Barber. 1992a. Photosynthetic characteristics and estimated growth rates indicate grazing is the proximate control of primary production in the equatorial Pacific. Journal of Geophysical Research **97:** 639-654.

Cullen, J. J., and E. H. Renger. 1979. Continuous measurement of the DCMU-induced fluorescence response of natural phytoplankton populations. Marine Biology **53:** 13-20.

Cullen, J. J., X. Yang, and H. L. MacIntyre. 1992b. Nutrient limitation of marine photosynthesis, p. 69-88. *In* P. G. Falkowski [ed.], Primary productivity and biogeochemical cycles in the sea. Plenum Press.

Davison, I. R. 1991. Environmental effects on algal photosynthesis: temperature. Journal of Phycology **27:** 2-8.

Demers, S., S. Roy, R. Gagnon, and C. Vignault. 1991. Rapid light-induced changes in cell fluorescence and in xanthophyll-cycle pigments of *Alexandrium excavatum* (Dinophyceae) and *Thalassiosira pseudonana* (Bacillariophyceae): a photo-protection mechanism. Marine Ecology Progress Series **76:** 185-193.

Demmig, B., K. Winter, A. Kruger, and F. C. Czygan. 1987. Photoinhibition and zeaxanthin formation in intact leaves. A possible role of the xanthophyll cycle in the dissipation of excess light energy. Plant Physiology **84:** 218-224.

Demmig-Adams, B. 1990. Carotenoids and photoprotection in plants. A role for the xanthophyll zeaxanthin. Biochimica Biophysica Acta **1020:** 1-24.

---. 1998. Survey of thermal energy dissipation and pigment composition in sun and shade leaves. Plant and Cell Physiology **39:** 474-482.

Demmig-Adams, B., and W. W. Adams III. 1992. Photoprotection and other responses of plants to high light stress. Annual Reviews of Plant Physiology and Plant Molecular Biology **1992:** 599-626.

Demmig-Adams, B., and W. W. Adams. 2000. Harvesting sunlight safely. Nature **403:** 371-374.

Dubinsky, Z. 1992. The functional and optical absorption cross-sections of photosynthesis. *In* P. G. Falkowski and A. Woodhead [eds.], Primary Productivity and Biogeochemical Cycles in the Sea. Plenum Press.

Dubinsky, Z., P. G. Falkowski, and K. Wyman. 1986. Light harvesting and utilization by phytoplankton. Plant Cell Physiology **27:** 1335–1349.

Dugdale, R. C. 1967. Nutrient limitation in the sea: dynamics, identification, and significance. Limnology and Oceanography **12:** 685-695.

Eppley, R. W. 1968. An incubation method for estimating the carbon content of phytoplankton in natural samples. Limnology and Oceanography **13:** 574-582.

---. 1972. Temperature and phytoplankton growth in the sea, p. 1063-1085, Fisheries Bulletin.

---. 1980. Estimating phytoplankton growth rates in the central oligotrophic oceans, p. 231–242. *In* P. G. Falkowski [ed.], Primary Productivity in the Sea. Plenum.

---. 1981. Relations between nutrient assimilation and growth rate in phytoplankton with a brief review of estimates of growth rate in the ocean, p. 251-263. *In* T. Platt [ed.], Physiological Bases of Phytoplankton Ecology. J. Can. Fish. Res. Bd.

Eppley, R. W., and E. H. Renger. 1974. Nitrogen assimilation of an oceanic diatom in nitrogen-limited continuous culture. Journal of Phycology **10:** 15-23.

Falkowski, P. G. 1980. Light-shade adaptation in marine phytoplankton, p. 99–119. *In* P. G. Falkowski [ed.], Primary Productivity in the Sea. Plenum Press.

---. 1992. Molecular ecology of phytoplankton photosynthesis, p. 47-67. *In* P. G. Falkowski and A. Woodhead [eds.], Primary Productivity and Biogeochemical Cycles in the Sea. Plenum.

Falkowski, P. G., R. Greene, and Z. Kolber. 1994. Light utilization and photoinhibition of photosynthesis in marine phytoplankton, p. 407-432. *In* N. R. Baker and J. R. Bowyer [eds.], Photoinhibition of Photosynthesis from molecular mechanisms to the field. Environmental plant biology. BIOS Scientific.

Falkowski, P. G., R. M. Greene, and R. J. Geider. 1992. Physiological limitations on phytoplankton productivity in the ocean. Oceanography Magazine **5:** 84-91.

Falkowski, P. G., and Z. Kolber. 1993. Estimation of phytoplankton photosynthesis by active fluorescence. ICES Marine Science Symposium **197:** 92-103.

---. 1995. Variations in chlorophyll fluorescence yields in phytoplankton in the world oceans. Australian Journal of Plant Physiology **22:** 341-355.

Falkowski, P. G., T. Owens, A. Ley, and D. Mauzerall. 1981. Effects of growth irradiance levels on the ratio of reaction centers in two species of marine phytoplankton. Plant Physiology **68:** 969-973.

Falkowski, P. G., and J. A. Raven. 1997. Aquatic Photosynthesis, 1 ed. Blackwell Science.

Falkowski, P. G., A. Sukenik, and R. Herzig. 1989. Nitrogen limitation in *Isochrysis galbana* (Haptophyceae). 2. Relative abundance of chloroplast proteins. Journal of Phycology **25:** 471-478.

Falkowski, P. G., K. Wyman, A. Ley, and D. Mauzerall. 1986. Relationship of steady state photosynthesis to fluorescence in eucaryotic algae. Biochimica Biophysica Acta **849:** 183-192.

Flameling, I. A., and J. Kromkamp. 1998. Light dependence of quantum yields for PSII charge separation and oxygen evolution in eucaryotic algae. Limnology and Oceanography **43:** 284-297.

Fryer, M. J., J. R. Andrews, K. Oxborough, D. A. Blowers, and N. R. Baker. 1998. Relationship between CO_2 assimilation, photosynthetic electron transport, and active O_2 metabolism in leaves of maize in the field during periods of low temperature. Plant Physiology **116:** 571-580.

Geel, C., W. Versluis, and J. F. H. Snel. 1997. Estimation of oxygen evolution by marine phytoplankton from measurement of the efficiency of Photosystem II electron flow. Photosynthesis Research **51:** 61-70.

Geider, K. J., H. L. MacIntyre, and T. M. Kana. 1996. A dynamic model of photoadaptation in phytoplankton. Limnology and Oceanography **41:** 1-15.

Geider, R. J. 1992a. Quantitative phytoplankton ecophysiology: implications for primary production and phytoplankton growth. ICES mar Sci. Symp. **194.**

---. 1992b. Respiration: Taxation without representation, p. 333-360. *In* P. G. Falkowski and A. Woodhead [eds.], Primary Productivity and Biogeochemical Cycles in the Sea. Plenum.

Geider, R. J., R. M. Greene, Z. Kolber, H. L. MacIntyre, and P. G. Falkowski. 1993a. Fluorescence assessment of the maximum quantum efficiency of photosynthesis in the western North Atlantic. Deep-Sea Research **40:** 1204-1224.

---. 1993b. Fluorescence assessment of the maximum quantum efficiency of photosynthesis in the western North Atlantic. Deep-Sea Research I **40:** 1205-1224.

Geider, R. J., H. L. MacIntyre, L. M. Graziano, and R. M. L. McKay. 1998. Responses of the photosynthetic apparatus of *Dunaliella tertiolecta* (Chlorophyceae) to nitrogen and phosphorous limitation. European Journal of Phycology **33:** 315-332.

Geider, R. J., H. L. MacIntyre, and T. M. Kana. 1997. Dynamic model of phytoplankton growth and acclimation: responses of the balanced growth rate and the chlorophyll *a*: carbon ratio to light, nutrient-limitation and temperature. Marine Ecology Progress Series **148:** 187-200.

Geider, R. J., B. A. Osborne, and J. A. Raven. 1986. Growth, photosynthesis and maintenance metabolic cost in the diatom *Phaeodactylum tricornutum* at very low light levels. Journal of Phycology **22:** 39-48.

Genty, B., J. M. Briantais, and N. R. Baker. 1989. The relationship between the quantum yield of photosynthetic electron transport and quenching of chlorophyll fluorescence. Biochimica Biophysica Acta**:** 87-92.

Gilbert, M., A. Domin, A. Becker, and C. Wilhelm. 2000. Estimation of primary productivity by chlorophyll *a in vivo* fluorescence in freshwater phytoplankton. Photosynthetica **38:** 111-126.

Gilmore, A. M., and Govindjee. 1999. How higher plants respond to excess light: Energy dissipation in photosystem II, p. 513-548. *In* G. S. Singhal, R. Renger, S. K. Sopory, K.-D. Irrgang and Govindgee [eds.], Concepts in photobiology: photosynthesis and photomorphogenesis. Concepts in photobiology. Narosa-Publishing.

Glover, H. E. 1980. Assimilation numbers in cultures of marine phytoplankton. Journal of Plankton Research **2:** 69-79.

Goh, C. H., U. Schreiber, and R. Hedrich. 1999. New approach of monitoring changes in chlorophyll a fluorescence of single guard cells and protoplasts in response to physiological stimuli. **22:** 1057-1070.

Goldman, J. C. 1980. Physiological processes, nutrient availability, and concept of relative growth rate in marine phytoplankton ecology., p. 179-194. *In* P. G. Falkowski [ed.], Primary Productivity in the Sea. Plenum.

Govindjee. 1995. Sixty-three years since Kautsky: Chlorophyll a fluorescence. Australian Journal of Plant Physiology **22:** 131-160.

Grasshoff, K., M. Ehrhardt, and K. Kremling. 1976. Methods of Seawater Analysis, p. 125-157. Verlag Chemie.

Graziano, L. M., R. J. Geider, W. K. W. Li, and M. Olaizola. 1996. Nitrogen limitation of North Atlantic phytoplankton: analysis of physiological condition in nutrient enrichment experiments. Aquatic Microbial Ecology **11:** 53-64.

Greene, R. M., Z. S. Kolber, D. G. Swift, N. W. Tindale, and P. G. Falkowski. 1994. Physiological limitation of phytoplankton photosynthesis in the eastern equatorial Pacific determined from variability in the quantum yield of fluorescence. Limnology and Oceanography **39:** 1061-1074.

Guillard, R. R. L., and J. H. Ryther. 1962. Studies of marine plankton diatoms I. *Cyclotella nana* Hustedt, and *Detonula confervacea* (Cleve) Gran. Canadian Journal of Microbiology **8:** 229-239.

Harris, G. P. 1978. Photosynthesis, productivity and growth: The physiological ecology of phytoplankton. Archive of Hydrobiology Beih. Ergebn. Limnology **10:** 1-171.

---. 1980. Spatial and temporal scales in phytoplankton ecology. Mechanisms, methods, models and management. Canadian Journal of Fisheries and Aquatic Sciences **37:** 877-900.

Harrison, W. G., T. Platt, and M. R. Lewis. 1985. The utility of light-saturation models for estimating marine primary productivity in the field: a comparison with conventional "simulated" in situ methods. Can. J. Fish. Aquat. Sci. **42:** 864-872.

Hartig, P., K. Wolfstein, S. Lippemeier, and F. Colin. 1998. Photosynthetic activity of natural microphytobenthos populations measured by fluorescence (PAM) and C-14-tracer methods: a comparison. Marine Ecology Progress Series **166:** 53-62.

Havaux, M., R. J. Strasser, and H. Greppin. 1991. A theoretical and experimental analysis of the qP and qN coefficients of chlorophyll fluorescence quenching and their relation to photochemical and non-photochemical events. Photosynthesis Research **27:** 41-55.

Head, E. J. H., and E. P. W. Horne. 1993. Pigment transformation and vertical flux in an area of convergence in the North Atlantic. Deep Sea Research **40:** 329-346.

Henley, W. F. 1993. Measurement and interpretation of photosynthetic light-response curves in algae in the context of photoinhibition and diel changes. Journal of Phycology **29:** 729-739.

Herzig, R., and P. G. Falkowski. 1989. Nitrogen limitation in *Isochrysis galbana* (Haptophyceae). I. Photosynthetic energy conversion and growth efficiencies. Journal of Phycology **25:** 462-471.

Horton, P., and A. Hague. 1988. Studies on the induction of chlorophyll fluorescence in isolated barley protoplasts. IV. Resolution of non-photochemical quenching. Biochimica Biophysica Acta **931:** 107-115.

Horton, P., A. V. Ruban, and R. G. Walters. 1994. Regulation of light harvesting in plants. Plant Physiology **106:** 415-420.

---. 1996. Regulation of light harvesting in green plants. Annual Reviews of Plant Physiology **47:** 655-684.

Huppe, H. C., and D. H. Turpin. 1994. Integration of carbon and nitrogen metabolism in plant and algal cells. Annual Reviews of Plant Physiology and Molecular Biology **45:** 577-607.

Ibelings, B. W., B. M. A. Kroon, and L. R. Mur. 1994. Acclimation of photosystem II in a cyanobacterium and a eukaryotic green alga to high and fluctuating photosynthetic photon flux densities, simulating light regimes induced by mixing in lakes. New Phytologist **128:** 407-424.

Jassby, A. D., and T. Platt. 1976. Mathematical formulation of the relationship between photosynthesis and light for phytoplankton. Limnology and Oceanography **21:** 540–547.

Johnson, Z. 2001. Regulation of Marine Photosynthetic Efficiency by Photosystem II, p. 200, Department of Botany. Duke University.

Kana, T. M., and P. M. Gilbert. 1987a. Effect of irradiances up to 2000 μE m^{-2} s^{-1} on marine *Synechococcus* WH7803–I. Growth, pigmentation, and cell composition. Deep-Sea Research **4:** 479-495.

Kashino, Y. and others 2002. Strategies of phytoplankton to perform effective photosynthesis in the North Water. Deep Sea Research **49:** 5049-5061.

Keller, M. D., R. C. Selvin, W. Claus, and R. R. L. Guillard. 1987. Media for the culture of oceanic ultraphytoplankton. Journal of Phycology **23:** 633-638.

Kiefer, D. A. 1973. Chlorophyll *a* fluorescence in marine diatoms: responses of chloroplasts to light and nutrient stress. Marine Biology **23:** 39-46.

Kiefer, D. A., and R. A. Reynolds. 1992. Advances in understanding phytoplankton fluorescence and photosynthesis, p. 155-174. *In* P. G. Falkowski and A. Woodhead [eds.], Primary Productivity and Biogeochemical Cycles in the Sea. Plenum.

Kirk, J. T. O. 1994. Light and Photosynthesis in Aquatic Ecosystems, 2nd ed. Cambridge University Press.

Kolber, Z., and P. G. Falkowski. 1993. Use of active fluorescence to estimate phytoplankton photosynthesis in situ. Limnology and Oceanography **38:** 1646-1665.

Kolber, Z., K. D. Wyman, and P. G. Falkowski. 1990. Natural variability in photosynthetic energy conversion efficiency: A field study in the Gulf of Maine. Limnology and Oceanography **35:** 72-79.

Kolber, Z., J. R. Zehr, and P. G. Falkowski. 1988. Effects of growth irradiance and nitrogen limitation on photosynthetic energy conversion in photosystem II. Plant Physiology **88:** 923-929.

Kolber, Z. S., O. Prásil, and P. G. Falkowski. 1998. Measurements of variable chlorophyll fluorescence using fast repetition rate techniques: defining methodology and experimental protocols. Biochimica and Biophysica Acta **1367:** 88-106.

Kooten, O. V., and J. F. H. Snel. 1990. The use of chlorophyll fluorescence nomenclature in plant stress physiology. Photosynthesis Research **25:** 147-150.

Krause, G. H., and E. Weis. 1988. The photosynthetic apparatus and chlorophyll fluorescence. An introduction, p. 3-11. *In* H. K. Lichtenthaler [ed.], Application of Chlorophyll Fluorescence. Kluwer Academic.

---. 1991. Chlorophyll fluorescence: The basics. Annual Reviews of Plant Physiology **42:** 313-349.

Kroon, B., B. B. Prézelin, and O. Schofield. 1993. Chromatic regulation of quantum yields for photosystem II charge separation, oxygen evolution, and carbon fixation in *Heterocapsa pygmaea* (Pyrrophyta). Journal of Phycology **29:** 453-462.

Kühl, M., R. M. Glud, J. Borum, R. Roberts, and S. Rysgaard. 2001. Photosynthetic performance of surface-associated algae below sea ice as measured with a pulse-

amplitude-modulated (PAM) fluorometer and O_2 microsensors. Marine Ecology Progress Series **223:** 1-14.

Kyle, D. J., I. Ohad, and C. J. Arntzen. 1984. Membrane protein damage and repair: Selective loss of a quinone-protein function in chloroplast membranes. Proceedings of the National Academy of Science USA **81:** 4070-4074.

Laisk, A., and V. Oja. 2000. Alteration of Photosystem II properties with non-photochemical excitation quenching. Philosophical Transactions of the Royal Society London **355:** 1405-1418.

Lalli, C. M., and T. R. Parsons. 1993. Biological Oceanography- An Introduction, 1 ed. Pergamon Press.

Langdon, C. 1988. On the causes of interspecific differences in the growth-irradiance relationship for phytoplankton. II. A general review. Journal of Plankton Research **10:** 1291-1312.

Latasa, M., and E. Berdalet. 1994. Effect of nitrogen or phosphorous starvation on pigment composition of cultures *Heterocapsa* sp. J. Plank. Res. **16:** 83-94.

Lavergne, J., and H.-W. Trissl. 1995. Theory of fluorescence induction in photosystem II: Derivation of analytical expressions in a model including exciton-radial-pair equilibrium and restricted energy transfer between photosynthetic units. Biophysical Journal **68:** 2474-2492.

Lawlor, D. W. 2001. Photosynthesis. Molecular, Physiological, & Environmental Processes. Springer Verlag.

Leipner, J., Y. Fracheboud, and P. Stamp. 1999. Effect of growing season on the photosynthetic apparatus and leaf antioxidative defenses in two maize genotypes of different chilling tolerance. Environmental and Experimental Botany **42:** 129-139.

Letelier, R. M., M. R. Abbott, and D. M. Karl. 1997. Chlorophyll fluorescence response to upwelling events in the Southern Ocean. Journal of Geophysical Research **24:** 409-412.

Levasseur, M., P. A. Thompson, and P. J. Harrison. 1993. Physiological acclimation of marine phytoplankton to different nitrogen sources. Journal of Phycology **29:** 587-595.

Lewis, M. R., and J. C. Smith. 1983. A small volume, short–incubation–time method for measurement of photosynthesis as a function of incident irradiance. Marine Ecology Progress Series **13:** 99–102.

Li, X. and others 2000. A pigment-binding protein essential for regulation of photosynthetic light harvesting. Nature **403:** 391-395.

Lomas, M. W., and P. M. Glibert. 1999. Interactions between NH_4^+ and NO_3^- uptake and assimilation: comparison of diatoms and dinoflagellates at several growth temperatures. Marine Biology **133:** 541-551.

Long, S. P., S. Humphries, and P. G. Falkowski. 1994. Photoinhibition of photosynthesis in nature. Annual Reviews of Plant Physiology and Plant Molecular Biology **45:** 633-662.

MacIntyre, H. L., T. M. Kana, T. Anning, and R. J. Geider. 2002. Photoacclimation of photosynthesis irradiance response curves and photosynthetic pigments in microalgae and cyanobacteria. Journal of Phycology **38:** 17-38.

MacIntyre, J. G., J. J. Cullen, and A. D. Cembella. 1997. Vertical Migration, nutrition and toxicity in the dinoflagellate *Alexandrium tamarense*. Marine Ecology Progress Series **148:** 201-216.

Marra, J. 1978. Effect of short-term variation in light intensity on photosynthesis of a marine phytoplankter: a laboratory simulation study. Marine Biology **46:** 191-202.

Marra, J., C. C. Trees, R. R. Bidigare, and R. T. Barber. 2000. Pigment absorption and quantum yields in the Arabian Sea. Deep Sea Research II **47:** 1279-1300.

Maxwell, D. P., S. Falk, C. G. Trick, and N. P. A. Huner. 1994. Growth at low-temperature mimics high-light acclimation in *Chlorella vulgaris*. Plant Physiology **105:** 535-543.

Maxwell, K., and G. N. Johnson. 2000. Chlorophyll fluorescence - a practical guide. Journal of Experimental Botany **51:** 659-668.

Morris, I. 1981. Photosynthetic products, physiological state and phytoplankton growth, p. 83-101. *In* T. Platt [ed.], Physiological bases of phytoplankton ecology. Canadian bulletin of fisheries and aquatic sciences. Department of Fisheries and Oceans.

Muller, P., X. Li, and K. K. Nyogi. 2001. Non-photochemical quenching. A response to excess light energy. Plant Physiology **125:** 1558-1566.

Neale, P. J. 1987. Algal photoinhibition and photosynthesis in the aquatic environment, p. 35- 65. *In* D. J. Kyle, C. B. Osmond and C. J. Arntzen [eds.], Photoinhibition. Elsevier.

Neale, P. J., J. J. Cullen, and C. M. Yentsch. 1989. Bio-optical inferences from chlorophyll a fluorescence: What kind of fluorescence is measured in flow cytometry? Limnology and Oceanography **34:** 1739-1748.

Neale, P. J., and P. J. Richerson. 1987. Photoinhibition and the diurnal variation of phytoplankton photosynthesis - I. Development of a photosynthesis-irradiance model from studies of in situ responses. Journal of Plankton Research **9:** 167-193.

Neubauer, C., and U. Schreiber. 1989. Photochemical and non-photochemical quenching of chlorophyll fluorescence induced by hydrogen peroxide. Zeitschrift für Naturforschung Biosciences **44:** 262-270.

Niyogi, K. K. 1999. Photoprotection revisited: Genetic and molecular approaches. Annual Reviews of Plant Physiology and Plant Molecular Biology **50:** 333-359.

Olaizola, M., R. J. Geider, W. G. Harrison, L. M. Graziano, G. M. Ferrari, and P. M. Schlittenhardt. 1996. Synoptic study of variations in the fluorescence-based maximum quantum efficiency of photosynthesis across the North Atlantic Ocean. Limnology and Oceanography **41:** 755-765.

Olaizola, M., and H. Y. Yamamoto. 1994. Short-term response of the diadinoxanthin cycle and fluorescence yield to high irradiance in *Chaetoceros muelleri* (Bacillariophyceae). Journal of Phycology **30:** 606-612.

Oquist, G., and W. S. Chow. 1992. On the relationship between the quantum yield of photosystem II electron transport, as determined by chlorophyll fluorescence and the quantum yield of CO2-dependent O2 evolution. Photosynthesis Research **33:** 51-62.

Osborne, B. A., and R. J. Geider. 1986. Effect of nitrate-nitrogen limitation on photosynthesis of the diatom *Phaeodactylum tricornutum* Bohlin (Bacillariophyceae). Plant Cell Environment **9:** 617-625.

Osmond, C. B. 1994. What is photoinhibition? Some insights from comparison of shade and sun plants., p. 1-24. *In* N. R. Baker and J. R. Bowers [eds.], Photoinhibition of photosynthesis: from molecular mechanisms to the field. Bios Scientific.

Owens, T. G. 1991. Energy transformation and fluorescence in photosynthesis, p. 101-136. *In* S. Demers [ed.], Particle Analysis of Oceanography. Springer-Verlag.

---. 1994. Excitation energy transfer between chlorophylls and carotenoids. A proposed molecular mechanism for non-photochemical quenching, p. 95-109. *In* N. R. Baker and J. R. Bowyer [eds.], Photoinhibition of photosynthesis from molecular mechanisms to the field. Environmental Plant Biology. BIOS Scientific Publishers Ltd.

Park, Y. I., W. S. Chow, and J. M. Anderson. 1995. The quantum yield of photoinactivation of photosystem II in peas is greater at low than high photon exposure. Plant and Cell Physiology **36:** 1163-1167.

Park, Y. I., W. S. Chow, J. M. Anderson, and M. H. Vaughan. 1996. Differential susceptibility of photosystem II to light stress in light acclimated pea leaves depends on the capacity for photochemical and non-radiative dissipation of light. Plant Science **115:** 137-149.

Parkhill, J. P., G. Maillet, and J. J. Cullen. 2001. Fluorescence-based maximal quantum yield for photosystem II as a diagnostic of nutrient stress. Journal of Phycology **37:** 517-529.

Pospisil, P. 1997. Mechanisms of non-photochemical chlorophyll fluorescence quenching in higher plants. Photosynthetica **34:** 343-355.

Prasil, O., N. Adir, and I. Ohad. 1992. Dynamics of photosystem II: mechanism of photoinhibition and recovery processes., p. 295-348. *In* J. R. Barber [ed.], The photosystems: structure, function, and molecular biology. Elsevier.

Prézelin, B. B. 1981. Light reactions in photosynthesis, p. 1–43. *In* T. Platt [ed.], Physiological Bases of Phytoplankton Ecology.

Prézelin, B. B., and A. C. Ley. 1980. Photosynthesis and chlorophyll a fluorescence rhythms of marine phytoplankton. Marine Biology **55:** 295-307.

Prézelin, B. B., B. W. Meeson, and B. M. Sweeney. 1977. Characterization of photosynthetic rhythms in marine dinoflagellates. II. Photosynthesis-irradiance curves and *in vivo* chlorophyll *a* fluorescence. Plant Physiology: 388-392.

Ralph, P. J., R. Gademann, A. W. D. Larkum, and U. Schreiber. 1999. *In situ* underwater measurements of photosynthetic activity of coral zooxanthellae and other reef dwelling dinoflagellate endosymbionts. Marine Ecology Progress Series **180:** 139-147.

Rees, D., C. B. Lee, D. J. Gilmour, and P. Horton. 1992. Mechanisms between controlling balance between light input and utilization in the salt tolerant alga *Dunaliella* C9AA. Photosynthesis Research **32:** 181-191.

Richerson, P. J., R. Armstrong, and C. R. Goldman. 1970. Contemporaneous disequilibrium. A new hypothesis to explain the "paradox of the plankton". Proceedings of the National Academy of Science **67:** 1710-1714.

Roháček, K., and M. Barták. 1999. Technique of the modulated chlorophyll fluorescence: basic concepts, useful parameters, and some applications. Photosynthetica **37:** 339-363.

Roy, S., and L. Legendre. 1979. DCMU-enhanced fluorescence as an index of photosynthetic activity in phytoplankton. Marine Biology **55:** 93-101.

Ruban, A. V., and P. Horton. 1995. Regulation of non-photochemical quenching of chlorophyll fluorescence in plants. Australian Journal of Plant Physiology **22:** 221-230.

Ruban, A. V., M. Wentworth, and P. Horton. 2001. Kinetic analysis of Nonphotochemical quenching of chlorophyll fluorescence. 1. Isolated chloroplasts. Biochemistry **40:** 9896-9901.

Samuelsson, G., and G. Öquist. 1977. A method for studying photosynthetic capacities of unicellular algae based on in vivo chlorophyll fluorescence. Plant Physiology **40:** 315-319.

Schofield, O., T. J. Evens, and D. F. Millie. 1998. Photosystem II quantum yields and xanthophyll-cycle pigments of the macroalga *Sargassum natans* (Phaeophyceae): responses under natural sunlight. Journal of Phycology **34:** 104-112.

Schreiber, U., and W. Bilger. 1993. Progress in chlorophyll fluorescence research: major developments during the last years in retrospect. Progress in Botany **54:** 151-173.

Schreiber, U., R. Gademann, P. J. Ralph, and A. W. D. Larkum. 1997. Assessment of photosynthetic performance of *Prochloron* in *Lissoclinum patella* in hospite by chlorophyll fluorescence measurements. Plant Cell Physiology **38:** 945-951.

Schreiber, U., H. Hormann, C. Neubauer, and C. Klughammer. 1995. Assessment of photosystem II photochemical quantum yield by chlorophyll fluorescence quenching analysis. Australian Journal of Plant Physiology **22:** 209-220.

Schreiber, U., U. Schliwa, and W. Bilger. 1986. Continuous recording of photochemical and non-photochemical chlorophyll fluorescence quenching with a new type of modulation fluorometer. Photosynthesis Research **10:** 51-62.

Schubert, H., B. M. A. Kroon, and H. C. P. Matthijs. 1994. In vivo manipulation of the xanthophyll cycle and the role of zeaxanthin in the protection against photodamage in the green alga, *Chlorella pyrenoidosa*. Journal of Biology and Chemistry **269:** 7267-7272.

Shuter, B. 1979. A model of physiological adaptation in unicellular algae. Journal of Theoretical Biology **78:** 519–552.

Sosik, H. M., and B. G. Mitchell. 1991. Absorption, fluorescence, and quantum yield for growth in nitrogen-limited *Dunaliella tertiolecta*. Limnology and Oceanography **36:** 910-921.

Steemann-Nielsen, E. 1952. The use of radio-active carbon (^{14}C) for measuring organic production in the sea. Journal for Conservation and International Exploration of the Sea **18:** 117-140.

Strickland, J. D. H., and T. R. Parsons. 1972. A Practical handbook of seawater analysis. Bulletin of the Fisheries and Research Board of Canada **167:** 1-310.

Suggett, D., G. Kraay, P. Holligan, M. Davey, J. Aiken, and R. Geider. 2001. Assessment of photosynthesis in spring cyanobacterial bloom by use of a fast repetition rate fluorometer. Limnology and Oceanography **46:** 802-810.

Terry, K. L., J. Hirata, and E. A. Laws. 1985. Light-, nitrogen-, and phosphorus-limited growth of *Phaeodactylum tricornutum* Bohlin Strain TFX-1 : chemical composition, carbon partitioning, and the diel periodicity of physiological processes. Journal of Experimental Marine Biology and Ecology **86:** 85-100.

Thomas, W. H., and A. N. Dodson. 1972. On nitrogen deficiency in tropical Pacific oceanic phytoplankton. II. Photosynthetic and cellular characteristics of a chemostat-grown diatom. Limnology and Oceanography **17:** 515-523.

Ting, C. S., and T. G. Owens. 1992. Limitations of the Pulse Modulated Technique for measuring the fluorescence characteristics of algae. Plant Physiology **100:** 367-373.

---. 1994. The effects of excess irradiance on photosynthesis in the marine diatom *Phaeodactylum tricornutum*. Plant Physiology **106:** 763-770.

Turpin, D. H. 1991. Effects of inorganic N availability on algal photosynthesis and carbon metabolism. Journal of Phycology **27:** 14-20.

Uhrmacher, S., D. Hanelt, and W. Nultsch. 1995. Zeaxanthin content and the degree of photoinhibition are linearly correlated in the brown algae *Dictyota dichotoma*. Marine Biology **123:** 159-165.

Vasilikiotis, C., and A. Melis. 1994. Photosystem II reaction center damage and repair cycle: Chloroplast acclimation strategy to irradiance stress. Proceedings of the National Academy of Science **91:** 7222-7226.

Vass, I., and S. Styring. 1992. Spectroscopic characterization of triplet forming states in photosystem II. Biochemistry **31:** 5957-5963.

Verhoeven, A. S., B. Demmig-Adams, and W. W. Adams. 1997. Enhanced employment of the xanthophyll cycle and thermal energy dissipation in spinach exposed to high light and N-stress. Plant Physiology **113:** 817-824.

Walters, R. G. 1991. Resolution of components of non-photochemical quenching in barley leaves. Photosynthesis Research **27:** 121-133.

Weger, H. G., D. G. Birch, I. R. Elrifi, and D. Turpin. 1988. Ammonium assimilation requires mitochondrial respiration in the light. A study with the green alga *Selenastrum minutum.* Plant Physiology **86:** 688-692.

Weis, E., and J. A. Berry. 1987. Quantum efficiency of photosystem II in relation to "energy"-dependent quenching of chlorophyll fluorescence. Biochimica and Biophysica Acta **894:** 198-208.

Welschmeyer, N. A., and C. J. Lorenzen. 1981. Chlorophyll-specific photosynthesis and quantum efficiency at subsaturating light intensities. Journal of Phycology **17:** 283–293.

White, A. J., and C. Critchley. 1999. Rapid light curves: A new fluorescence method to assess the state of the photosynthetic apparatus. Photosynthesis Research **59:** 63-72.

Wood, M. D., and R. L. Oliver. 1995. Fluorescence transients in response to nutrient enrichment of nitrogen- and phosphorus-limited *Microcystis aeruginosa* cultures and natural phytoplankton population: a measure of nutrient limitation. Australian Journal of Plant Physiology **22:** 331-340.

Zhu, M., X. Yang, and J. J. Cullen. 1992. The study of fluorescence characteristics and biochemical composition of a marine diatom *Thalassiosira pseudonana* 3H in light dark cycles. Acta Oceanologica Sinica **12:** 457-464.

Zimmerman, R. C., J. B. Soohoo, J. N. Kremer, and D. Z. D'argenio. 1987. Evaluation of variance approximation techniques for non-linear photosynthesis-irradiance models. Marine Biology **95:** 205-215.